THERMAL ANALYSIS AND OPTIMIZATION OF ANNULAR FINS WITH SIMULTANEOUS HEAT AND MASS TRANSFER

BY

ABDURRAHMAN MOINUDDIN

A Thesis Presented to the
DEANSHIP OF GRADUATE STUDIES

KING FAHD UNIVERSITY OF PETROLEUM & MINERALS
DHAHRAN, SAUDI ARABIA

In Partial Fulfillment of the
Requirements for the Degree of

MASTER OF SCIENCE

In

MECHANICAL ENGINEERING

MAY 2009

KING FAHD UNIVERSITY OF PETROLEUM AND MINERALS

DHAHRAN 31261, SAUDI ARABIA

DEANSHIP OF GRADUATE STUDIES

This thesis, written by **ABDURRAHMAN MOINUDDIN** under the direction of his thesis advisor and approved by his thesis committee, has been presented to and accepted by the Dean of Graduate Studies, in partial fulfillment of the requirements for the degree of **MASTER OF SCIENCE IN MECHANICAL ENGINEERING.**

Thesis Committee

Dr. Syed M. Zubair (Advisor)

Dr. Shahzada Z. Shuja (Co-Advisor)

Dr. Mohammed A. Antar (Member)

Dr. Amro M. Al- Qutub

Department Chairman

Dr. Salam A. Zummo

Dean of Graduate Studies

8/12/09

Date

Dedicated to

My Parents

And

My Siblings

ACKNOWLEDGEMENTS

All praises, all glory and all thanks are due to Allah, The Majestic, The Almighty for bestowing me with knowledge, guidance, patience, courage and health to achieve this work. May peace and blessings be upon prophet Muhammad (PBUH), his family and his companions.

I would like to acknowledge KFUPM for the support extended towards my research through its remarkable facilities and for providing me the opportunity to pursue graduate studies.

I deeply acknowledge with gratitude, the valuable time, effort, encouragement, admiration and guidance given by my thesis committee chairman, Dr. Syed M. Zubair. Secondly, I am grateful to my committee co-chairman, Dr. Shazada Z. Shuja for his constructive guidance, technical support, valuable time and effort. I am indebted to Dr. Mohammed A. Antar for his continuous support, and valuable suggestions during this research.

Special thanks to my seniors Shaikh Imran, Misbahuddin, Abdurrahmaan, Mumtaz, Shaikh Rizwan, Omer, Mazher, Murtaza, Mujahid, Fareed, Asrar, Nizam, for their overall valuable guidance during this journey. I would also like to thanks my friends Ammar, Hussain, Hasan, Sarfaraz, Owais, Nadeem, Imran Ghani, Abdul Malik, Shahid, Naeem, Rizwan and all others who provided wonderful company and good memories that will last a life time.

Finally, from the bottom of my heart, I thanks my mother and father, and all my family members for their continuous love, encouragement, prayers, emotional and moral

support throughout my life. Words fall short in conveying my gratitude towards them. A prayer is the simplest way I can repay them - May Allah (S.W.T.) give them good health and give me ample opportunity to be of service to them throughout my life.

TABLE OF CONTENTS

LIST OF TABLES

LIST OF FIGURES

Appendix

THESIS ABSTRACT (ENGLISH)

NAME: ABDURRAHMAN MOINUDDIN

TITLE: THERMAL ANALYSIS AND OPTIMIZATION OF ANNULAR FINS WITH SIMULTANEOUS HEAT AND MASS TRANSFER

MAJOR: MECHANICAL ENGINEERING

DATE: MAY 2009

Finned tube heat exchangers are widely used in industrial applications. In general, the energy exchange between the fin and surrounding gas stream takes place solely by sensible heat transfer. however, in various applications such as, air conditioning, refrigeration, evaporative air coolers, environmental control system of aircrafts and chemical processing systems, heat transfer between moist air and the fin is accompanied by diffusion mass transfer of water vapor. The prime reason for this simultaneous heat and mass transfer is that the coil surface temperature is below the dew point temperature of air being cooled. So it is important to study the most widely used fins, namely annular or circular fins, under these conditions.

One dimensional fin model is developed and studied for five types of annular fins that is constant cross-section, triangular, concave parabolic, convex parabolic and hyperbolic profiles under fully as well as partially wet conditions. In addition to studying the thermal performance numerically, their optimization is also done in the present work. An analytical solution for hyperbolic profile is introduced and compared with corresponding numerical results. Besides this, a two-dimensional fin model for rectangular profile annular fin is derived and analyzed for constant as well as distinct thermal conductivities in the fundamental directions. Furthermore, the optimum dimension for a given quantity of fin material is also laid out.

MASTER OF SCIENCE DEGREE

KING FAHD UNIVERSITY OF PETROLEUM and MINERALS

Dhahran, Saudi Arabia

THESIS ABSTRACT (ARABIC)

الاسم: عبد الرحمن معين الدين

العنوان: الحراري والامثل للزعانف الحلقية بالتزامن الحراري والكتلي

التخصص: الهندسة الميكانيكية

التاريخ: مايو 2009

المبادلات الحرارية الأنبوبية المزعنفة تستخدم بشكل واسع في التطبيقات الصناعية .بشكل عام،التبادل في الطاقة بين الزعنفة و الغاز المحيط المتدفق تأخذ حيزا " بانتقال الحرارة المحسوس ، ومع ذلك في تطبيقات مختلفة مثل أجهزة التكييف والتبريد ، والتبخر ومبردات الهواء ، ونظام مراقبة البيئة للطائرات ونظم المعالجة الكيماوية انتقال الحرارة بين الهواء الرطبة والزعنفة يرافق بنشر وانتقال كتلي لبخار الماء.يرجع السبب الرئيسي لنقل الحرارة والكتلة في وقت واحد وهو أن درجة حرارة سطح الملف أقل من درجة حرارة نقطة الندى للهواء المراد تبريده . لذا من المهم دراسة أكثر الزعانف المستخدمة على نطاق واسع، والتي أعني الشكل الزعنفي الحلقي او الزعنفي الدائري ، تحت هذه الظروف

نموذج زعنفي ذا بعد واحد تم تطويره ودراسته لخمسة أنواع من الزعانف الحلقية والتي هي ذات مقطع ثابت، مثلثيه، مقعر مكافئ، محدب مكافئ، محدب مكافئ مفرق السطح تحت الظروف الرطبة الكاملة والجزئية. بالإضافة إلى دراسة الأداء الحراري عدديا وكيفية تحسينه أيضا تم في هذا العمل. الحل التحليلي للسطح المغرق قدم وتم مقارنته مع النتائج العددية المناظرة . إلى جانب هذا نموذج زعنفي ذو بعدين لسطح زعنفي حلقي مستطيل تم اشتقاقه وتحليله لموصلات حرارية ثابتة ومميزه في الاتجاهات الأساسية .علاوة على ذلك ، البعد الأمثل لكمية معطاة من المواد الزعنفية وضعت

درجة الماجستير في العلوم

جامعة الملك فهد للبترول و المعادن

الظهران المملكة العربية السعودية

CHAPTER 1

INTRODUCTION

1.1 Background

An ever-increasing number of engineering problems are concerned with energy transitions requiring the speedy movement of heat. This requires high performance heat transfer components with relatively smaller weights, volumes, costs, or acceptable shapes. Extended surfaces or fins are widely used in our day-to-day life. Typical examples are air-land-space vehicles and their power sources; refrigeration, cryogenic and chemical processes; electrical circuits; process heat dissipaters; nuclear fuel modules and so forth. Wherever there is a need of efficient heat transfer, we see extended surfaces doing the job.

In heat transfer phenomenon, transfer of energy takes place from a body at high temperature (sometimes-called source) to another body, which is at relatively lower temperature (called sink). These are the heat rejecting and heat absorbing surfaces also known as prime surfaces. A prime surface is extended by attaching additional objects like metal tapes or spines to it; these added surfaces are known as extended surfaces or fins.

Some commonly used extended surfaces are, depicted in Figure 1-1

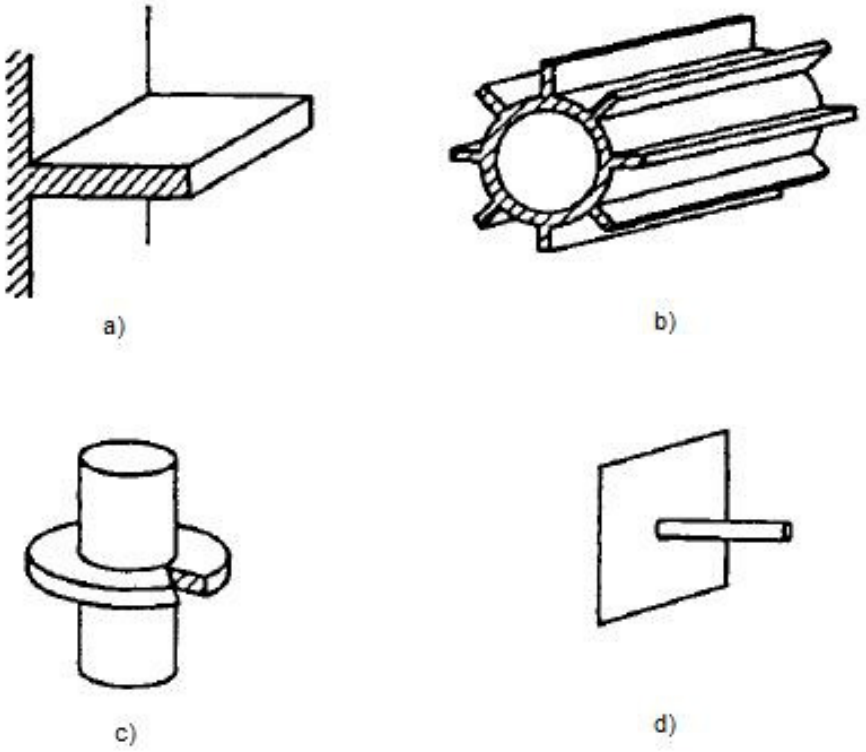

Figure 1-1 a) Longitudinal fin; b) Cylindrical tube with fin of rectangular profile; c) Annular fin; d) Spine

One of the most common of all types of fins is annular fin from the standpoint of finned tube heat exchangers. Depending on the requirement of the process, space availability and ease of manufacturing, different types of annular fins are utilized. These are shown schematically in Figure 1-2.

.

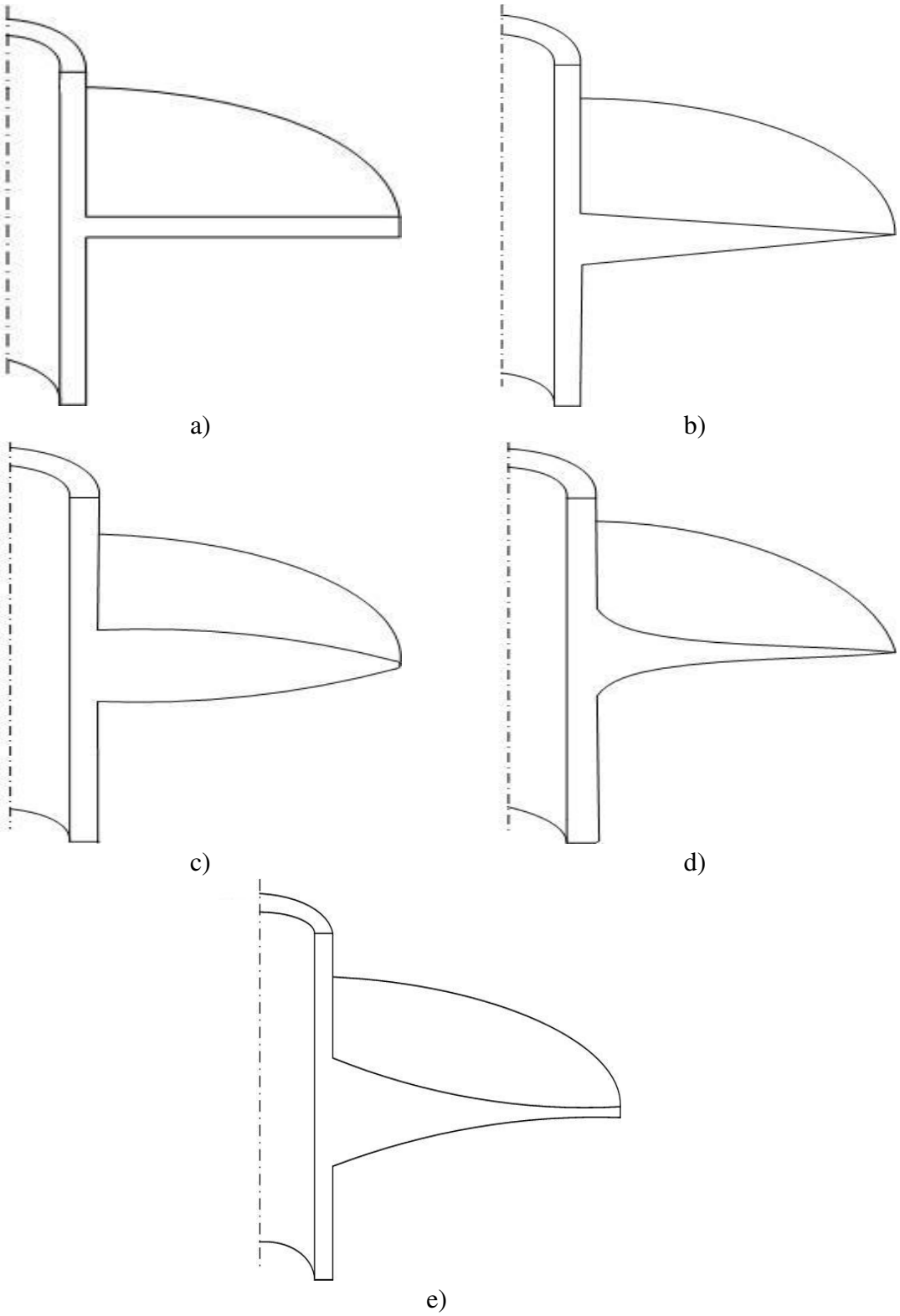

Figure 1-2 Different kinds of annular fins: a) Rectangular b) Triangular c) Convex parabolic d) Concave parabolic e) Hyperbolic profile fin

Generally, the heat transfer from/to the fin surface takes place solely by sensible heat transfer, like in automobile radiators. However, in certain application the temperature of the surrounding atmosphere is higher than the fin surface temperature. Under these circumstances, if the temperature of the fin surface is less than or equal to the dew point temperature of the humid surrounding air then, in addition to sensible heat transfer, mass transfer also takes place. This mass transfer is actually the result of latent heat of condensation being absorbed by the fin, thereby increasing its temperature and causing the water in the air to condense. Such phenomenon is observed in evaporative air coolers, dehumidifying coils of air conditioners and in environmental control system of aircrafts. Now, depending upon the extent the condensed water covers the fin surface, we classify them as fully wet, partially wet or fully dry fins. As the names suggest, if the water film covers the fin completely we call it fully wet, if partially, we say it is partially wet and if none of the two we call it a fully dry fin.

1.2 Research Objectives

The objectives of this study are summed up and presented as follows:

1) To analyze various types of annular fins numerically and/or analytically under simultaneous heat and mass transfer using one-dimensional heat transfer approach.
2) Using the same one-dimensional model determine the optimum dimensions of the fin that should give us the maximum amount of heat transfer rate under a specified operating conditions, for a fixed quantity of fin material.

3) To present a two-dimensional numerical solution for analysis of annular fin with rectangular profile under both heat and mass transfer interaction considering equal as well as different thermal conductivity values in the fundamental directions.
4) Finally, study the optimum dimensions for the two-dimensional rectangular profile fin when subjected to both heat and mass transfer.

1.3 Layout of the Thesis

This thesis is divided in to five sections including the present chapter. In chapter 2, we have reviewed the available literature related to fins in respect of heat transfer, simultaneous heat and mass transfer as well as those dealing with optimization of the fins. Detail investigation of annular fins in one-dimension is presented in chapter 3, which includes analysis as well as results and discussion for temperature distribution, fin efficiency, and optimal fin dimensions. In a similar fashion, a two-dimensional model is derived for annular profile fin of constant cross-section and the results are discussed in chapter 4. Finally, in chapter 5 the conclusions and some recommendations for future work related to fins is presented.

CHAPTER 2

LITERATURE REVIEW

This chapter provides a review of previous and ongoing research work performed by different researchers during more than past half-century. Knowledge gained through this review was crucial during the analysis work of this study. In section 2.1.1, review of one-dimensional approach to fin problems for only heat transfer and for heat and mass transfer is presented. Section 2.1.2 discusses the review of optimization techniques in one-dimensional problems. In section 2.2, two-dimensional analysis of different fin types and their optimization is reviewed.

2.1 One Dimensional Fin Analysis

There has been numerous works on one-dimensional fin analysis. Researchers have from time to time, presented their work trying to understand the different aspects of heat transfer in/from various type of fins in more realistic, applicable and economical point of view. The interest of different authors can be classified into two categories. One related to determination of fin efficiency and the other one for optimization.

2.1.1 Efficiency of Fin

The fin efficiency, for a dry fin is defined by Kern and Kraus [1] as "the ratio of actual heat dissipation of a fin to its ideal heat dissipation if the entire fin surface were at the same temperature as its base". The following section 2.1.1. (a), deals with the review of work in this respect whereas section 2.1.1. (b) consider mass transfer also in addition to heat transfer from the fin surface.

2.1.1. (a) Heat Transfer Only

Kern and Kraus [1] divided the extended surfaces into three fundamental geometries. Namely, these are longitudinal fins, radial fins and spine fins. They employed the assumptions of Murray [2] and Gardner [3], which are almost always referred to as *Murray-Gardner assumption*, and are as follows:

1. The heat flow in the fin and its temperatures remain constant with time.
2. The fin material is homogeneous, its thermal conductivity is the same in all directions, and it remains constant.

3. The convective heat transfer coefficient on the faces of the fin is constant and uniform over the entire surface of the fin.
4. The temperature of the medium surrounding the fin is uniform.
5. The fin thickness is small, compared with its height and length, so that temperature gradients across the fin thickness and heat transfer from the edges of the fin may be neglected.
6. The temperature at the base of the fin is uniform.
7. There is no contact resistance where the base of the fin joins the prime surface.
8. There are no heat sources within the fin itself.
9. The heat transferred through the tip of the fin is negligible compared with the heat leaving its lateral surface.
10. Heat transfer to or from the fin is proportional to the temperature excess between the fin and the surrounding medium.

Kraus [4] surveyed the progress of extended surface technology in the past 65 years. One-dimensional steady state solution including three different boundary conditions on fin tip has been summarized by Incropera and DeWitt [5].

In recent years Alam and Ghoshdastidar [6] presented a finite-difference based numerical simulation of steady, laminar heat transfer in circular tubes fitted with a number of identical longitudinal fins having tapered lateral profiles. They used a temperature dependent thermal conductivity and viscosity. In another study, Kou *et al.* [7] divided a singular fin of variable thermal properties into many sections and combined the solution of each one of them into one by using the recursive numerical formulation. Lane and Heggs [8] derived a generalized analytical solution for various fin profiles and provided

performance and design charts. Bouaziz and Hanini [9] used a temperature dependent thermal conductivity to provide a simplified analytical solution for temperature distribution and fin efficiency.

There have also been many studies concerning annular fins. Ullmann and Kalman [10] adopted the same approach as that of Brown [11] and numerically studied four types of annular fins. Their results suggested that out of the four types, parabolic fins have the best performance. In a technical paper Arauzo *et al.* [12] came up with an approximate solution of the quasi-one-dimensional heat conduction equation for annular fin of hyperbolic profile. For the same fin configuration, Campo and Cui [13] presented an simple analytic procedure for approximate solution of the quasi-1D heat equation. By using this technique, they transformed the generalized Airy equation into an equivalent quasi-1D heat equation for a straight fin of uniform profile. In another attempt, a semi-analytical technique was given by Kundu and Das [14] for studying the performance of elliptic disc fins by making use of sector method.

Assis and Kalman [15] numerically study the transient behavior of different kind of fins by varying the step initial conditions. The reason for their transient study was the fact that the path to steady state condition is different for both situations i.e. the base of the fin subjected to constant temperature and to constant heat flux. In another generalized study by Loar and Kalman [16], the performance of longitudinal, spine and annular fins were studied numerically with temperature dependent heat transfer coefficient. They used the simplifying assumptions of Ref. [2] and Gardner [3]. Kundu and Das [17] thermally analyzed fins of straight taper with the help of Frobenius expanding series. Using a linear variation of the convective heat transfer coefficient along the fin surface and relaxing

assumptions like length of arc idealization and insulated fin tip, they studied longitudinal fin, spine and annular fins. In a recent study, Kundu and Das [18] developed a model to analytically study the performance of four different fin arrays. They reported that conduction through the supporting structure and the convection from the inter-fin spacing plays a vital role in fin performance.

2.1.1. (b) Heat and Mass Transfer

Therlkeld [19] obtained an analytical expression for the overall fin efficiency by using the enthalpy difference as the driving force for the combined heat and mass transfer process. He assumed a linear relationship between the air temperature and corresponding saturated air enthalpy. The overall efficiency of a wet fin, calculated with his method, does not depend much on the relative humidity of the air. Physically, the differences in temperature and humidity ratio between the incoming air and existing one on the fin surface are driving forces for the heat and mass transfer, respectively. It is important to note that the two driving forces can be combined into one to be converted into the enthalpy difference under the assumption that the Lewis number is equal to one.

McQuiston [20] studied analytically the overall efficiency of a fully wet straight fin of uniform thickness. He assumed that the driving force for the mass transfer, as given by the difference in the humidity ratio between the incoming air and the existing one on the fin surface, is linearly related to the corresponding temperature difference. An analytical solution was obtained for the fin efficiency similar to that of the fin efficiency with only heat transfer (no mass transfer). He demonstrated that the overall fin efficiency depends strongly on the relative humidity of the incoming air stream. Another analytical solution

was obtained by Wu and Bong [21] for the efficiency under both fully wet and partially wet conditions by using the temperature and humidity ratio differences as the driving forces for heat and mass transfer. The linear relationship they assumed between the humidity ratio of the saturated air on the fin surface and its temperature was that of Elmahdy and Biggs [22]. Their result shows that there is not much change in the fin efficiency, of a fully wet fin, with the relative humidity however, fin efficiency does change appreciably when the fin is partially wet. Similar conclusions were drawn by Kundu [23] who presented an analytical method for the performance of longitudinal and pin fins of uniform thickness under fully wet as well as partially wet conditions. He used a similar relationship between specific humidity and corresponding temperature as Wu and Bong [21]. An additional conclusion he drawn from his work was that the fin efficiency is highest for a dry fin under same conditions.

Kazeminejad [24] studied a rectangular fin assembly under fully wet condition. He used the concept of the sensible to total heat ratio, which is used in the psychrometric calculations to get a numerical solution for his model. His results showed that a significant decrease in fin effectiveness occurs as the amount of dehumidification increases .Sharqawy and Zubair [25] recently studied straight fins of different configurations when subjected to simultaneous heat and mass transfer. They also assumed a linear relation between the humidity ratio and temperature but different from Elmahdy and Biggs's [22] work. They concluded that the linear approximation model used by Wu and Bong [21] cannot be used without knowing the fin tip temperature. Their results also indicated that as the atmospheric pressure increases the fin efficiency also increases. Another lately study done by Kundu and Miyara [26], analytically established

the performance of a fully wet fin assembly under dehumidifying conditions assuming a cubic relation, taken by Liang *et al.* [27], between humidity ratio of saturated air and its temperature. The authors used Adomian decomposition method for finding the solution. This method is mentioned by Adomain [28]. They compared the results obtained by their model with that of Sharqawy and Zubair [29] model and found noticeable discrepancy.

Fins of straight taper have also attained reasonable attention of the researchers. Kundu [30] presented an analytical study of a cooling and dehumidifying straight taper longitudinal fin under fully wet conditions. He used the model of Wu and Bong [21] to relate the specific humidity of the air and the local fin temperature. According his observation, relative humidity does not significantly affect the temperature distribution, fin efficiency and the fin effectiveness, rather the condition of the fin surface does. Kundu and Das [31] developed a generalized analytical technique for various geometries namely; longitudinal, annular and spine fins; under dry and fully wet conditions. Their mathematical formulation was based on the assumption of a linear relationship between temperature and humidity ratio, while the method of Frobenius power series expansion has been used to solve the governing differential equation. They concluded that the wet fin's efficiency and effectiveness depends on the base temperature and the ambient conditions. In another analytical approach, Kundu *et al.* [32] used cubic polynomial relationship (Ref. [27;33]) between specific humidity and the corresponding saturation temperature for studying the performance of a triangular fin under dehumidifying condition.

The earliest work on annular fins with simultaneous heat and mass transfer was done by Elmahdy and Biggs [22]. They numerically studied the overall fin efficiency of a fully

wet circular fin. They assumed a linear relationship between the humidity ratio of the saturated air on the fin surface and its temperature, which was somewhat different than McQuiston's [20] model. Numerical solutions for a specific circular fin were obtained but no close-form solution was presented. Their results indicates that the fin efficiency strongly depend on the relative humidity. Another work in this regard was done by Rosario and Rahman [34] . They investigated the radial fin assembly under fully wet operating conditions assuming a fixed sensible to total heat ratio to obtain their numerical solution. The results found suggested that the heat transfer rate increased with increment in dry bulb temperature as well as the relative humidity of the air. Another outcome of their study showed that there is a strong relationship between the fin efficiency and relative humidity of the incoming air.

Naphon [35] studied annular fin under dry-surface conditions, partially wet-surface conditions, and fully wet-surface conditions. He used a third-degree polynomial correlation given by Laing *et al.* [36] for the relationship between the dry bulb temperature and the humidity ratio for the saturated air. Sharqawy and Zubair [29] suggested a more practical linear relationship between the humidity ratio and dry bulb temperature. This relation can be calculated without knowing the fin tip temperature. Rather ambient air conditions and base temperature were needed instead. They used this relationship to derive an analytical solution for an annular fin of constant cross-section area when subjected to heat and mass transfer. The authors established that the closed-form solutions for a dry-fin case presented in many text books is a special case for the analytical solution, which they presented. In addition, a correction scheme to modify the fin parameter in the case of fully wet fin surface condition was also presented.

On the other hand, Kundu [37] disagreed with the suggestion of Sharqawy and Zubair [29] that the dew point temperature of air may be taken as the fin tip temperature for calculating the psychrometric parameters in the study of fully wet fins. Instead, he asserted that local tip temperature should also be at hand for calculating psychrometric parameters in addition to dew point temperature of air. The author presented an iterative scheme to compute the fin tip temperature first and then the fin surface temperature. Incorporating this modification, the author thermally studied a new type of fin geometry called Annular Step Fin (ASF).

Coney *et al.* [38] studied heat and mass transfer mechanism in a layer adjacent to the condensate layer, with heat conduction through the fin. They predicted numerically the fin temperature distribution, condensate film thickness and fin efficiency for a fin in a laminar humid cross flow air arrangement. They observed that fin efficiency is substantially reduced when condensation takes place. Moreover they reported that air flow plays an important role in heat and mass transfer.

2.1.2 Fin Optimization

Optimization of fins can be described as a process through which we find the most advantageous dimensions of the fin in question for a required amount of heat transfer or if the dimensions of the fin is given, then determining the maximum possible heat transfer from the fin.

2.1.2. (a) Heat Transfer Only

For only conducting and convecting fins, the criterion for optimal fin was first reported by Schmidt [39]. Brown [11] derived an equation for a dry uniform annular fin relating the optimum dimensions to the heat transfer and thermal properties of the fin and the heat transfer coefficient between the fin and coolant. The results presented graphically were in terms of dimensionless parameters based on dry fin condition. Ullmann and Kalman [10] adopted the same approach as that of Ref. [11] and numerically determined the optimized dimension for four types of annular fins. Zubair *et al.* [40] determined the optimum dimensions of annular fins with power law profile in addition to temperature dependent thermal conductivity. They neglected the effect of curvature and heat transfer from the tip. They found that a circular fin of (quadratic) hyperbolic profile gives an optimum performance. In another study Khan [41] studied the optimum dimension of convecting-radiating circular fins with variable profiles. They incorporated variable thermal conductivity, variable heat transfer coefficient as well as radiation from the fin surface.

Campo *et al.* [42] addressed the problem of optimizing the hyperbolic annular fin by numerically solving it using two different method. One is with finite difference techniques using coarse mesh and the other is shooting method. Arslanturk [43] analytically obtained some correlation equations expressing the optimum heat transfer rate and optimum radii ratio of the fin in terms of the fin volume and Biot number. Annular fin arrays in heat sink is studied by Lai *et al.* [44]. These authors derived analytically a transcendental equation to find the optimal radius of annular fins. A semi-analytical technique was used by Kundu and Das [14] employing sector method for optimization of elliptic fins circumscribing circular tubes. The authors noted that when

there is restriction on both sides of the fin, rate of heat transfer from elliptic fins is significantly greater than concentric annular fins. Kumar *et al.* [45] described a method through which they obtained a preliminary approximate solution of hyperbolic profile annular fin using finite difference technique and then refining it with the help of C programme. Subsequently they obtained the optimum dimensions of the fin in question.

Sonn and Bar-Cohen [46] presented an analysis for the determination of an expression for the diameter of the least material cylindrical pin fin. This relation was based on dry fin condition. They briefly discussed and compared the optimum performance and the dimensional relations for cylindrical pin fin and longitudinal fin. They pointed out that due to the similarity in the governing equations of the two fins, sometimes error is made in finding the optimum pin fin diameter by using optimum fin parameter for the longitudinal fin. Almogbel and Bejan [47] optimized the cylindrical tree of pin fin in terms of maximizing the global conductance for a fixed total volume and fin material. Bahadur and Bar-Cohen [48] optimized thermally conductive polyphenylene sulphide (PPS) polymer pin fin heat sink. They calculated the coefficient of thermal performance for the PPS polymer and compared with conventional aluminum, and suggested the PPS as an alternative future material for heat sinks. Another study done by Chen *et al.* [49] concentrated on thermally optimizing a fully confined Pin Fin Heat Sink (PFHS) with the constraints of pressure drop, mass and space. A similar Response Surface Methodology was used by Chiang and Chang [50] for optimizing PFHS but dropping the first of the three constraints of [49].

Ignoring the length of arc assumption, Hanin and Campo [51] tried to obtained an exact analytical form of optimum profile for straight fin for minimizing the volume for a given

amount of heat transfer per unit depth. According to their calculation, circular arc turns out to be the optimum fin profile and one of the most salient finding was that the volume of optimal circular arc fin was on average 7 times smaller than that of Schmidt [39]. Kundu and Das [31] addressed the thermal analysis and optimization of straight fins. They suggested a generalized approach for optimizing longitudinal, radial and pin fin with straight taper. Their analysis did not include assumptions of Length of arc idealization and insulated tip. Moreover, a linear variation of convective heat transfer coefficient at the fin surface was considered. Using Frobenius expanding series, the generalized fin equation was analytically solved and a single expression was provided for the temperature distribution. A simplified solution for optimizing a rectangular fin with variable thermal conductivity was proposed by Bouaziz and Hanini [9].

2.1.2. (b) Heat and Mass Transfer

Sharqawy and Zubair [29] presented an analytical solution to find the optimum fin dimensions, for annular fin under fully wet condition with simultaneous heat and mass transfer, which gives the maximum heat transfer rate. The results shown were in same graphical format as a that of Ref. [11]. Temperature and humidity ratio differences were used as the driving forces for heat and mass transfer. Kundu [37] thermally optimized a new type of annular fin called Annular Step Fin (ASF) under fully wet conditions. The motivation behind this optimizing study was that the rate of heat conduction decreases from fin base to tip and annular disc fins might not be the best geometry for effective utilization of the fin material. The author found out that the heat transfer rate per unit volume of ASF is always higher in comparison to annular fin for the same design conditions.

Kundu [30] used Lagrange multiplier technique to analytically optimize the dimensions of straight taper wet fins. He stated that wet fins transfer more heat and has a larger aspect ratio then the dry fins for the same amount of the fin material. Another conclusion he drawn was that the optimum aspect ratio increases from rectangular to triangular cross section wet for the same fin volume and psychrometric conditions. Using the same Lagrange multiplier technique, Kundu and Das [31] presented the numerical optimization of different straight taper fins integrating linear relationship between temperature and specific humidity. From both of the above studies [30;31] one can find out either of two, optimum dimension or maximum heat transfer by keeping the other parameter constant. Razelos [52] presented a critical analysis on the work of [31]. He mentioned some of the irregularities and questioned the method of problem description. For example, the author pointed out some of the mistake in the nomenclature, keywords, incorrect equation, undefined parameters and so forth.

Analytical optimization of longitudinal and pin fins of uniform thickness was considered by Kundu [23] for fully as well as partially wet surface conditions. The results were shown in the form of design curves. In another study Sharqawy and Zubair [25] carried out an analytical study to find out the efficiency of fully wet straight fins of different configurations under simultaneous heat and mass transfer, in addition to optimization. Same driving forces was considered for heat and mass transfer as that in their previous study Ref. [29] .

2.2 Two Dimensional Fin Analysis

Analysis of fins in two-dimensional domain has received relatively much lesser attention if we compare to that of one-dimension. Utilizing the assumption of Murray and Gardner, Look and Kang [33] presented an optimization procedure for constant thickness rectangular profile fin for dissimilar heat transfer coefficient values at different surfaces of the fin as well as variable base temperature. Again Kang and Look [53] studied the heat transfer in two-dimensional trapezoidal fins for a variety of slopes, varying from triangular to rectangular. Unlike Ref. [33] the fin's base temperature was assumed constant as well as the convective heat transfer coefficients on different surfaces of the fin. The solution for heat transfer from the fin was obtained for Biot number values of less than equal to 0.1.

Trapezoidal fin was analyzed by Kang and Look [54] by four different methods. The four methods were one-dimensional and two-dimensional analytical solution, two-dimensional finite difference method and two-dimensional modified finite difference method. For the Biot number ranging from 0.01 to1 and non-dimensional length assumed, there results showed that all the four methods are within 3% of error with each other when calculating heat transfer from the fin. Moreover, one-dimensional analytical solution does not give accurate results for non-dimensional temperature when the Biot number is 1.0. There results also proved that two-dimensional modified finite difference method reduces the error considerably in comparison to two-dimensional finite difference method.

A similar work, in the sense of employing difference level of modeling dimension, has been done Liang *et al.*[55] . They investigated the wet fin efficiency of plate-fin-tube heat

exchanger using one-dimensional analytical model, one-dimensional numerical model as well as two-dimensional numerical model. The performance of the plate-fin-tube heat exchanger was studied for wide range of values of geometric parameters, air flow conditions and varying degree of relative humidity. In another effort Lin [56] presented two dimensional efficiency of elliptic fin under simultaneous heat and mass transfer conditions. There results obtained were for $r-\theta$ plane and function of air humidity, axis ratios and Biot numbers. They concluded that the conventional 1-D sector method overestimated the fin efficiency, although marginally. Furthermore, the elliptic fin performs well when compared to circular fins under both dry and wet conditions. Arslanturk [57] did a two-dimensional analytical study for annular fin of uniform thickness under thermally non-symmetric convective boundary conditions to find the optimum dimensions. Some of the interesting findings of the author are that, for non-insulated fin tip, on increasing the fin ratio (outer radius to inner radius ratio) first the minimum and then the maximum heat transfer occurs. Another finding of the work is that the fin ratio for optimum annular fin decreases as the convective heat transfer coefficient is increased on the tip of the fin.

Malekzadeh and Rahideh [58] did a two-dimensional non-linear transient study on annular fins of variable cross-section. They divided the heat transfer domain into sub-domain and discretized each domain by differential quadrature method. Assuming both convection as well as radiation from the fin surfaces, the effect of time and space dependent temperature and convective heat transfer coefficient as two different boundary conditions on the base of the fin is investigated.

Due to the advance in material manufacturing, new types of materials are available in the market, which are moldable to achieve different geometries, have high thermal conductivity and significantly lesser density, providing a window for lighter next generation fin materials. However, unlike traditional materials, aluminum and copper, they have anisotropic thermal conductivity, which translates to having different values of thermal conductivity in the fundamental directions. Bahadur and Bar-cohen [59] studied this aspect for heat transfer in cylindrical pin fins. They concluded that heat transfer from the fin increases with the increase in the radial Biot number (Biot number based on thermal conductivity in radial direction) and decreases with increase in the radial to axial thermal conductivity ratio and fin aspect ratio.

CHAPTER 3

ONE-DIMENSIONAL FIN ANALYSIS

In this chapter we have developed the annular fin model of variable geometric profile for fully as well as partially wet case. Section 3.2 and 3.3 deals with the mathematical analysis of fins. Whereas in section 3.4 we have reduced our general fin analysis to that of constant cross-section annular fin. In section 3.5 an analytical solution for a fully wet hyperbolic profile annular fin is developed. After that in section 3.6, the outline of our numerical solution procedure is explained followed by grid independence test in section 3.7. Finally, after validating the mathematical model, the results for fin efficiency and optimum dimensions are presented in sections 3.9 and 3.10 respectively.

3.1 Assumptions and Problem Statement

Similar to the classical work on extended surfaces, we have also considered certain assumptions for the one-dimensional analysis of the fins subjected to both heat and mass transfer in extended surfaces. The assumptions considered in the present study are:

- The thermal conductivity of the fin, heat transfer coefficient and latent heat of condensation of the water vapor are constant;
- The heat and mass transfer are under steady-state condition;
- The base temperature and it's specific humidity are always constant;
- The thermal resistance associated with the presence of thin water film due to condensation is small and may be neglected; and
- The effect of air pressure drop due to airflow is ignored.

These are some of the classical assumptions that have been used for the analysis of conducting-convecting finned surfaces. It may be noted that the assumption of negligible thermal resistance in the condensate film is applicable as demonstrated by Coney *et al.* [60;61]. For example, during the humidification process, the thickness of the condensate film is much smaller compared to the boundary layer thickness for forced convection. The rate of condensation increases with increase of both dry bulb temperature and relative humidity of the incoming air. However, the condensate film drains off the fin surface due to gravity as well as by forced airflow.

The problem statement can be presented as; we have an annular fin of general profile with base thickness of t_b^* and temperature T_b. The tip thickness could be zero or it could be the same as that of the fin base if the fin has constant thickness profile. The

temperature at tip is T_t which for fully wet situation, should be less than the dew point temperature of the ambient air at temperature T_a and relative humidity ω_a.The length of the fin is L. Figure 3-1 depicts the problem statement.

3.2 Fully Wet Fin Model

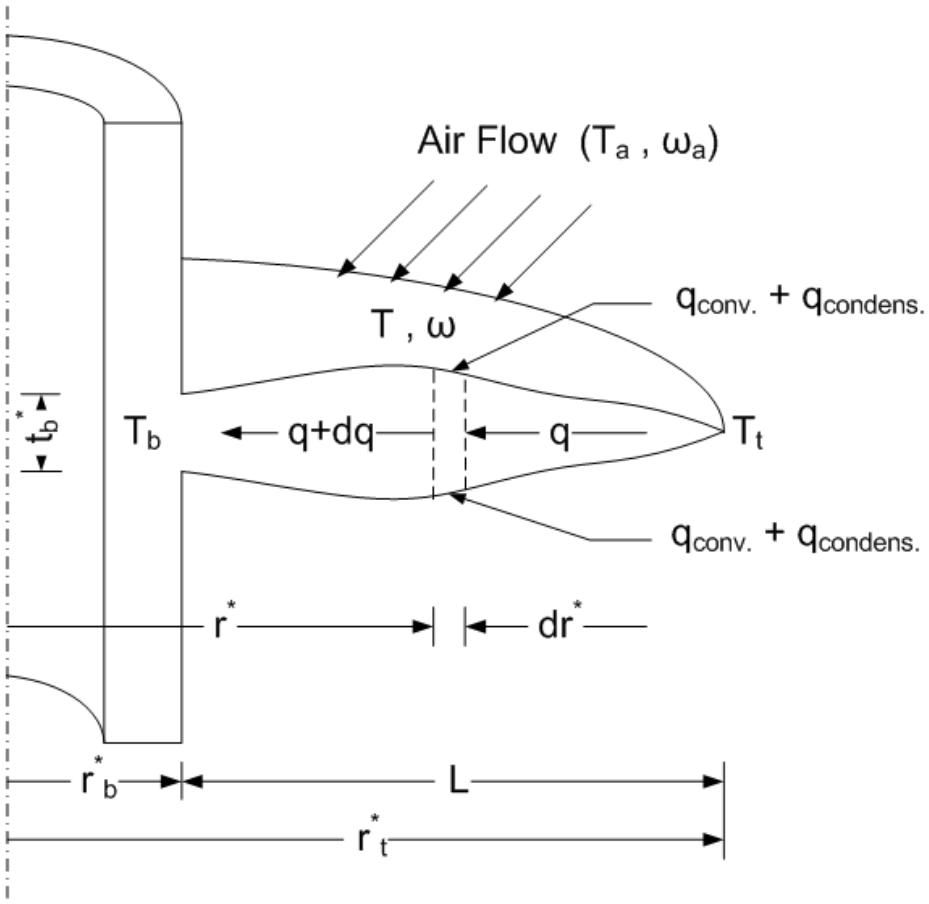

Figure 3-1 Schematic of a Completely Wet Annular Fin.

Applying the energy balance on the infinitesimal circular ring of width dr^*, which has an average thickness of t^*, at a radius of r^* from the center of the tube

$$\dot{E}_{in} = \dot{E}_{out} \tag{3.2.1}$$

$$q_{convection} + q_{condensation} + q_{r^*+dr^*} = q_{r^*} \tag{3.2.2}$$

Where q_{r^*} is the conduction heat transfer rate and from Fourier's law of heat transfer is given by

$$q_{r^*} = k\,A\frac{dT}{dr^*} \tag{3.2.3}$$

$$A = 2\pi r^*\, t(r^*) \tag{3.2.4}$$

$t(r^*)$ shows the variable thickness of the fin along its length

$$q_{r^*+dr^*} = q_{r^*} + \frac{\partial q_{r^*}}{\partial r^*}dr^* \tag{3.2.5}$$

$$q_{r^*+dr^*} = q_{r^*} + k\left[2\pi r^*\, t(r^*)\frac{d^2T}{dr^{*2}} + 2\pi\, t(r^*)\frac{dT}{dr^*} + 2\pi r^*\,\frac{dt(r^*)}{dr^*}\frac{dT}{dr^*}\right]dr^* \tag{3.2.6}$$

$$q_{convection.} = 2\,(2\,\pi\, r^*)\,h\,(T_a - T)\,dr^* \tag{3.2.7}$$

$$q_{condensation} = 2\left(2\pi r^* h_D\, i_{fg}(\omega_a - \omega)\,dr^*\right) \tag{3.2.8}$$

The heat and mass transfer coefficients are related by the Chilton-Colburn [62] analogy, and is represented as

$$\frac{h}{h_D} = C_p\, Le^{\frac{2}{3}} \tag{3.2.9}$$

Where

$$h_D\, i_{fg} = h\, B \tag{3.2.10}$$

And

$$B = \frac{i_{fg}}{C_p\, Le^{\frac{2}{3}}} \tag{3.2.11}$$

Substituting all the above terms in equation, (3.2.2) we get

$$k\left[2\pi r^* t(r^*)\frac{d^2T}{dr^{*2}} + 2\pi t(r^*)\frac{dT}{dr^*} + 2\pi r^* \frac{dt(r^*)}{dr^*}\frac{dT}{dr^*}\right]dr^* + 4\pi r^* h(T_a - T)\,dr^* + 4\pi r^* h_D\, i_{fg}\,(T_a - T)\,dr^* = 0 \tag{3.2.12}$$

Cancelling dr^* & dividing throughout by $2\pi r^* t(r^*)k$

$$\frac{d^2T}{dr^{*2}} + \frac{1}{r^*}\frac{dT}{dr^*} + \frac{1}{t(r^*)}\frac{dt(r^*)}{dr^*}\frac{dT}{dr^*} + \frac{2h}{k\,t(r^*)}(T_a - T) + \frac{2h_D}{k\,t(r^*)} i_{fg}\,(\omega_a - \omega) = 0 \tag{3.2.13}$$

Normalizing the above equation using the following relations

$$r = \frac{r^*}{L} \tag{3.2.14}$$

$$\theta = \frac{T_a - T}{T_a - T_b} \tag{3.2.15}$$

$$\Omega = \frac{\omega_a - \omega}{\omega_a - \omega_b} \tag{3.2.16}$$

$$t(r^*) = t^*_b \left(\frac{r^*_t - r^*}{L}\right)^n \tag{3.2.17}$$

$$t = \frac{t^*}{L} \tag{3.2.18}$$

Here n is the fin profile index,

$$\begin{aligned} &n = 0 \rightarrow \text{Constant thickness Profile} \\ &n = 1 \rightarrow \text{Triangular Profile} \\ &n = 0.5 \rightarrow \text{Convex parabolic profile} \\ &n = 2 \rightarrow \text{Concave parabolic profile} \end{aligned} \tag{3.2.19}$$

Substituting

$$Co = B\left(\frac{\omega_a - \omega_b}{T_a - T_b}\right) \tag{3.2.20}$$

and putting

$$m_0 = \sqrt{\frac{2h}{k\, t^*_b}} \tag{3.2.21}$$

We get

$$\frac{d^2\theta}{dr^2} + \left[\frac{1}{r} - \frac{n}{r_t - r}\right]\frac{d\theta}{dr} = \left(m_o L\right)^2 \left(\frac{1}{r_t - r}\right)^n \left[\theta + Co\Omega\right] \tag{3.2.22}$$

However, if we consider an annular fin of hyperbolic profile, then we will have another relation to govern the fin profile instead of equation (3.2.17) which is

$$t(r^*) = t^*_b(\frac{r_b^*}{r^*}) \tag{3.2.23}$$

And the equation (3.2.22) becomes

$$\frac{d^2\theta}{dr^2} = (m_o L)^2 \frac{r}{r_b}[\theta + Co\,\Omega] \tag{3.2.24}$$

One of the boundary condition for the cases in question was mentioned in the assumptions, i.e.

- At the base of the fin, the temperature and humidity ratio is constant.

$$\text{at } r = r_b,\ \theta = 1 \ \textit{and}\ \ \Omega = 1 \tag{3.2.25}$$

- The other boundary condition, which is at the fin tip, can be one of the two following

$$\text{at } r = r_t,\ \frac{d\theta}{dr} = 0 \qquad \text{for insulated tip} \tag{3.2.26}$$

or

$$\text{at } r = r_t,\ \frac{d\theta}{dr} = \psi (m_o L)^2 (\theta + Co\,\Omega) \qquad \text{for convective tip} \tag{3.2.27}$$

Where $\psi = (t_b^* / 2) / L$ is the fin aspect ratio.

For a given air condition, T_a and ω_a are known. Nevertheless, equation (3.2.22) is not closed because it still has two unknowns θ and Ω to be determined. To solve equation (3.2.22), an additional relation for Ω and θ is needed. To solve this problem, various

attempts have been made. Ref. [20] used a linear relationship between $(\omega_a - \omega)$ and $(T_a - T)$ as given below

$$(\omega_a - \omega) = C\,(T_a - T) \tag{3.2.28}$$

where C is a constant. Although this assumption simplifies the solution of the differential equation, it does not represents the physical situation. Ref. [22] solved equation (3.2.22) by making use of the fact that the air near the fin surface is saturated and using a linear relation between ω and T. However we know from the psychrometric correlations of an air-water vapor mixture given by Hyland and Wexler [63], that there is no such linear relation between the two, rather the humidity ratio ω of the saturated air on the wet surface is known as a function of the local fin temperature T and the atmospheric pressure.

The heat transfer to the fin is the summation of heat transferred by convection and condensation, which is given by the following relation for an infinitesimal area.

$$q_{fin} = 2\left(2\pi r^* dr^*\right) h\left(T_a - T\right) + 2\left(2\pi r^* dr^*\right) h_D\, i_{fg}\left(\omega_a - \omega\right) \tag{3.2.29}$$

We define the dimensionless heat transferred to the infinitesimal fin surface, dQ as

$$dQ = \frac{2\left(2\pi r^* dr^*\right) h\left(T_a - T\right) + 2\left(2\pi r^* dr^*\right) h_D\, i_{fg}\left(\omega_a - \omega\right)}{2\pi r_b^{\,*}\, k\left(T_a - T_b\right)} \tag{3.2.30}$$

When we integrate for the whole fin the equation simplifies to

$$Q = 2\psi\left(m_0\, L\right)^2 \left(R - 1\right) \int_{r_b}^{r_t} \left(\theta + Co\ \Omega\right) r\, dr \tag{3.2.31}$$

Here R denotes the radius ratio of tip to base of the fin. The maximum heat transfer rate $q_{\max}$ would exist if the entire fin surface were at the fin base temperature and base humidity ratio and can be written as:

$$Q^*_{\max} = 2\left[\pi\left(r_t^{*2} - r_b^{*2}\right)\right]h\left(T_a - T_b\right) + 2\left[\pi\left(r_t^{*2} - r_b^{*2}\right)\right]h_D\, i_{fg}\left(\omega_a - \omega_b\right) \quad (3.2.32)$$

Dividing by the same denominator as of equation (3.2.30) to make it dimensionless we have

$$Q_{\max} = \frac{2\left[\pi\left(r_t^{*2} - r_b^{*2}\right)\right]h\left(T_a - T_b\right) + 2\left[\pi\left(r_t^{*2} - r_b^{*2}\right)\right]h_D\, i_{fg}\left(\omega_a - \omega_b\right)}{2\pi\, r_b^{*}\, k\left(T_a - T_b\right)} \quad (3.2.33)$$

Or upon substitution of various parameters

$$Q_{\max} = \psi\left(m_0\, L\right)^2\left(R+1\right)\left(1+Co\right) \quad (3.2.34)$$

Introducing fin efficiency as the ratio of the actual total heat transfer rate to the maximum total heat transfer, from equations (3.2.31) and (3.2.34) we get

$$\eta = \frac{Q}{Q_{\max}} = \frac{2\left(R-1\right)\int_{r_b}^{r_t}\left(\theta + Co\,\Omega\right) r\, dr}{\left(R+1\right)\left(1+Co\right)} \quad (3.2.35)$$

In other words, we can describe the above derivation for the total heat transfer from/ to fin as; for a fin subjected to combined heat and mass transfer, the total heat transfer comprises both the sensible as well as the latent heat transfer caused by the temperature difference and mass transfer, respectively. Moreover, the amount of heat transferred, Q, from the air to the fin surface is a function of the temperature and humidity ratio

differences between the air and fin surface. Furthermore, the mathematical expression for the efficiency of a fully wet fin given by equation (3.2.35) depends on the distribution of temperature as well as humidity ratio on the fin surface.

3.3 Partially Wet Fin Model

A partially wet fin is encountered when the fin base temperature is lower but the fin tip temperature is higher than the dew point of the air. Under such situation, there is a radius, $r = r_\zeta$, where the surface temperature equals the dew point of the air, i.e. $T\left(r_\zeta\right) = T_{dew}$. The fin is then divided into two regions: a wet region for $r_b \le r \le r_\zeta$, with the surface temperature lower than T_{dew} and a dry region from $r_\zeta \le r \le r_t$, with the surface temperature higher than T_{dew} (see Figure 3-2). In this regard, separate governing differential equations must be written for each region.

For $r_b \le r \le r_\zeta$

$$\frac{d^2\theta}{dr^2} + \left[\frac{1}{r} - \frac{n}{r_t - r}\right]\frac{d\theta}{dr} = \left(m_o\, L\right)^2 \left(\frac{1}{r_t - r}\right)^n \left[\theta + Co\,\Omega\right] \tag{3.3.1}$$

$$\frac{d^2\theta}{dr^2} = \left(m_o L\right)^2 \frac{r}{r_b}\left[\theta + Co\,\Omega\right] \qquad \text{Hyperbolic Profile} \tag{3.3.2}$$

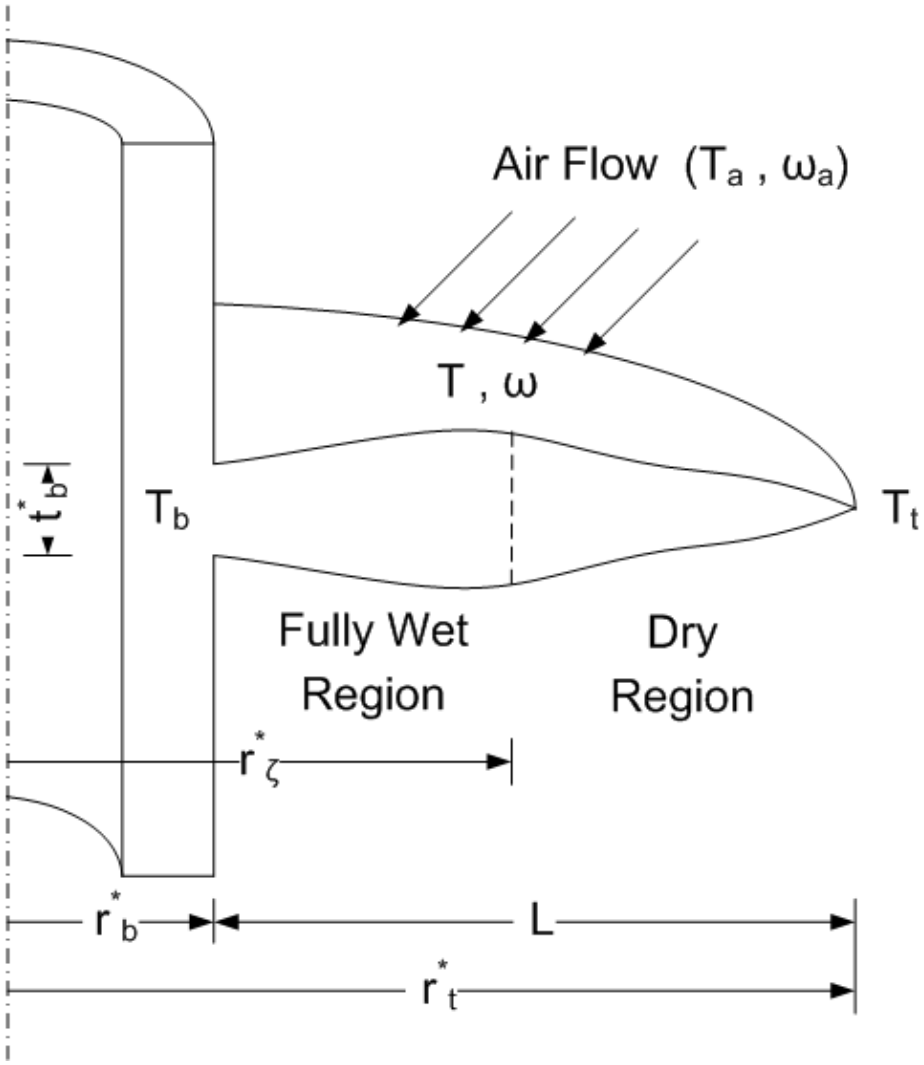

Figure 3-2 Schematic of a Partially Wet Fin

And for $r_\zeta \le r \le r_t$

$$\frac{d^2\theta}{dr^2}+\left[\frac{1}{r}-\frac{n}{r_t-r}\right]\frac{d\theta}{dr}=\left(m_o\,L\right)^2\left(\frac{1}{r_t-r}\right)^n\theta \tag{3.3.3}$$

$$\frac{d^2\theta}{dr^2}=\left(m_oL\right)^2\frac{r}{r_b}[\theta] \qquad \text{Hyperbolic Profile} \tag{3.3.4}$$

The boundary conditions are as follows,

- At fin base

$$\text{at } r = r_b, \quad \theta = 1, \quad \Omega = 1 \tag{3.3.5}$$

- At the section separating the fully wet and fully dry region

$$\text{at } r = r_\zeta \ , \ \theta = \theta_{dew} \tag{3.3.6}$$

- For the tip, again we can have either insulation or convection, given by the following

$$\text{at } r = r_t \ , \ \frac{d\theta}{dr} = 0 \tag{3.3.7}$$

or

$$\text{at } r = r_t \ , \frac{d\theta}{dr} = -\left(m_o L\right)^2 \psi \theta \tag{3.3.8}$$

The actual heat transferred to the infinitesimal wet fin surface, $q_{wet\ fin}$ is,

$$q_{wet\ fin} = 2\left(2\pi r^* dr^*\right) h\left(T_a - T\right) + 2\left(2\pi r^* dr^*\right) h_D \, i_{fg} \left(\omega_a - \omega\right) \tag{3.3.9}$$

While for dry fin surface is reduces to

$$q_{dry\ fin} = 2\left(2\pi r^* dr^*\right) h\left(T_a - T\right) \tag{3.3.10}$$

So the total heat transferred to a partially wet fin will be

$$Q^*_{fin} = \int_{r_b}^{r_\zeta} dq_{wet\ fin} + \int_{r_\zeta}^{r_t} dq_{dry\ fin} \tag{3.3.11}$$

Now we make it dimensionless as follows

$$Q = \frac{\int_{r_b}^{r_\zeta} dq_{wet\ fin} + \int_{r_\zeta}^{r_t} dq_{dry\ fin}}{2\pi\, r_b^{\,*}\, k\left(T_a - T_b\right)} \tag{3.3.12}$$

Finally it becomes,

$$Q = 2\left(m_0\, L\right)^2 \psi \left(R-1\right)\left[\int_{r_b}^{r_\zeta} \left(\theta + Co\ \Omega\right) r\, dr + \int_{r_\zeta}^{r_t} \theta\, r\, dr\right] \tag{3.3.13}$$

The maximum heat transfer rate $Q_{\max}$ can be calculated using the same equation as for fully wet fin i.e. equation (3.2.34),. Substituting the expressions for Q and $Q_{\max}$ into the fin efficiency equation, we get

$$\eta = \frac{2\left(R-1\right)\left[\int_{r_b}^{r_\zeta} \left(\theta + Co\ \Omega\right) r\, dr + \int_{r_\zeta}^{r_t} \theta\, r\, dr\right]}{\left(R+1\right)\left[1+Co\right]} \tag{3.4.1}$$

3.4 Analytical Solution for Fully Wet Constant Thickness Annular Fin

Just as cross check of our mathematical model's validity, we substitute the profile index, $n = 0$, and try to obtain an analytical solution to compare with the available results in the literature. On doing so, the equation (3.2.22) reduces to

$$\frac{d^2\theta}{dr^2}+\frac{1}{r}\frac{d\theta}{dr}=\left(m_oL\right)^2\left[\theta+Co\,\Omega\right] \tag{3.4.2}$$

Using the definitions of θ, r, Co and Ω

$$\frac{L^2}{\left(T_a-T_b\right)}\left[\frac{d^2(T_a-T)}{dr^{*2}}+\frac{1}{r^*}\frac{d(T_a-T)}{dr^*}\right]=\left(m_oL\right)^2\left[\frac{T_a-T}{T_a-T_b}+B\frac{\left(\omega_a-\omega_b\right)}{\left(T_a-T_b\right)}\frac{\left(\omega_a-\omega\right)}{\left(\omega_a-\omega_b\right)}\right] \tag{3.4.3}$$

Cancelling and rearranging terms

$$\frac{d^2\left(T_a-T\right)}{dr^{*2}}+\frac{1}{r^*}\frac{d\left(T_a-T\right)}{dr^*}=m_o{}^2\left[\left(T_a-T\right)+B\left(\omega_a-\omega\right)\right] \tag{3.4.4}$$

Finally we get

$$\frac{d^2\theta^*}{dr^{*2}}+\frac{1}{r^*}\frac{d\theta^*}{dr^*}-m_0{}^2\theta^*-m_0{}^2B(\omega_a-\omega)=0 \tag{3.4.5}$$

Here

$$\theta^*=T_a-T \tag{3.4.6}$$

An additional equation to solve equation (3.4.5) as suggested by Ref. [29] is

$$\omega=a_2+b_2T \tag{3.4.7}$$

The constants a_2 and b_2 are defined as follows

$$a_2=\omega_b-\frac{\omega_{dew}-\omega_b}{T_{dew}-T_b}T_b \tag{3.4.8}$$

$$b_2=\frac{\omega_{dew}-\omega_b}{T_{dew}-T_b} \tag{3.4.9}$$

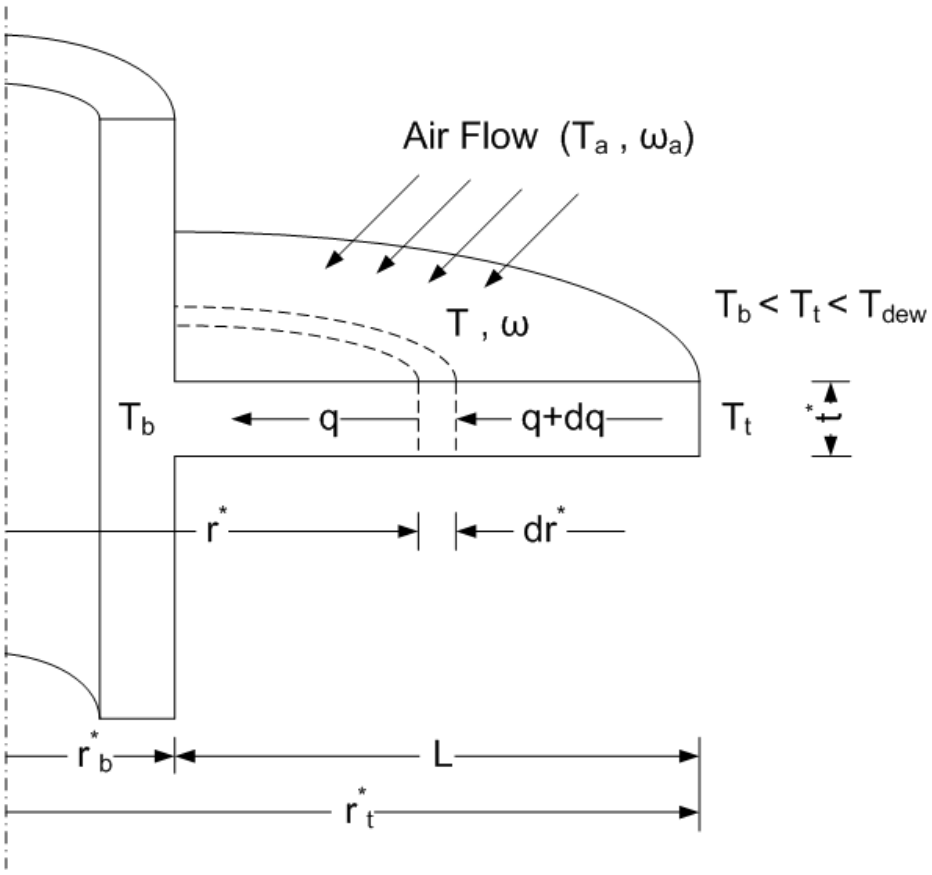

Figure 3-3 Annular Fin of Uniform Thickness (n=0)

Substituting equation (3.4.7) into equation (3.4.5)

$$\frac{d^2\theta^*}{dr^{*2}} + \frac{1}{r^*}\frac{d\theta^*}{dr^*} - m^2\theta^* = m_0{}^2 B\, D \tag{3.4.10}$$

Where

$$m^2 = m_0{}^2(1 + b_2 B) \tag{3.4.11}$$

$$D = \omega_a - a_2 - b_2 T_a \tag{3.4.12}$$

The boundary conditions used here are of that of the insulted tip

$$\theta^* = \theta_b{}^* = T_a - T_b \qquad \text{at} \quad r^* = r_b{}^* \tag{3.4.13}$$

$$\frac{d\theta^*}{dr^*} = 0 \qquad \text{at} \quad r^* = r_t^* \tag{3.4.14}$$

The solution of equation (3.4.10) subjected to the above boundary conditions is

$$\frac{\theta^* + \theta_p{}^*}{\theta_b{}^* + \theta_p{}^*} = \frac{I_0(mr^*)K_1(mr_t^*) + I_1(mr_t^*)K_0(mr^*)}{I_0(mr_b{}^*)K_1(mr_t^*) + I_1(mr_t^*)K_0(mr_b{}^*)} \tag{3.4.15}$$

In the above equation

$$\theta_p{}^* = \frac{B\,D}{(1 + b_2 B)} \tag{3.4.16}$$

Now to calculate the actual rate of heat transferred through the fin base is

$$Q^*{}_b = kA\left[\frac{dT}{dr^*}\right]_{r^* = r_b{}^*} \tag{3.4.17}$$

This gives,

$$Q^*{}_b = 2\pi\, r_b{}^*\, t^*\, k\, (\theta_b{}^* + \theta_p{}^*)\, m\left[\frac{I_1(mr_t^*)K_1(mr_b{}^*) - I_1(mr_b{}^*)K_1(mr_t^*)}{I_1(mr_t^*)K_0(mr_b{}^*) + I_0(mr_b{}^*)K_1(mr_t^*)}\right] \tag{3.4.18}$$

The relation presented in equation (3.4.15) and (3.4.18) are in accordance of the results of Ref. [29] and a similar approach is adopted for efficiency and is as follows. The maximum heat transfer rate, $Q^*{}_{\max}$ would be

$$Q^*{}_{\max} = \pi(r_t^{*2} - r_b^{*2})\, t^*\, k\, m^2\, (\theta_b{}^* + \theta_p{}^*) \tag{3.4.19}$$

Hence, the following relation gives the efficiency

$$\eta = \frac{2r_b^*}{m(r_t^{*2} - r_b^{*2})}\left[\frac{I_1(mr_t^*)K_1(mr_b^*) - I_1(mr_b^*)K_1(mr_t^*)}{I_1(mr_t^*)K_0(mr_b^*) + I_0(mr_b^*)K_1(mr_t^*)}\right] \tag{3.4.20}$$

As the authors [29] mentioned, the above expression, which is for fully wet fin is the same as the fully dry fin Ref. [11] except that the fin parameter m is modified by multiplying m_0 by $(1+b_2B)$.

In the following section 3.5, a similar linear model is assumed to obtain an analytical solution for hyperbolic fin.

3.5 Analytical Solution for Fully Wet Hyperbolic Profile Annular Fin

Using the same assumptions mentioned in section 3.1, we apply the conservation of energy on an infinitesimal ring of hyperbolic profile annular fin. Upon doing so we end up in equation (3.2.24) which can be restructured and may be written as

$$\frac{d^2\theta^*}{dr^{*2}} = m_o^{\,2}\frac{r^*}{r_b^*}\left[\theta^* + B(\omega_a - \omega)\right] \tag{3.5.1}$$

Now we need a relation between the temperature difference $\theta^{'}$ and humidity ratio $\omega$to close the above problem. We will use the same relation as that of Ref. [29] and is mentioned in equation (3.4.7). Inserting this very relation in equation (3.5.1) and defining

$$M_0^{\,2} = \left(\frac{m_0^{\,2}}{r_b^*}\right) \tag{3.5.2}$$

$$M^2 = M_0^{\,2}(1+b_2 B) \tag{3.5.3}$$

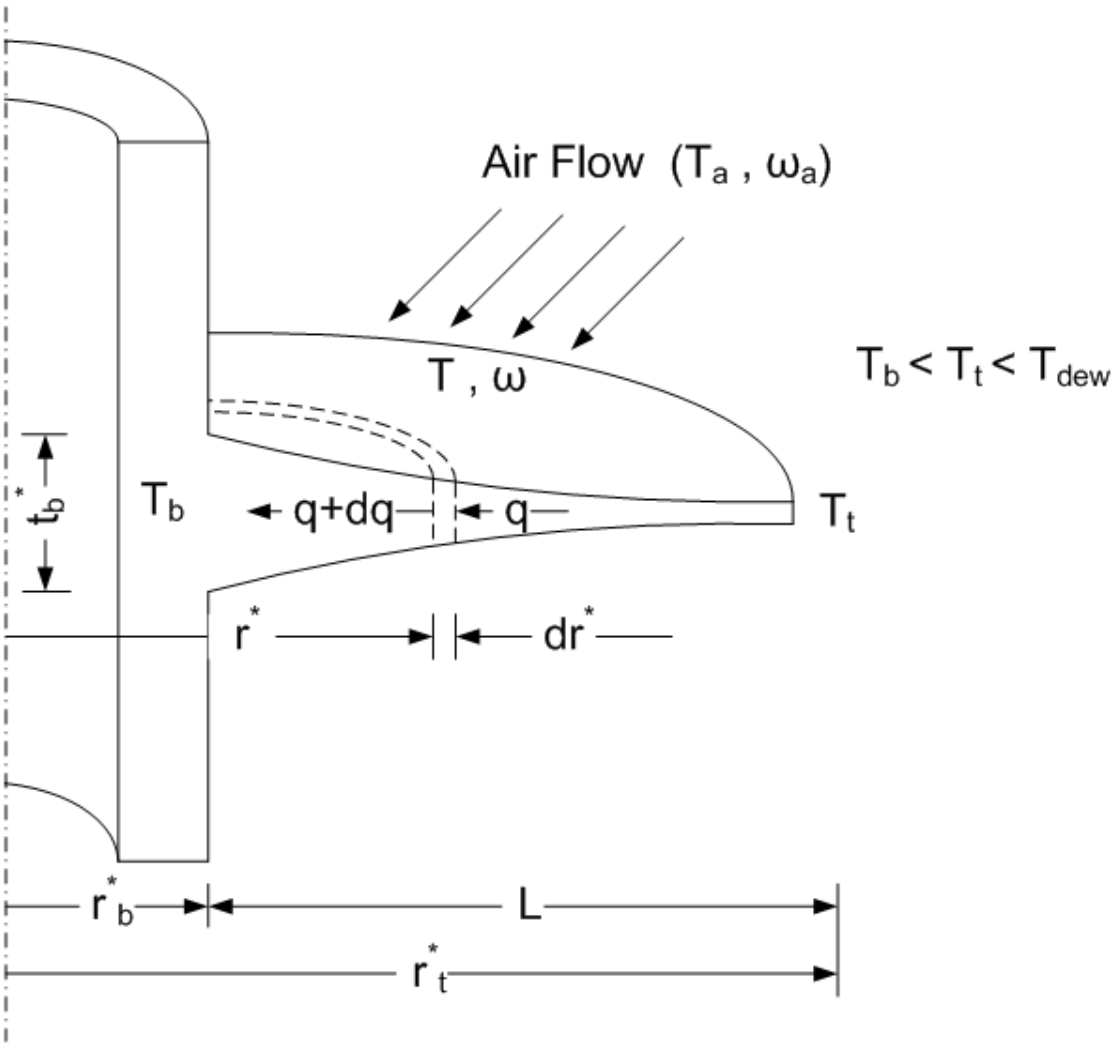

Figure 3-4 Schematic of a Completely Wet Hyperbolic Annular Fin.

We get

$$\frac{d^2\theta^*}{dr^{*2}} - M^2 r^* \theta^* = M_0{}^2 r^* B\left(\omega_a - \omega\right) \tag{3.5.4}$$

The boundary condition are same as that mentioned in equation (3.4.13) and (3.4.14). The solution is presented in the form of Airy function.

$$\frac{\theta^* + \theta_p^*}{\theta_b^* + \theta_p^*} = \left[\frac{Ai'\left(M^{\frac{2}{3}} r_t^*\right) Bi'\left(M^{\frac{2}{3}} r^*\right) - Ai\left(M^{\frac{2}{3}} r^*\right) Bi'\left(M^{\frac{2}{3}} r_t^*\right)}{Ai'\left(M^{\frac{2}{3}} r_t^*\right) Bi'\left(M^{\frac{2}{3}} r_b^*\right) - Ai\left(M^{\frac{2}{3}} r_b^*\right) Bi'\left(M^{\frac{2}{3}} r_t^*\right)} \right] \tag{3.5.5}$$

It is important to note that Airy functions are related to modified Bessel functions of the fractional order by the following equations (Abramowitz and Stegun [64])

$$Ai(X) = \frac{1}{\pi}\sqrt{\frac{1}{3}X}\, K_{1/3}\left(\frac{2}{3}X^{3/2}\right) \tag{3.5.6}$$

$$Bi(X) = \sqrt{\frac{1}{3}X}\left[I_{1/3}\left(\frac{2}{3}X^{3/2}\right) + I_{-1/3}\left(\frac{2}{3}X^{3/2}\right)\right] \tag{3.5.7}$$

Ai' and Bi' are their respective derivatives.

The actual rate of heat transfer from the fin is given by

$$Q^*_b = kA_b \left.\frac{dT}{dr^*}\right|_{r^*=r_b^*} = k\left(2\pi r_b^*\, t_b^*\right) \left.\frac{d\theta'}{dr^*}\right|_{r^*=r_b^*} \tag{3.5.8}$$

Which gives

$$Q^*_b = k\, A_b \left(\theta_b^* + \theta_p^*\right) M^{2/3} \left[\frac{-Ai'\left(M^{\frac{2}{3}} r_t^*\right) Bi'\left(M^{\frac{2}{3}} r_b^*\right) + Ai'\left(M^{\frac{2}{3}} r_b^*\right) Bi'\left(M^{\frac{2}{3}} r_t^*\right)}{Ai'\left(M^{\frac{2}{3}} r_t^*\right) Bi'\left(M^{\frac{2}{3}} r_b^*\right) - Ai\left(M^{\frac{2}{3}} r_b^*\right) Bi'\left(M^{\frac{2}{3}} r_t^*\right)} \right] \tag{3.5.9}$$

And the maximum heat transfer, which is the heat transfer from the fin surface if the entire fin is at the base temperature and base humidity ratio, is related as

$$Q^*_{\max} = m_0{}^2\, k\, t_b{}^*\, \pi\left(r_t{}^{*2} - r_b{}^{*2}\right)\left(1+b_2\, B\right)\left(\theta_b{}^* + \theta_p{}^*\right) \tag{3.5.10}$$

The fin efficiency is, as we know defined by

$$\eta = \frac{Q^*_b}{Q^*_{\max}} \tag{3.5.11}$$

Which yields

$$\eta = \frac{2M^{-4/3}}{\left(r_t{}^{*2} - r_b{}^{*2}\right)}\left[\frac{-Ai'\left(M^{\frac{2}{3}} r_t^*\right)Bi'\left(M^{\frac{2}{3}} r_b^*\right) + Ai'\left(M^{\frac{2}{3}} r_b^*\right)Bi'\left(M^{\frac{2}{3}} r_t^*\right)}{Ai'\left(M^{\frac{2}{3}} r_t^*\right)Bi'\left(M^{\frac{2}{3}} r_b^*\right) - Ai\left(M^{\frac{2}{3}} r_b^*\right)Bi'\left(M^{\frac{2}{3}} r_t^*\right)}\right] \tag{3.5.12}$$

3.6 Numerical Solution Procedure

The mathematical model developed; let it be of fully wet fin or partially wet fin, with the appropriate boundary condition, is written in finite difference form and solved using either successive over-relaxation (SOR) or under relaxation method as per need. SOR method is drafted by Patrick [65]. The convergence criterion used is of the order of $1X10^{-06}$. Since the analytical heat and mass transfer results are not available for triangular, concave parabolic and convex parabolic profile annular fins, we will compare with the one that is available i.e. rectangular profile fin and proceed for the other types. For the case of hyperbolic profile, we will compare our numerical results with the analytical ones obtained in this work. However, before moving to that part, we need to achieve the grid independence.

3.7 Grid Independence

Grid independence is described as the improvement in the results upon successive reduction in the cell size. As the grid is refined, grid cells become smaller, the number of cells in the domain grows, and the spatial discretization error asymptotically approaches zero (excluding the round-off error).

For our case, we have discretized the one-dimensional fin domain into 51 nodes as the starting point, there after increasing it up until 111 nodes in the step interval of 10 nodes. The grid independence test results for fin efficiency is shown in Table 3-1 and is plotted in Figure 3-5. From the figure and table, we can say that 101 nodes provide satisfactory accurate results without consuming unacceptable amount of time.

Table 3-1 Grid independence test data for fin efficiency for constant thickness annular fin

Case	Number of Nodes	Fin Efficiency
A	51	0.8257
B	61	0.8253
C	71	0.8251
D	81	0.8249
E	91	0.8247
F	101	0.8246
G	111	0.8245
Analytical solution Ref. [28]	-	0.8017

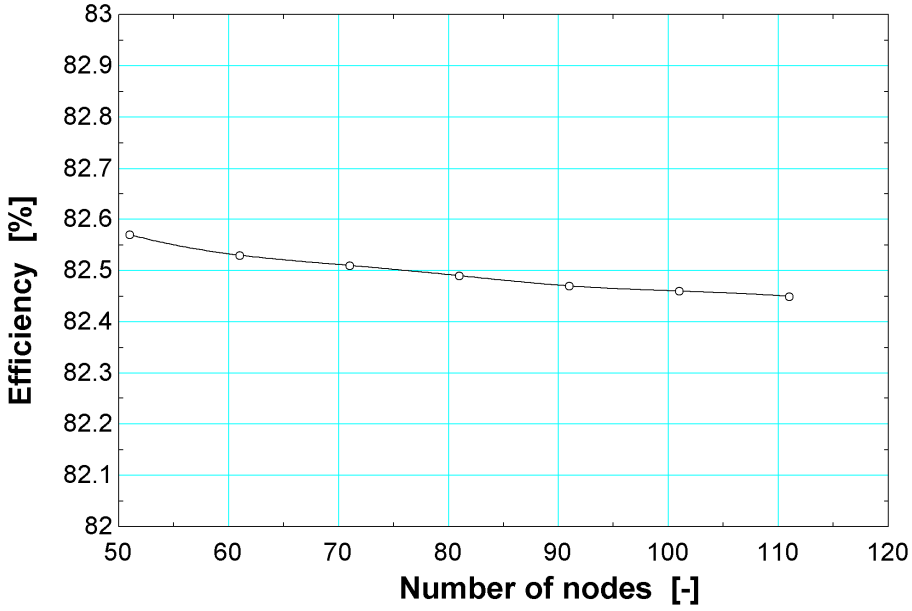

Figure 3-5 Grid independence test for fin efficiency

3.8 Validation

For validating the developed model, we compare our result with those available in the literature. Figure 3-6 shows the comparison of the dry fin efficiency result of the present work with that of Ref. [11]. As it is visible from the picture, it is a perfect match. The relative humidity of air, radius ratio of the fin and other ambient conditions are mentioned in the figure itself. The comparison of the results for simultaneous heat and mass transfer is shown in Figure 3-7. The numerical results with the present model are compared with the approximate linear model used by Ref. [29]. The figure clearly shows that the present model always gives a higher efficiency at any fin-parameter ($m_0 L$) value.

In the light of the above comparisons we can safely say that our mathematical modeling of an annular fin of general profile is acceptable, in fact better than that of Ref. [29], since

we are using actual psychrometric relation instead of any linear relation between humidity ratio and surface temperature.

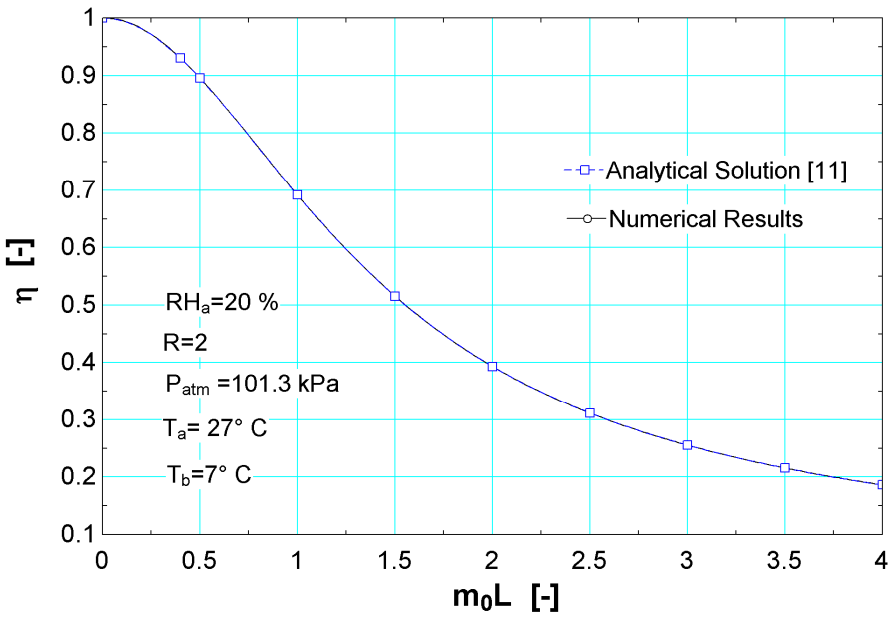

Figure 3-6 Comparison of fin efficiency for dry case

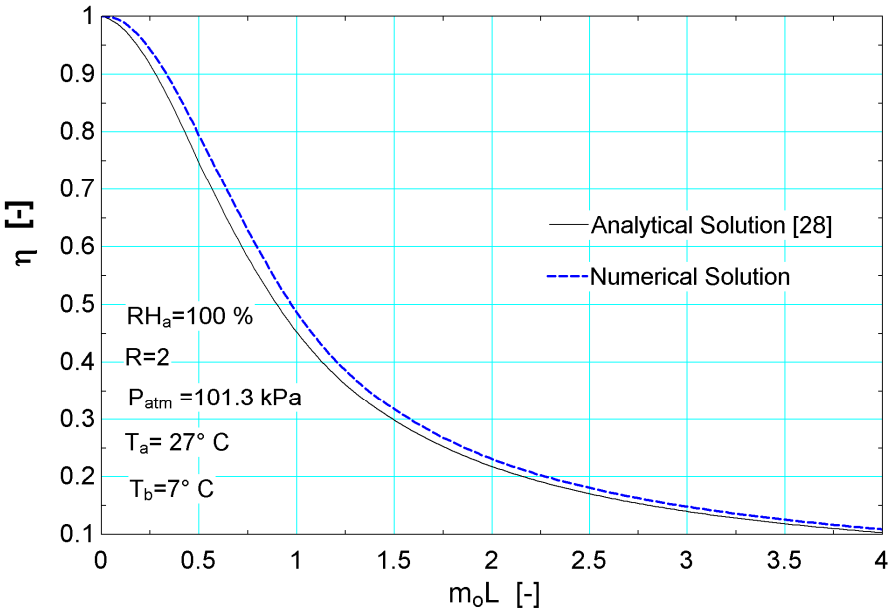

Figure 3-7 Comparison of fin efficiency for wet case

3.9 Fin Efficiency Results and Discussion

In the following sections, numerical results for temperature distribution, fin efficiency (η) and effect of difference of temperature between ambient and base temperature are presented for various thermo-geometric values.

3.9.1 Rectangular profile annular fin

Figure 3-8 demonstrate the temperature distribution over the rectangular profile fin for insulated as well convective tip condition under various relative humidity. The radius ratio R was assumed to be 2 and the fin parameter $m_0 L$ was taken as 1.5. These input values were randomly chosen and were used along with ambient temperature T_a of 27 ℃ and constant base temperature T_b of 7 ℃. Atmospheric pressure was assumed in all calculation unless otherwise mentioned.

For the case when the relative humidity (RH_a) is 0.2 i.e. 20%, the fin is completely dry which means that the entire surface temperature is higher than the dew point temperature of the ambient air at the above mentioned conditions. As we increase the relative humidity, the fin temperature starts reducing and a situation comes when the fin base temperature is lower but the tip temperature is higher than the dew point temperature. This leads to partial wet condition and is visible when the RH_a values are 40% and 60%. It is important to note that at relative humidity of 40%, the curve seems to overlap that of 20% relative humidity. The reason is that, although condensation has started on the fin surface however, at low relative humidity values as that of 40%, the result of this small amount of condensation is not appreciable so the difference on temperature profile is also

not very significant. Upon further increase in relative humidity, the whole fin surface temperature drops below dew point and the fin is fully covered by a thin water film. Thus we see that at any value of X, which represent the non-dimensional distance of the fin starting from the base as 0 and 1 for fin tip, the surface non-dimensional temperature becomes less upon increasing RH_a values.

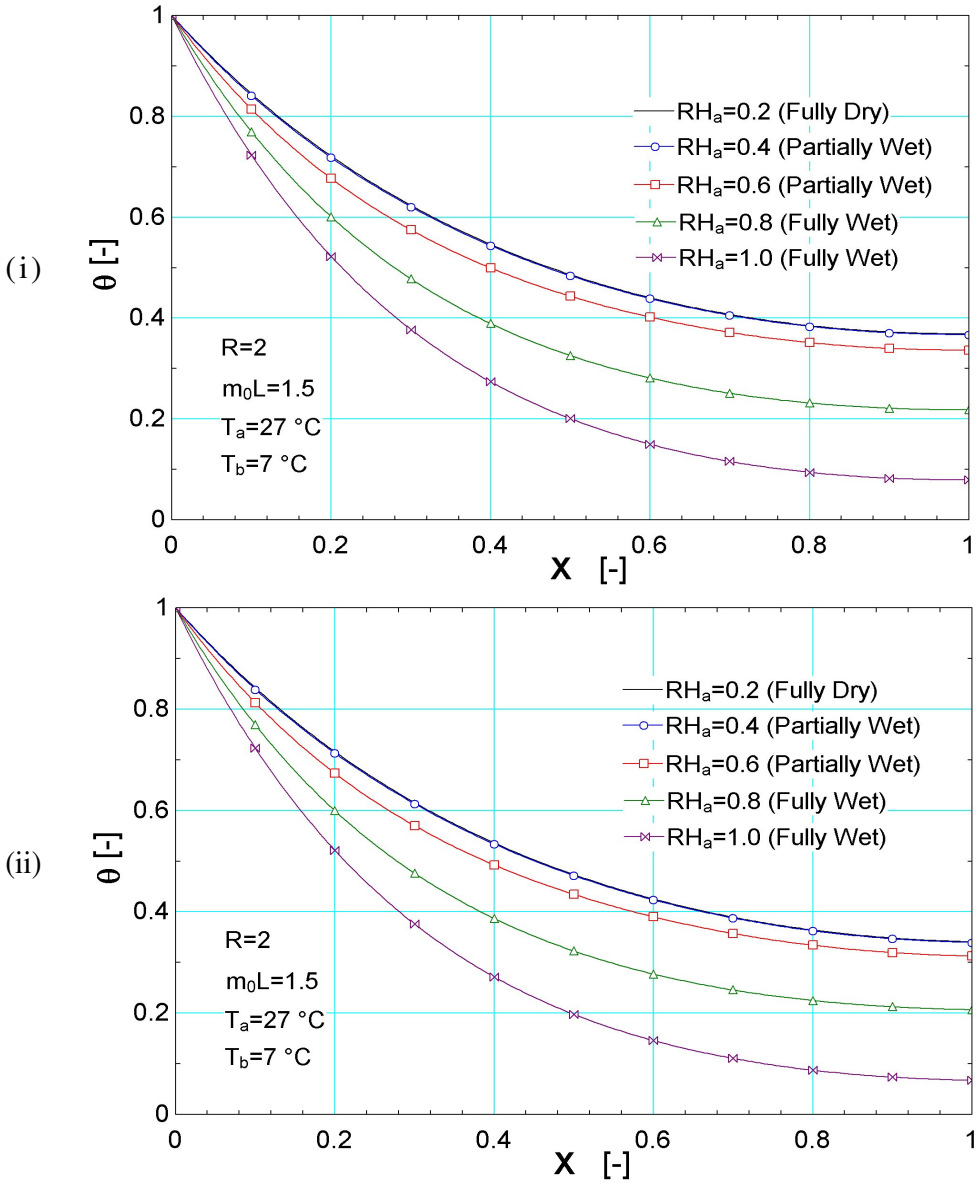

Figure 3-8 Non-dimensional temperature distribution for rectangular profile fin: (i) Insulated tip (ii) convective tip (ψ =0.05)

The effect of fin parameter, which represents conduction resistance to convection resistance, on the fin efficiency for different radius ratio values is plotted in Figure 3-9. The value of fin parameter at which the fin becomes partially wet is mentioned on the figure itself. It is observed that as the $m_0 L$ value is varied from zero to four, the fin efficiency starts reducing, and the reason being the introduction of more fin resistance because of additional fin material. At fin parameter equal to zero, the fin efficiency is 100%, which implies that there is no thermal resistance or no fin material at all. Another possibility might be that convective heat transfer coefficient to thermal conductivity ratio has approached zero and everywhere on the fin surface, the temperature is equal to the base temperature. It is also notable that there is a steep drop in the efficiency for $0 < m_0 L < 2$ after which the slope of the curve decreases and is almost zero at $m_0 L$of about four. This can be explained by the fact that as more fin material is attached, more resistance to heat flow occurs thereby reducing the fin efficiency. Upon further increase in the fin parameter, the effect of the reducing convection resistance becomes visible in the sense that the fin efficiency starts to normalize. The figure also points out that the difference in the fin efficiency between dry fin and partially wet fin is appreciable. Whereas the same difference between partially wet and fully wet condition is not there. The major reason for the difference in efficiency between relative humidity of 20% and 40%, despite the closeness in temperature distribution, is the increase in maximum heat transfer quantity. That is, the actual heat transfer difference for the two may not be very much but due to the appreciable change in the denominator, the efficiency for two conditions differs significantly.

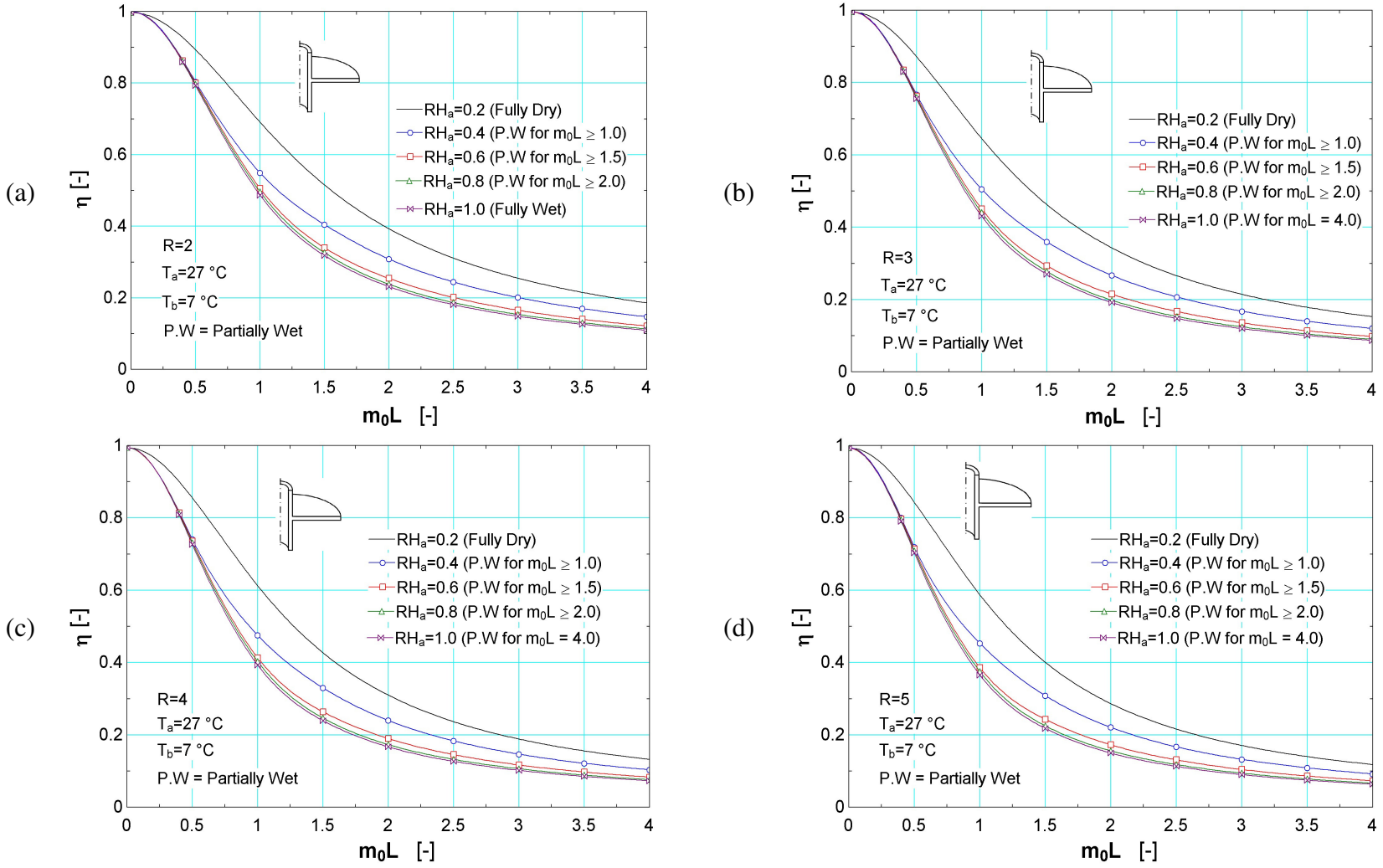

Figure 3-9 Effect of fin parameter on fin efficiency for rectangular profile fin at various air relative humidity:

(a) R=2 (b) R=3 (c) R=4 (d) R=5

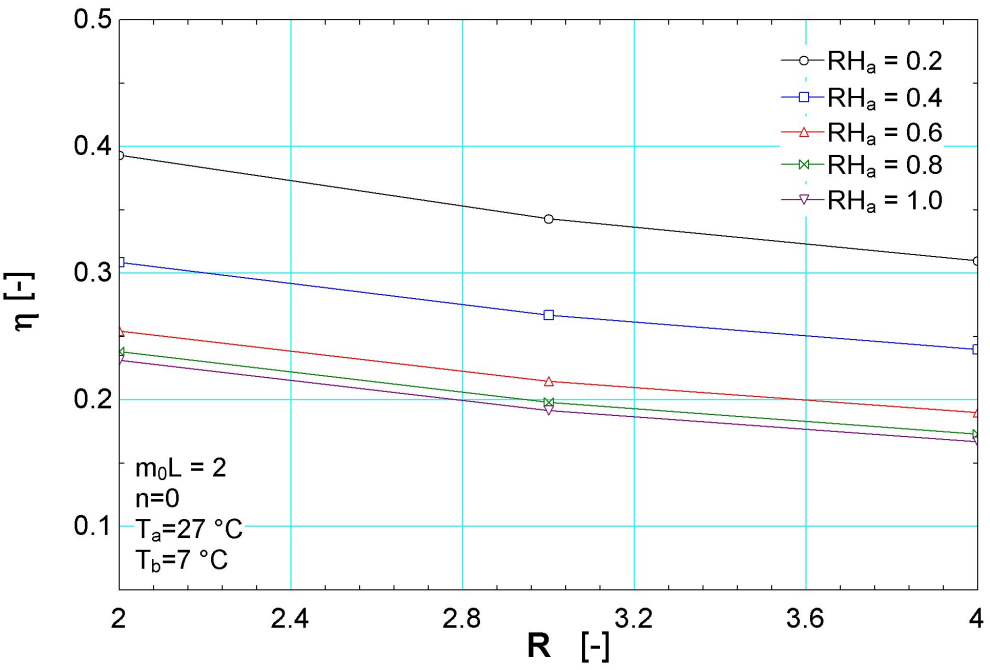

Figure 3-10 Effect of radius ratio on the fin efficiency for rectangular profile fin

Figure 3-10 shows the effect of radius ratio on the fin efficiency for various relative humidities, fin parameter of two and constant ambient and base temperatures. That is, if the tip radius is increased with respect to the base radius, how it is going to affect the fin performance. The curves are almost a straight line with a negative slope. This reduction in efficiency is due to increase in thermal resistance, as explained before, in the form of increasing fin length. It must be noted that Figure 3-9 was meant to show the effect of relative humidity on fin efficiency however here we are interested in finding the consequence of radius ratio on efficiency.

In all the previous results obtained for rectangular fin profile, the ambient and base temperatures were fixed at 27℃ and 7℃. The outcome of difference in ambient temperature T_a and base temperature T_b is shown in Figure 3-11 for three base

conditions i.e. T_b equal to 0℃, 5℃ and 10℃. For each base temperature, the ambient temperature is varied from 25℃ to 65℃. Again the curves show a near straight line relation between $(T_a - T_b)$ and fin efficiency with a negative slope. For same value of T_b, the efficiency decreases when T_a is increased. To explain this we need to take the help of analytical solution described in section 3.4. If look at the efficiency equation (3.4.20), we find that the only term effected by the variation of ambient temperature is m, which is in turn dependent on factor b_2. So as we change T_a, the fin efficiency changes. Moreover, as the ambient temperature increases, more heat transfer takes place but $Q_{\max}$ increases even higher, and consequently efficiency reduces.

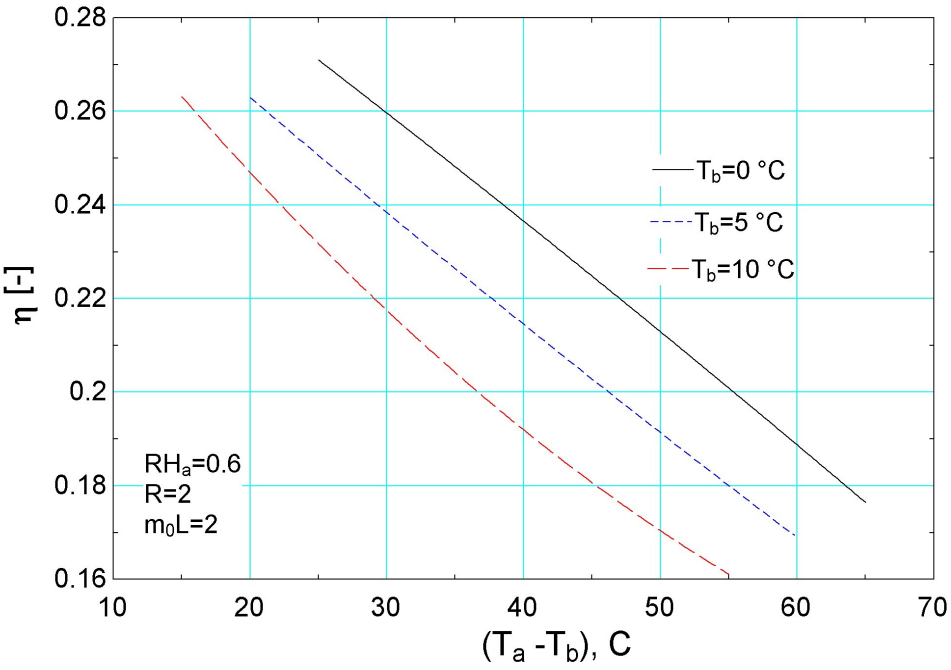

Figure 3-11 Effect of difference in temperature of ambient air and base of the fin on fin efficiency for rectangular profile fin

3.9.2 Triangular profile annular fin

Since for triangular, concave parabolic and convex parabolic profiles, the fin tip thickness is negligible, there is no heat and mass transfer there, which in turn implies that there will be no convective tip situations.

The effect of relative humidity on the temperature distribution for triangular profile annular fin is shown in Figure 3-12. The trend is similar to rectangular profile fin; furthermore, the curves for relative humidity of 20% and 40% almost coincide as was in the case of rectangular profile fin however; the variation is little bit different. For RH_a of 20% and 40%, the curves are almost linear. This linearity at low relative humidity shows that the heat flux through any cross-section in the fin is close to constant. So if heat flux is constant and the thermal conductivity is same then we will have a constant slope and that's what we see from the curve. The same decrease in temperature at any X location is observed upon increase in the relative humidity.

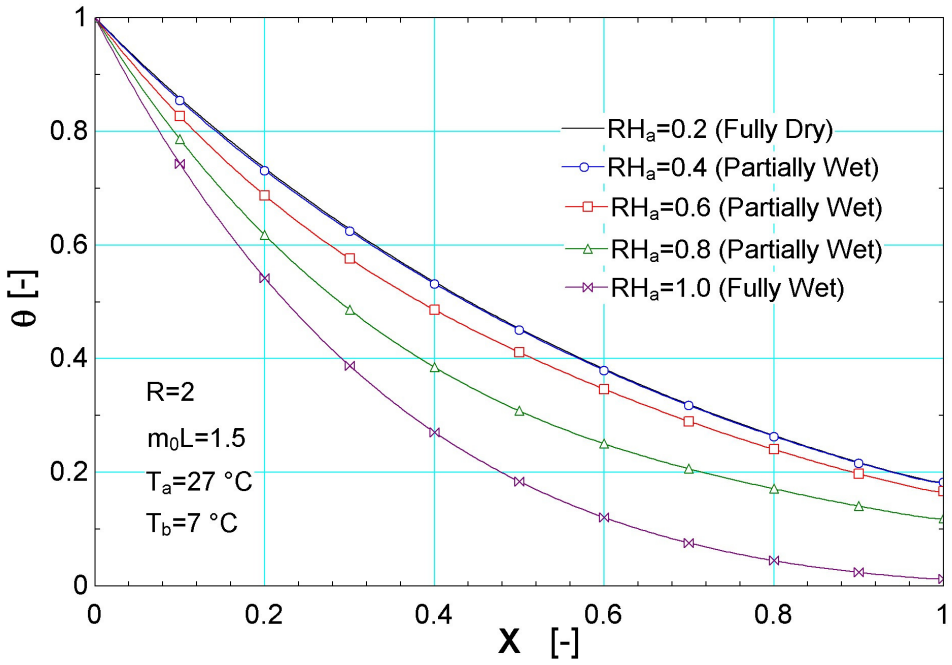

Figure 3-12 Non-dimensional temperature distribution for triangular profile fin with insulated tip

The plot of efficiency vs. fin parameter as a function of fin parameter (for the triangular profile fin), is shown in Figure 3-13 for various radius ratios. The fin is partially wet for all values of R and relative humidity except that of 20% at which the fin surface is completely dry. The figure suggests that there is no effect on fin efficiency at low fin parameter values regardless of air relative humidity neglecting the dry case. A similar steep curve is visible as that was for rectangular profile, until fin parameter value of two. Another noticeable point is that the threshold value of fin parameter for partially wet situation has shifted upon increasing the radius ratio when air relative humidity is 100%.

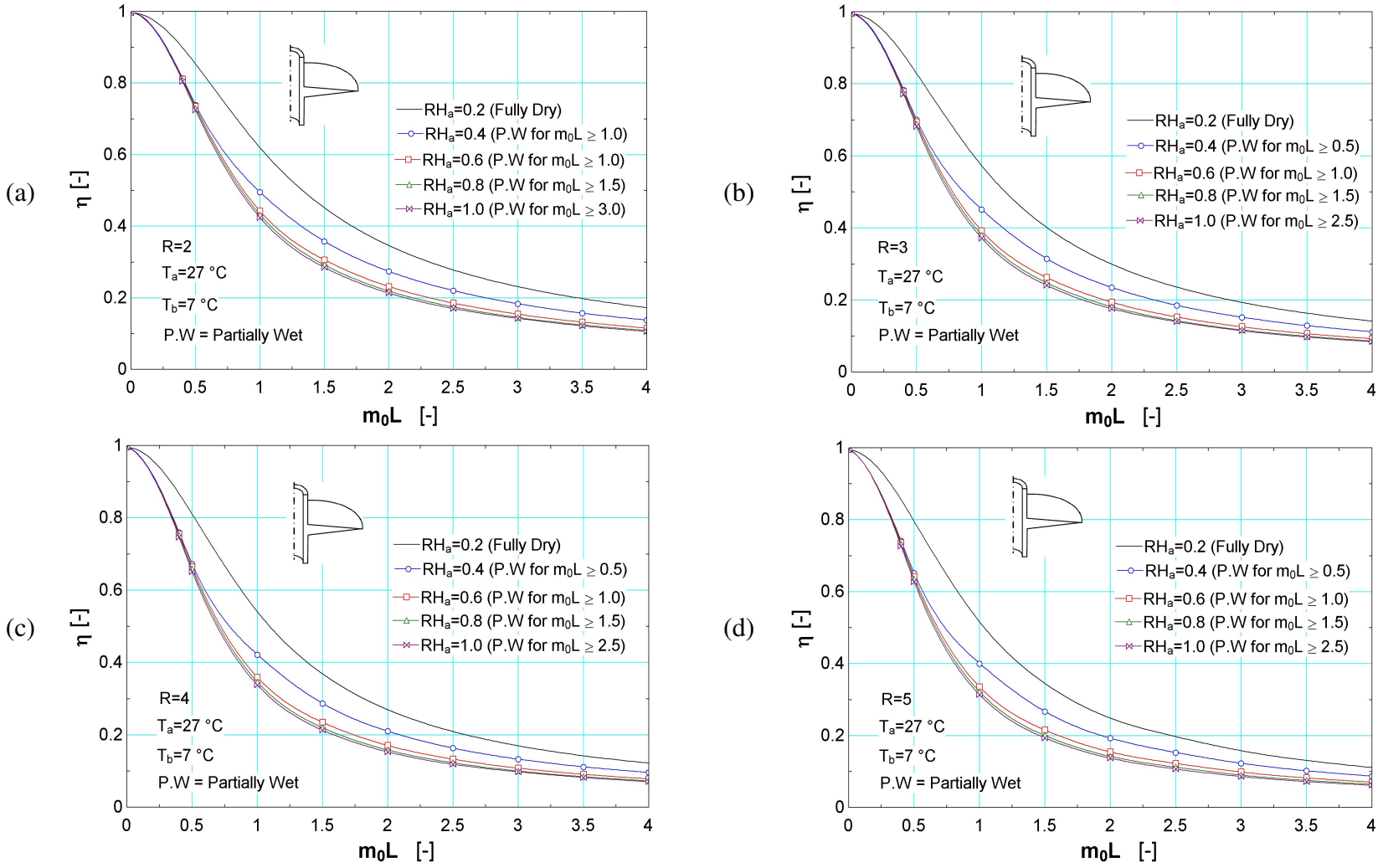

Figure 3-13 Effect of fin parameter on fin efficiency for triangular profile fin at various air relative humidity:

(a) R=2 (b) R=3 (c) R=4 (d) R=5

Figure 3-14 shows the dependence of fin efficiency on the radius ratio for triangular profile annular fin. The trend of the curve is similar to rectangular one although it has shifted a little bit down. The effect of ambient and base temperature difference on fin efficiency for triangular case plotted in Figure 3-15. The curves have been plotted for three fin base temperatures. The figure clearly shows the significance of fin base and fin tip temperatures on the efficiency.

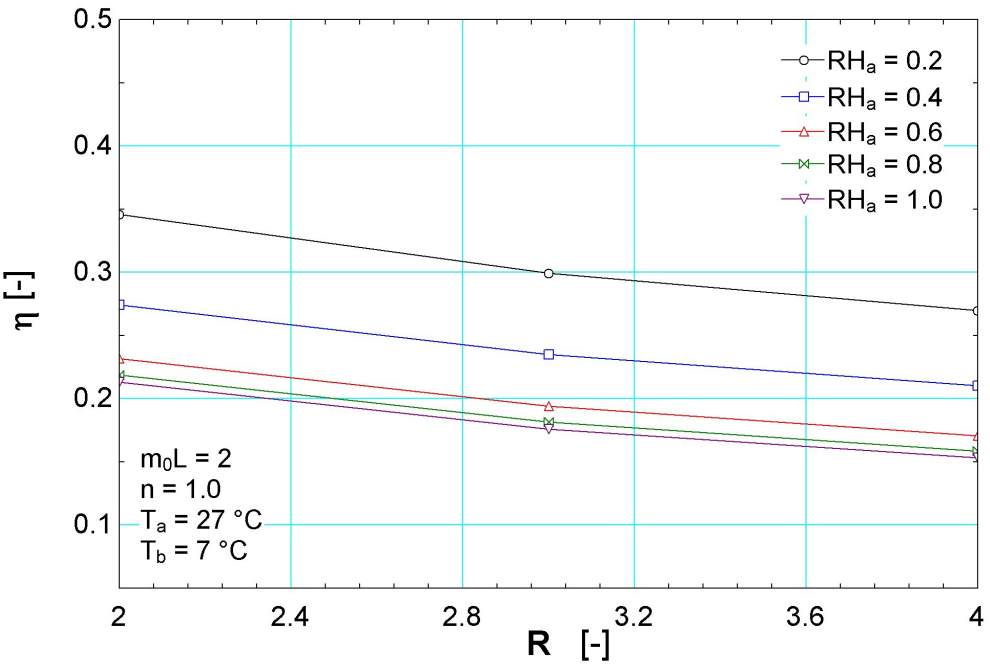

Figure 3-14 Effect of radius ratio on the fin efficiency for triangular profile fin

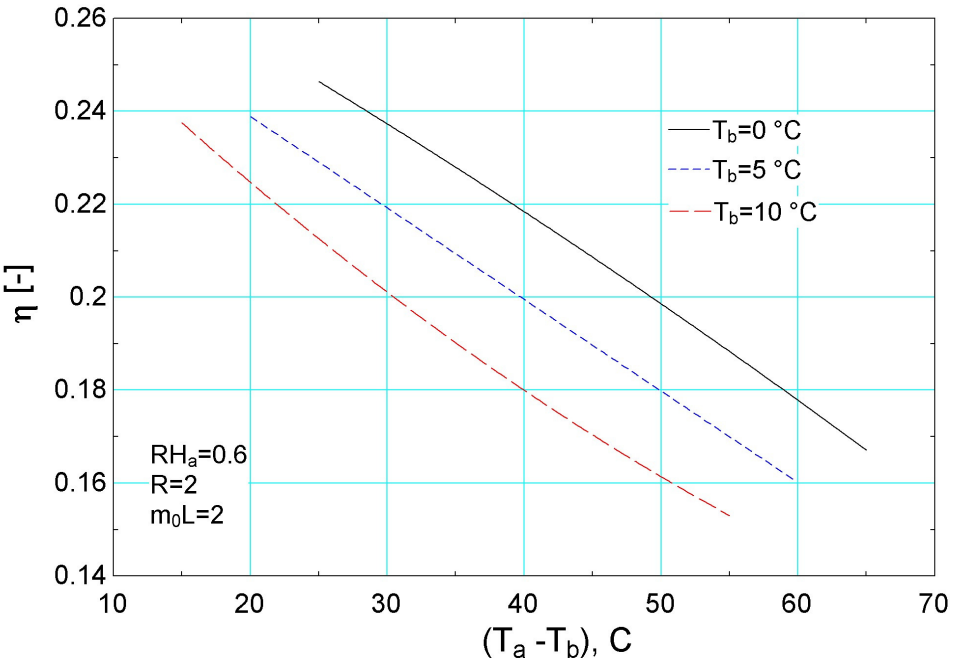

Figure 3-15 Effect of difference in temperature of ambient air and base of the fin efficiency for triangular profile fin

3.9.3 Convex parabolic profile annular fin

The temperature distribution curve for convex parabolic profile fin with insulted tip condition is shown in Figure 3-16. The result for relative humidity of 20% and 40% almost overlaps each other. Moreover, it clearly shows the effect of relative humidity on the surface temperature. As RH_a value increases, the local temperature reduces at any location X. At higher values of relative humidity, this effect cause the surface temperature to fall below than dew point temperature of the ambient air causing fully wet surface conditions.

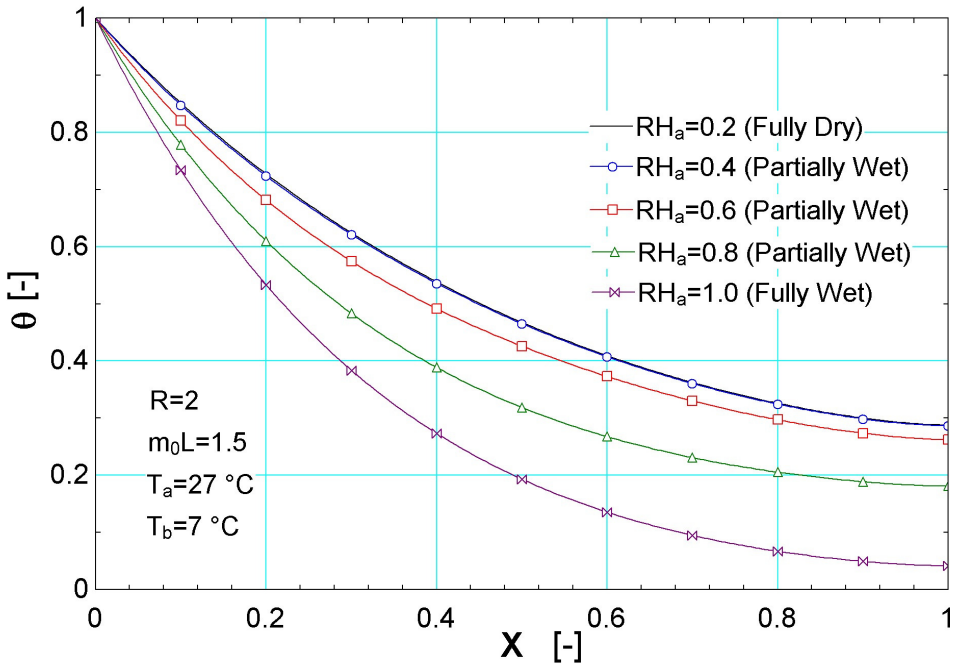

Figure 3-16 Non-dimensional temperature distribution for convex parabolic profile fin with insulated tip

Fin efficiency as a function of fin parameter is plotted in Figure 3-17 for convex parabolic profile annular fin. For various air relative humidity, the curves for efficiency are plotted. The fin efficiency decreases suddenly when fin parameter value starts increasing from zero until about it reaches the value of two. Thereafter this gradient is relatively smaller. For any value of RH_a from 40% to 100%, the fin efficiency does not depend on fin parameter at lower magnitudes (until about $m_0 L = 0.5$).

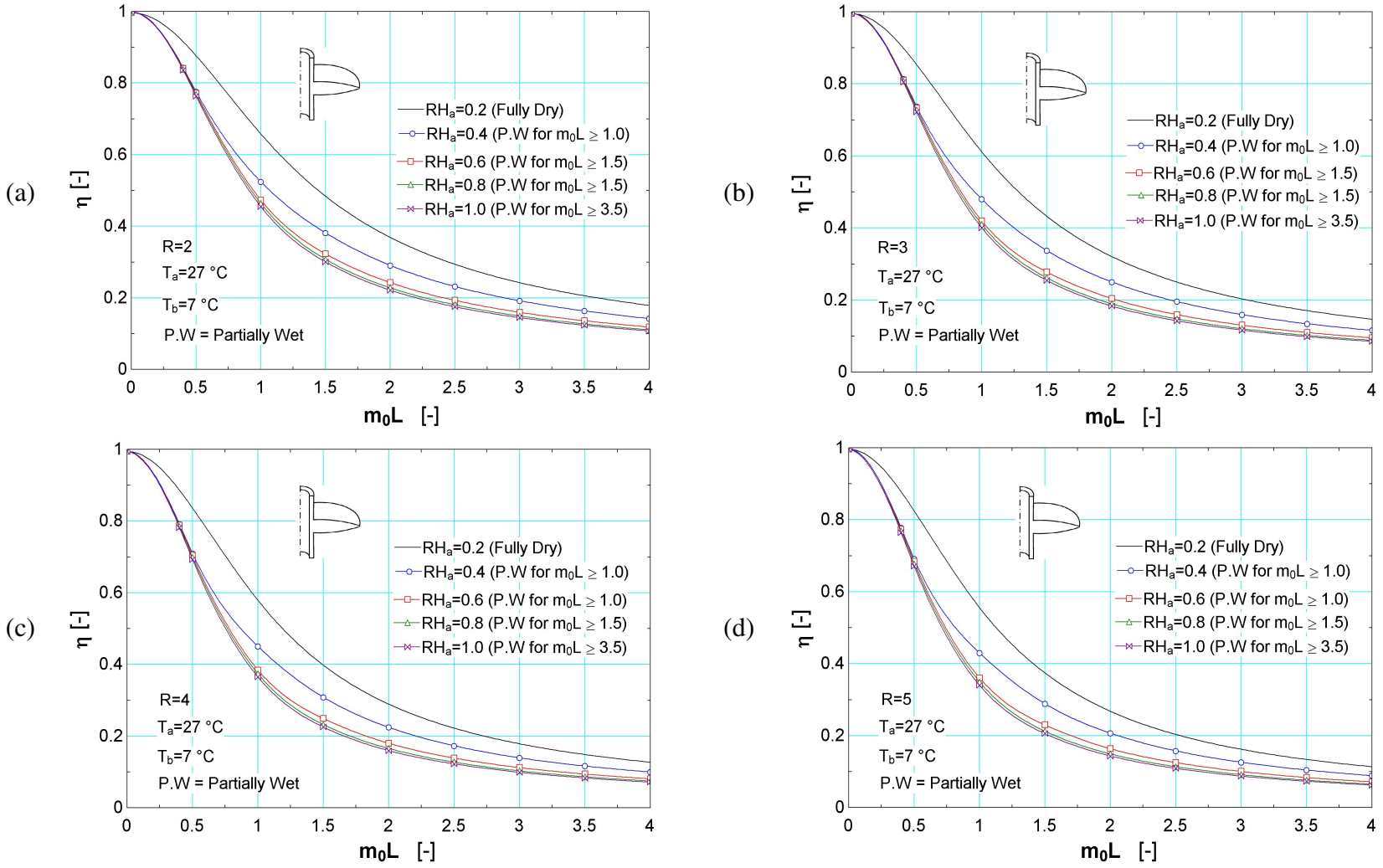

Figure 3-17 Effect of fin parameter on fin efficiency for convex parabolic profile fin at various air relative humidity:

(a) R=2 (b) R=3 (c) R=4 (d) R=5

Figure 3-18 shows the effect of radius ratio on the fin efficiency for various relative humidities, fin parameter of 2, ambient temperature of 27 ℃ and base temperature of 7 ℃. The figure shows a near straight line relationship as with the previous cases.

The temperature of ambient air and that of the fin base also plays an important role in determining the fin efficiency. This is clearly visible in Figure 3-19. For any fixed value of base temperature, if we increase the ambient air temperature, the fin efficiency reduces.

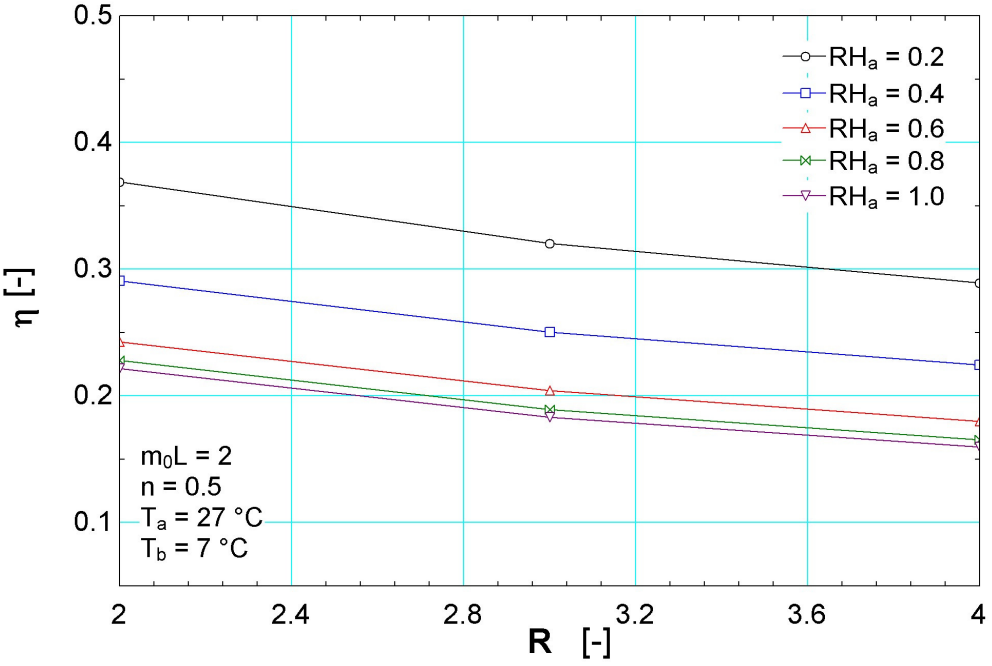

Figure 3-18 Effect of radius ratio on the fin efficiency for convex parabolic profile fin

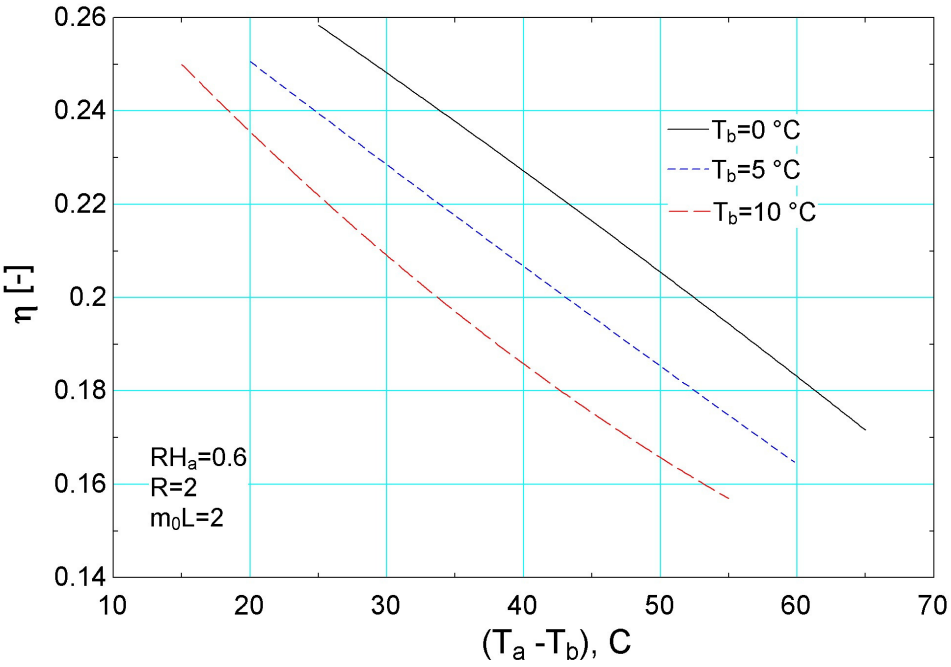

Figure 3-19 Effect of difference in temperature of ambient air and base of the fin on efficiency for convex parabolic profile fin

3.9.4 Concave parabolic annular fin

Temperature variation on a concave profile parabolic annular fin with insulated tip condition is shown in Figure 3-20. The first most important observation about this fin is that irrespective of relative humidity value, the temperature at the tip is zero. Moreover, for RH_a values of 0.2 and 0.4, the curve seems to be a straight line connecting the highest and lowest values of temperature. The reason for this linearity was mentioned when we discussed the triangular fin profile. Another interesting point is that in all the other profile fins, the fin was completely wet at 100% relative humidity but this not the case for this type of fine.

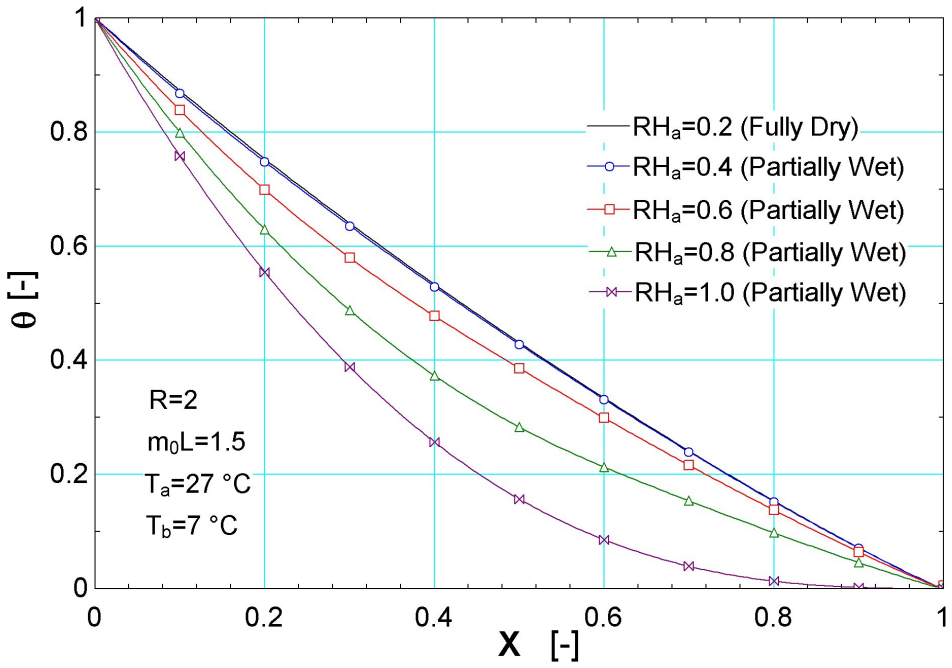

Figure 3-20 Non-dimensional temperature distribution for concave parabolic profile with insulated tip

The following Figure 3-21 depicts the efficiency variation of concave parabolic profile annular fin under different ambient air relative humidity as a function of fin parameter $m_0 L$. If we look at the fin efficiency at any fin parameter value and at any value of relative humidity and compare with the other fin results, we find that concave profile fin gives the lowest efficiency at the same thermo-geometric values. For all values of RH_a except 0.2, the fin efficiency trend is more or less a straight line for $0 \le m_0 L \le 0.75$. This phenomenon is not visible in any other type of fin. But what is observable is that like all fin types, the effect of higher values of relative humidity is not appreciable on fin efficiency.

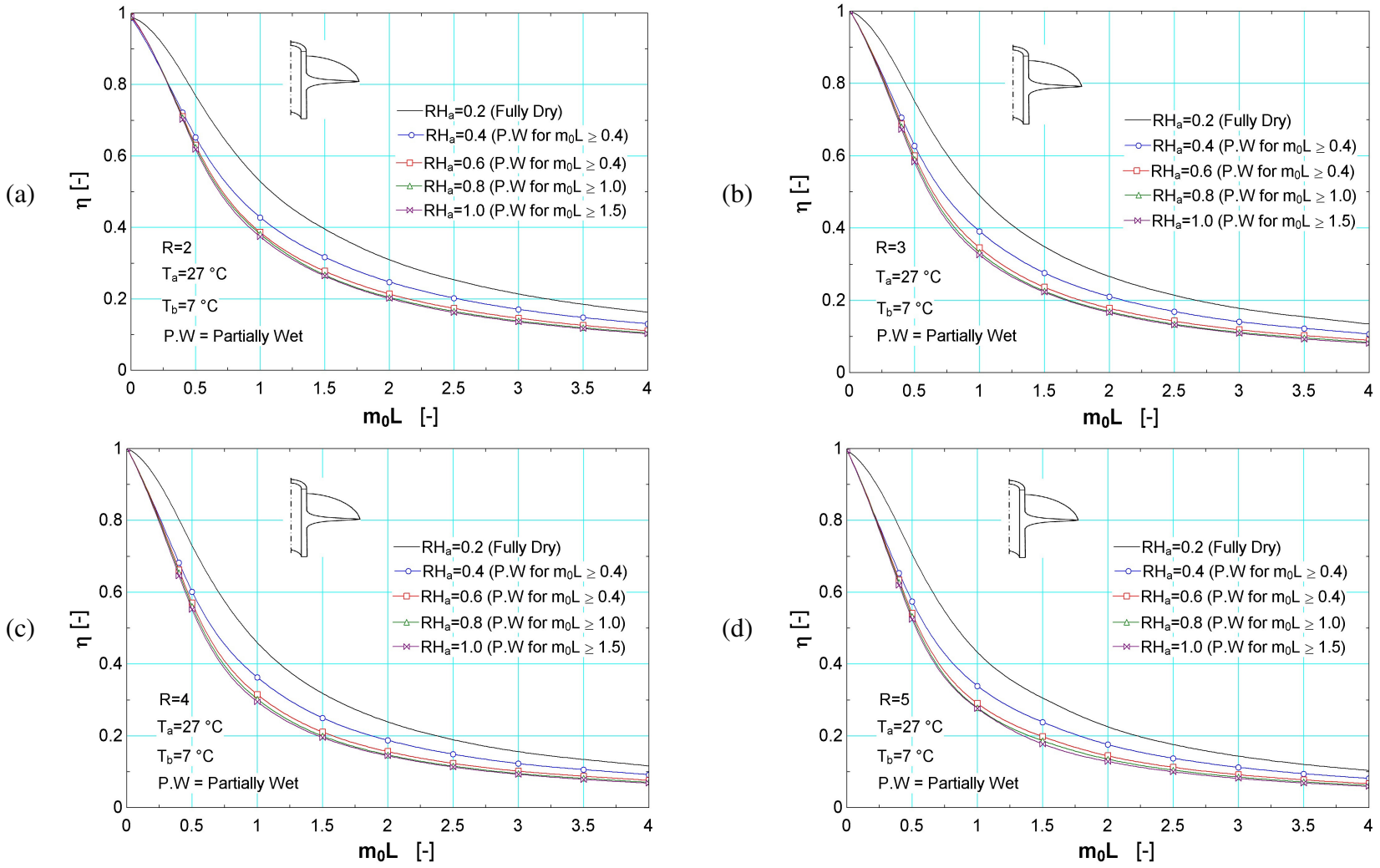

Figure 3-21 Effect of fin parameter on fin efficiency for concave parabolic profile fin at various air relative humidity: (a) R=2 (b) R=3 (c) R=4 (d) R=5

The effect of radius ratio on the fin efficiency is plotted in Figure 3-22 for concave parabolic profile with relative humidity ranging from 20 % to 60 % and fin parameter of two. Fin efficiency decreases on increasing the radius ratio as with other types of fins. The reason is that as the distance from the fin's base increases the surface temperature moves away from that of base toward the ambient, thus resulting in lesser temperature difference between local surface and ambient air which is the main driving force for heat transfer from the fin.

In Figure 3-23 the effect of temperature difference between ambient and base of the fin on the fin efficiency is shown. This plot demonstrates that lower values of base temperature will yield better performance even if the temperature difference ($T_a - T_b$) is same.

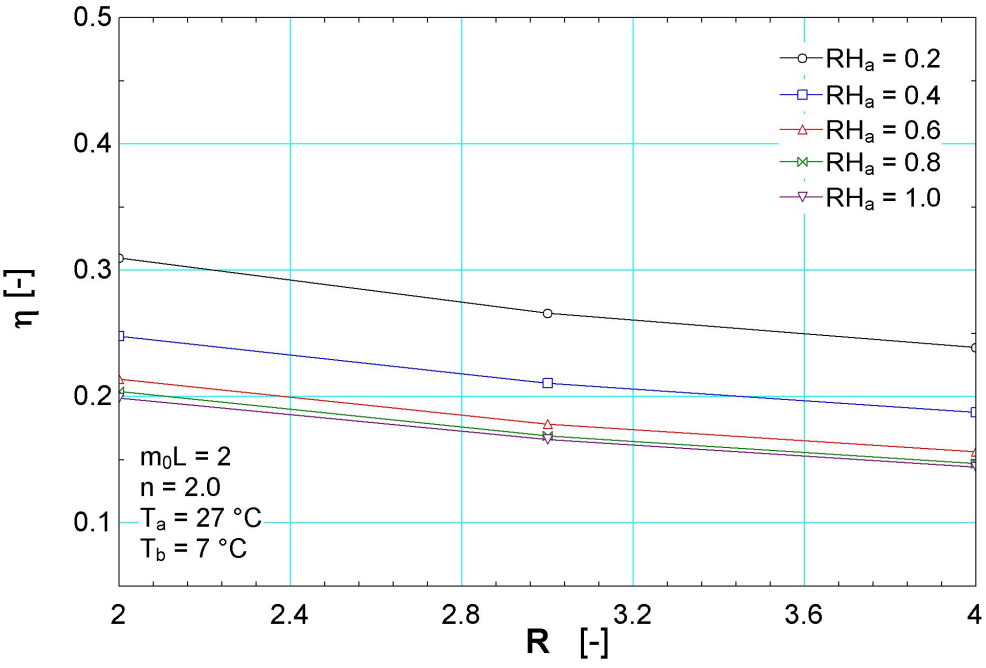

Figure 3-22 Effect of radius ratio on the fin efficiency for concave parabolic profile

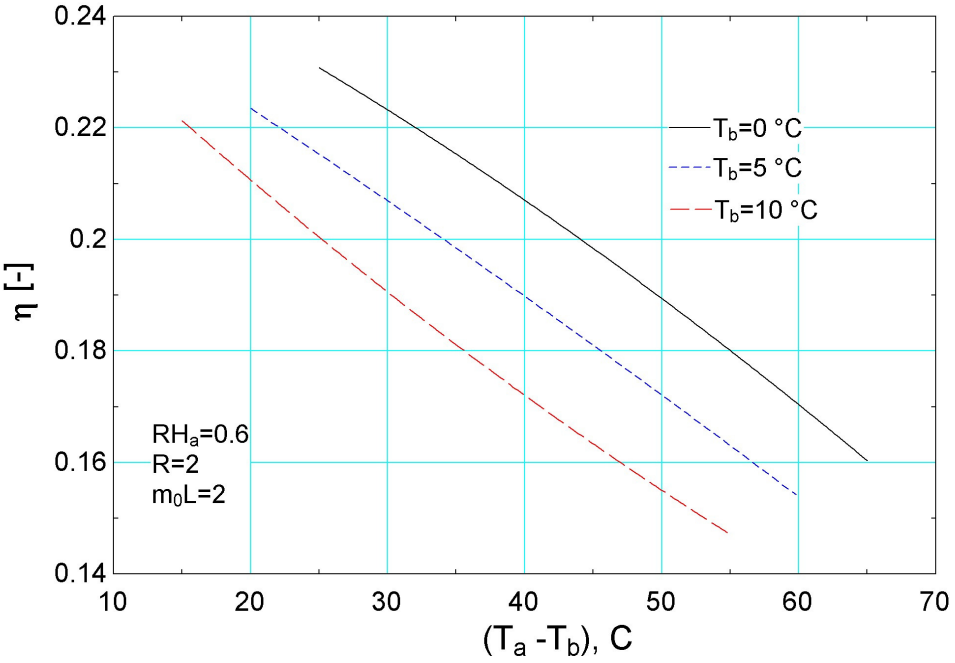

Figure 3-23 Effect of difference in temperature of ambient air and base of the fin on fin efficiency for concave parabolic profile

3.9.5 Hyperbolic profile annular fin

Non-dimensional temperature distribution for hyperbolic fin is presented in Figure 3-24 for insulated tip condition. The fin surface is fully dry at relative humidity of 20% whereas it becomes partially wet if we increase this value and finally reaches fully wet situation at $RH_a = 1$ for the given operating conditions. The effect of relative humidity is considerable on the fin temperature particularly at higher values in the sense that the curve deviates more from that of fully dry fin.

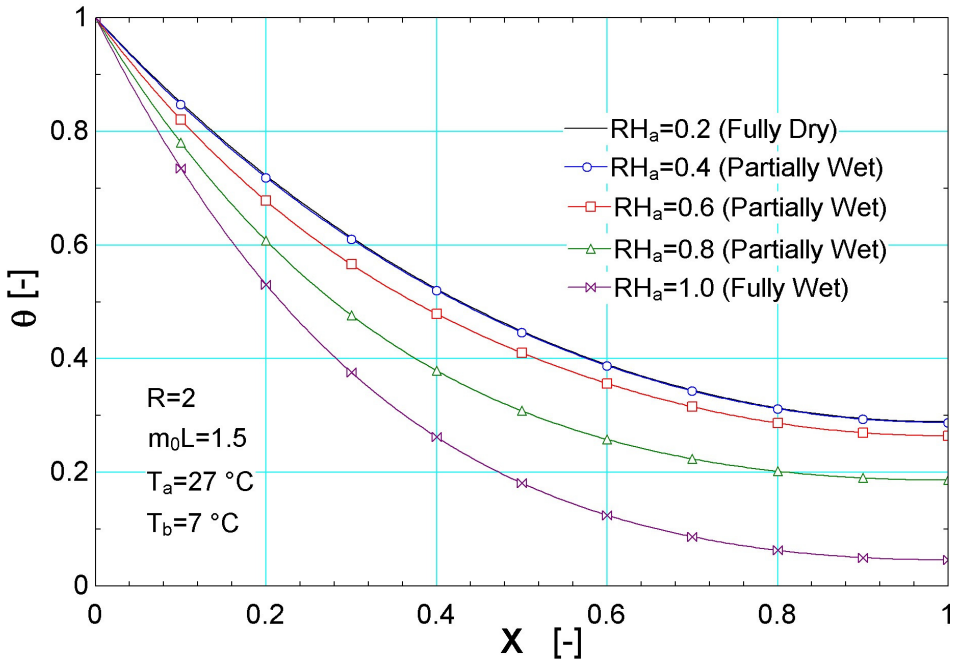

Figure 3-24 Non-dimensional temperature distribution for hyperbolic profile with insulated tip

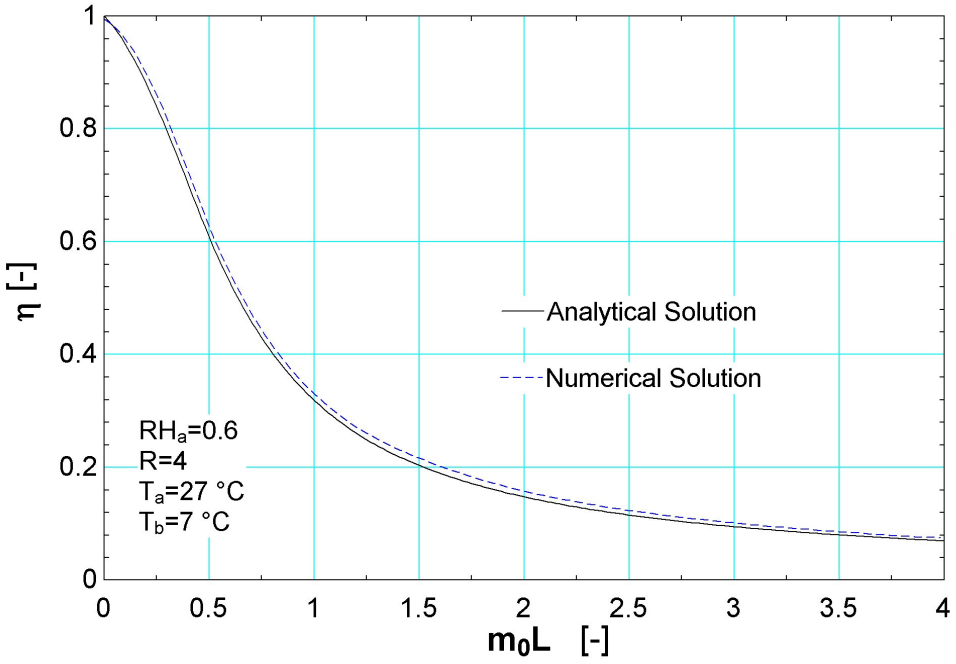

Figure 3-25 Comparison of efficiency for analytical and numerical solution presented in this work

Figure 3-25 shows the comparison of analytical solution presented in section 3.5 and the numerical approach in section 3.2 and 3.3. The graph depicts that, like it was for the case of rectangular fin, numerical solution always gives higher efficiency than the analytical solution. The reason might be that we are using approximate model for temperature and humidity ratio relationship in the analytical method whereas for numerical solution we have used the actual psychrometric relations.

Unlike concave parabolic profile annular fin and like all the other three types, hyperbolic fin has higher $m_0 L$ values at which the fin becomes partially wet. This value is constant for different radius ratio as can be seen from the efficiency vs. fin parameter graph from Figure 3-26 of hyperbolic profile fin. The dry fin condition throughout this work has been the winner in terms of giving superior efficiencies for any fin parameter and any radius ratio value. In addition, highest relative humidity has always given lowest efficiency.

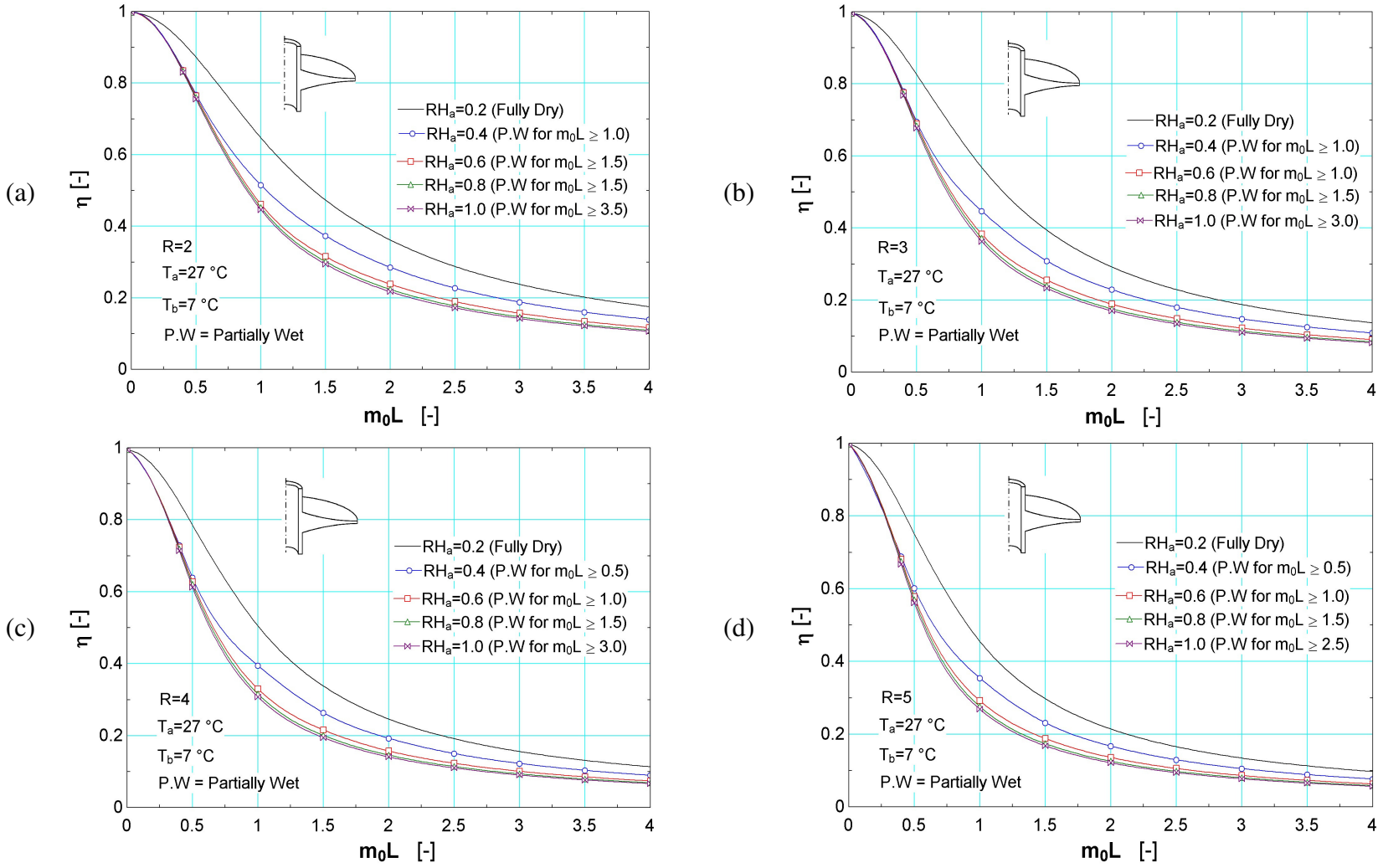

Figure 3-26 Effect of fin parameter on fin efficiency for hyperbolic parabolic profile fin at various air relative humidity: (a) R=2 (b) R=3 (c) R=4 (d) R=5

The effect of radius ratio on the fin efficiency for hyperbolic fin is shown in Figure 3-27. For different relative humidities, fin parameter of 2, ambient temperature of 27 ℃ and base temperature of 7 ℃; the drop in fin efficiency between radius ratio of 2 and 4 is maximum for the case of hyperbolic fin followed by rectangular fin then convex parabolic after that triangular fin and finally concave parabolic fin. Figure 3-28 shows the dependence of $(T_a - T_b)$ on the fin efficiency. If we do a similar comparison for highest efficiency at any $(T_a - T_b)$, let us say 45 and for $T_b = 0\,^{\circ}\mathrm{C}$, the descending order is rectangular, convex parabolic, hyperbolic, triangular and concave parabolic annular fin.

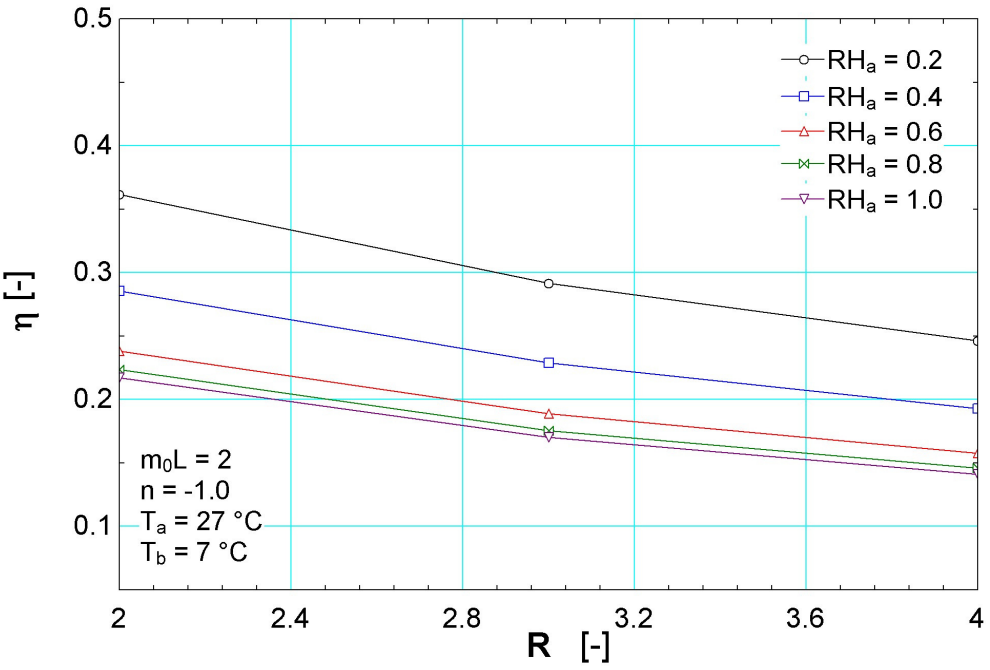

Figure 3-27 Effect of radius ratio on the fin efficiency for hyperbolic profile

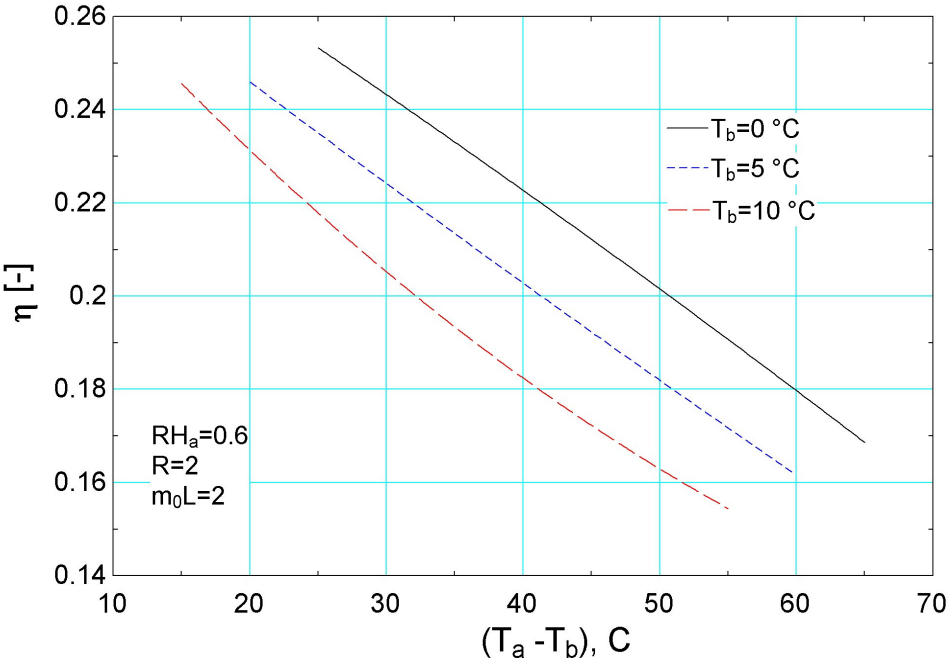

Figure 3-28 Effect of difference in temperature of ambient air and base of the fin on fin efficiency for hyperbolic profile

3.10 Fin Optimization and Results

As we know, optimization of fins are done in two ways i.e. either for a given heat transfer rate we minimize the volume or for a given quantity of fin material we find the fin dimensions that will give maximum heat transfer rate. We shall be following the latter approach.

If we look at equation (3.2.30), i.e.

$$Q = 2\psi \left(m_0 L\right)^2 \left(R-1\right) \int_{r_b}^{r_t} \left(\theta + Co\ \Omega\right) r\, dr \tag{3.8.1}$$

And define new dimensionless parameters as,

$$u = \sqrt{\frac{2\,h\,r_b^*}{k}} \tag{3.8.2}$$

$$v = \frac{V}{\pi\, r_b^{*3}} = \frac{2\pi\, t_b^* \left[\int_{r_b^*}^{r_t^*} r^* \left(\frac{r_t^* - r^*}{r_t^* - r_b^*} \right)^n dr \right]}{\pi\, r_b^{*3}} \tag{3.8.3}$$

$$v = \frac{V}{\pi\, r_b^{*3}} = \frac{2\pi\, t_b^*\, r_b^* \left(r_t^* - r_b^* \right)}{\pi\, r_b^{*3}} \qquad \text{for hyperbolic profile} \tag{3.8.4}$$

$$w = \frac{r_b^*}{t_b^*} \tag{3.8.5}$$

We observe that

$$\psi = \frac{1}{2\,w\left(R-1\right)} \tag{3.8.6}$$

$$m_0\, L = u\left(R-1\right)\sqrt{w} \tag{3.8.7}$$

$$r_b = \frac{1}{R-1} \tag{3.8.8}$$

$$r_t = \frac{R}{R-1} \tag{3.8.9}$$

$$R = \sqrt{v\,w+1} \tag{3.8.10}$$

i.e. ψ, $m_0 L$, r_b, r_t and R are all functions of u, v and w. A similar dissection of equation (3.3.13) will result in same conclusion. These parameters, u, v, w represents modified version of $m_o L$ (sort of conduction resistance to convection resistance ratio),

non-dimensional fin material volume and fin base ratio (outer radius of tube to thickness of fin at its conjunction with tube) respectively. So by keeping these two parameters constant (u and v), and considering w as the only independent variable, the maximum heat dissipated from the fin can be obtained. This in physical interpretation would mean that we have a finite quantity of material, which implies that we know the thermal properties of the material. Moreover, we have prior knowledge of the working environment in which we are going to employ the fin, thus completely defining u. Finally, we find the dimensions of the fin that will give us maximum heat transfer rate for the chosen thermo-geometric conditions.

3.10.1 Rectangular profile annular fin optimization

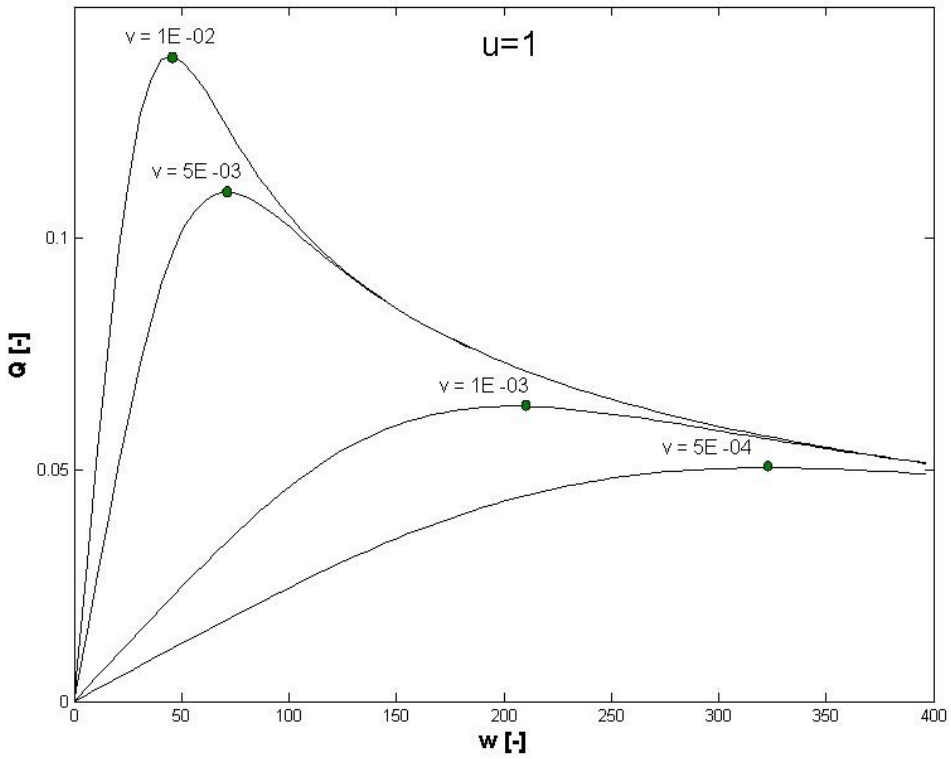

Figure 3-29 Optimum fin dimensions of rectangular fin for various non-dimensional volumes

Figure 3-29 shows the variation of non-dimensional heat transfer to the fin surface with fin base ratio (w) for rectangular profile annular fin. For a fixed quantity of fin material, we know that if we increase the fin base thickness the heat transfer from the fin increases. This increase is due to increase in conduction heat transfer area at the fin base. However, as we increase this base thickness, a value is reached beyond which there is no benefit of increasing the fin base thickness since the conduction resistance eclipses the benefit of increase conduction area. This phenomenon is clearly visible from the figure. The value of fin base ratio at which maximum heat transfer occurs is our optimum fin dimension.

The locus of optimum dimensions and the corresponding heat transfer is presented in the form of log-log graph in Figure 3-30. A comparison is also showed with Ref. [29]'s work. A salient feature of presenting the result in this graphical format is; although we started with a known volume of fin material and found the maximum heat transfer rate, now we can go in the reverse direction i.e. for a given heat transfer rate we can find the minimum required fin material. It is worth to note that the numerical solution gives higher Q than analytical solution but lesser value of w.

(i)

(ii)

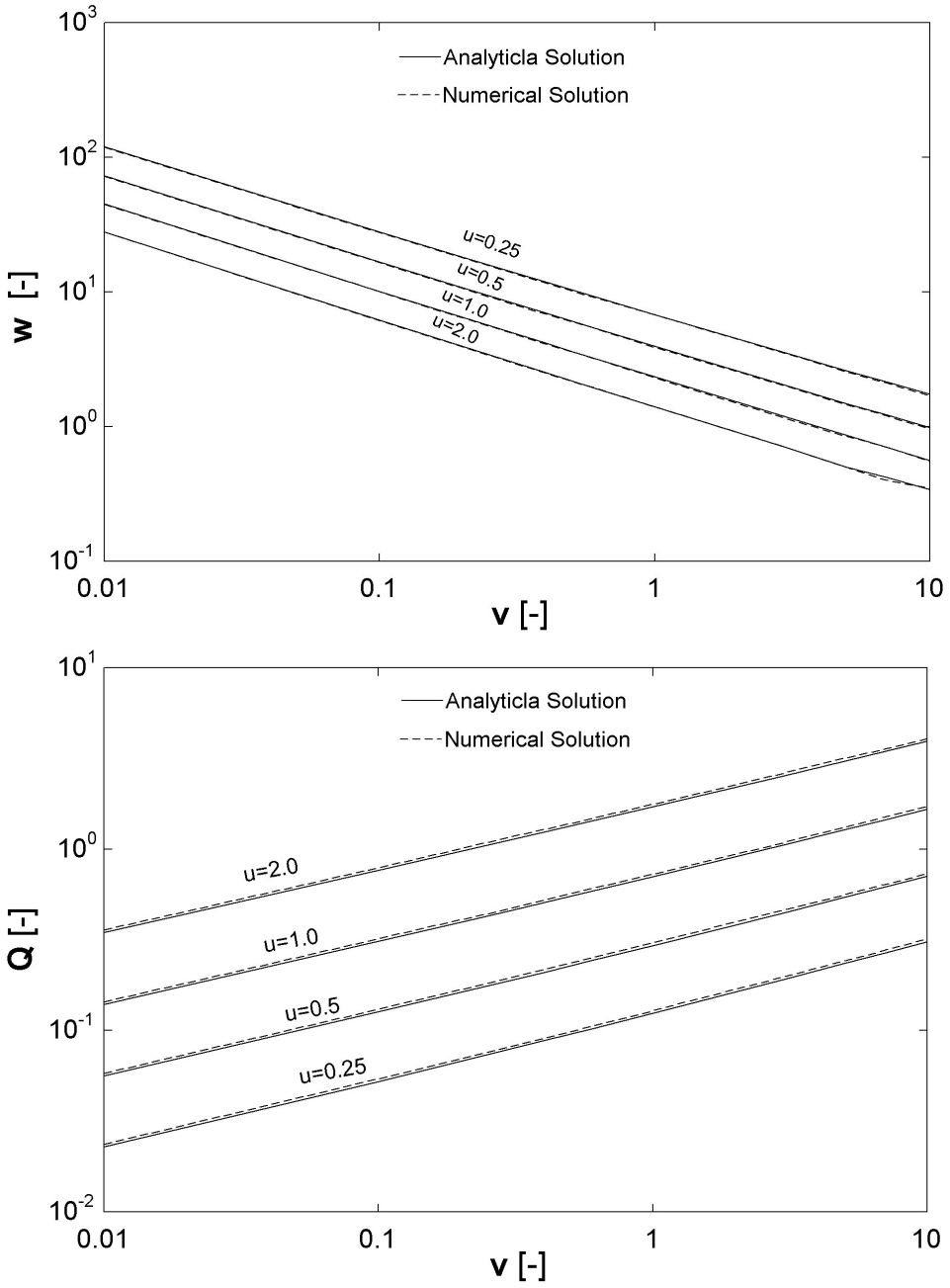

Figure 3-30 Optimization results comparison with analytical solution for rectangular profile annular fin

The following (regression) model is presented (within ± 1% of actual numerical data) for the above figure:

$$w = c1 \cdot v^{n1}$$

$$Q = c2 \cdot v^{n2}$$

where the various parameters are given by

$$c1 = 2.417 \cdot u^{-0.758}$$

$$c2 = 0.725 \cdot u^{1.258}$$

$$n1 = -0.628 - 0.0200005 \cdot ln(u)$$

$$n2 = 0.363 - 0.0149999 \cdot ln(u)$$

It is important to note that the regression equations shown above and in the following sections are applicable only in the range of the charts.

3.10.2 Triangular profile annular fin optimization

For triangular profile fin, the optimization results are presented in Figure 3-31. Unlike previous case, the results are not as evenly distributed as before. For $u = 0.25$ the graph shows a peculiar behavior. At the extreme high value of v, the w value is close to that of $u = 0.5$ however, this closeness in the result disappears when v reaches the other extreme value. This deviation is less visible in Q vs. v plot.

(i)

(ii)

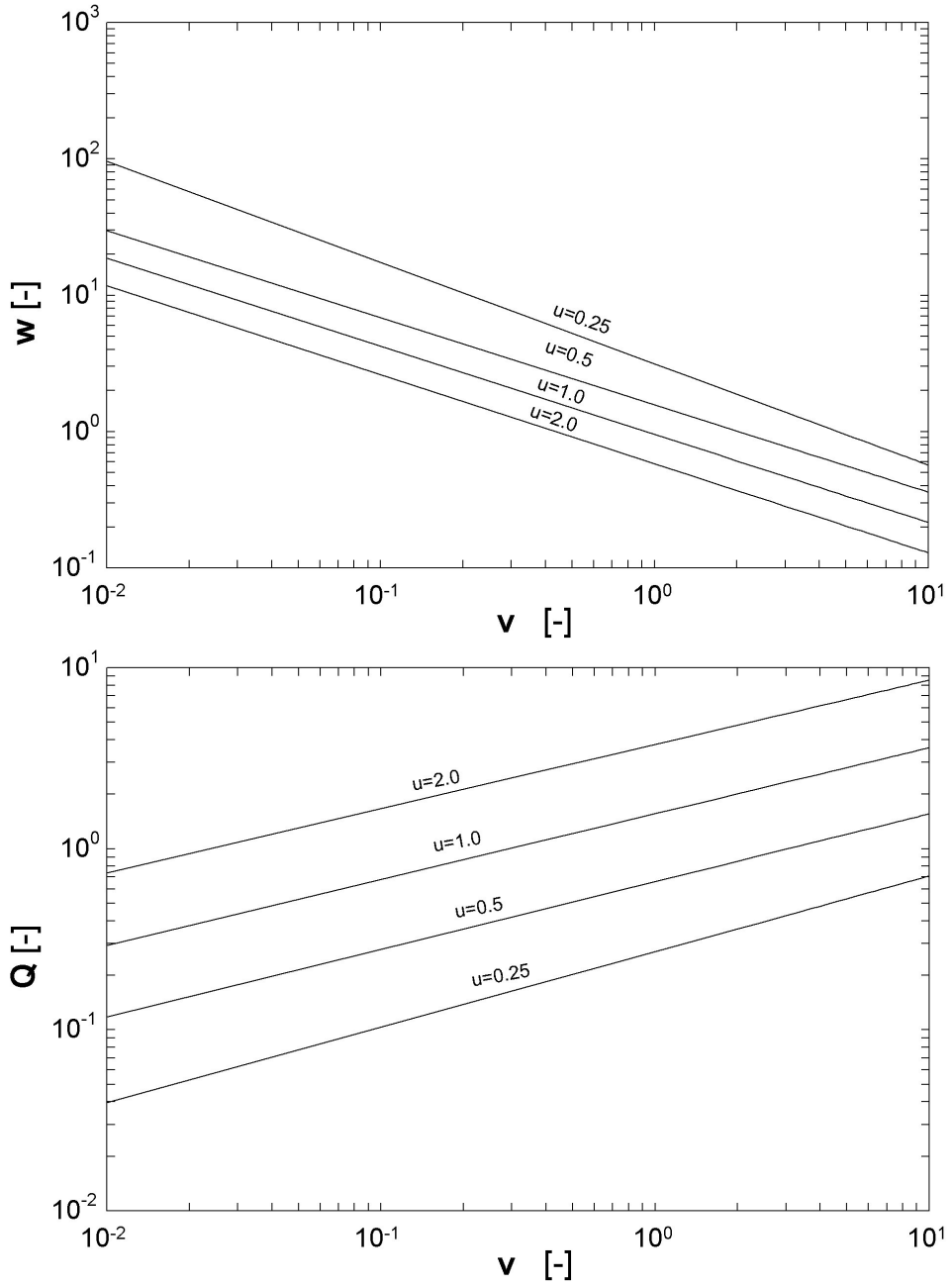

Figure 3-31 Optimization results triangular profile annular fin

The regression equations best representing the actual numerical data for the optimum dimension and corresponding heat transfer are shown below:

$$w = c1 \cdot v^{n1}$$

$$Q = c2 \cdot v^{n2}$$

the various parameters being

$$c1 = 0.974397 \cdot u^{-0.801609}$$

$$c2 = 1.57043 \cdot u^{1.26505}$$

$$n1 = -0.626549 + 0.0919242 \cdot ln(u) - 0.0679984 \cdot u \cdot ln(u)$$

$$n2 = 0.367768 - 0.0284883 \cdot ln(u)$$

3.10.3 Convex parabolic profile annular fin optimization

In Figure 3-32 we see nicely distributed optimization results for convex parabolic annular fin. For any non-dimensional heat transfer parameter value (u), as we increase the non-dimensional volume (v) the optimum non-dimensional heat transfer (Q) increases. On the other hand, a reverse trend is observed for optimum fin-base ratio. There is no abnormal behavior in the curves like that of the previous case and the trend is exactly that of rectangular fin. However, for any value of u and v this type of fin give higher Q than rectangular fin but lesser corresponding w. There is no clear winner when compared with triangular profile fin.

(i)

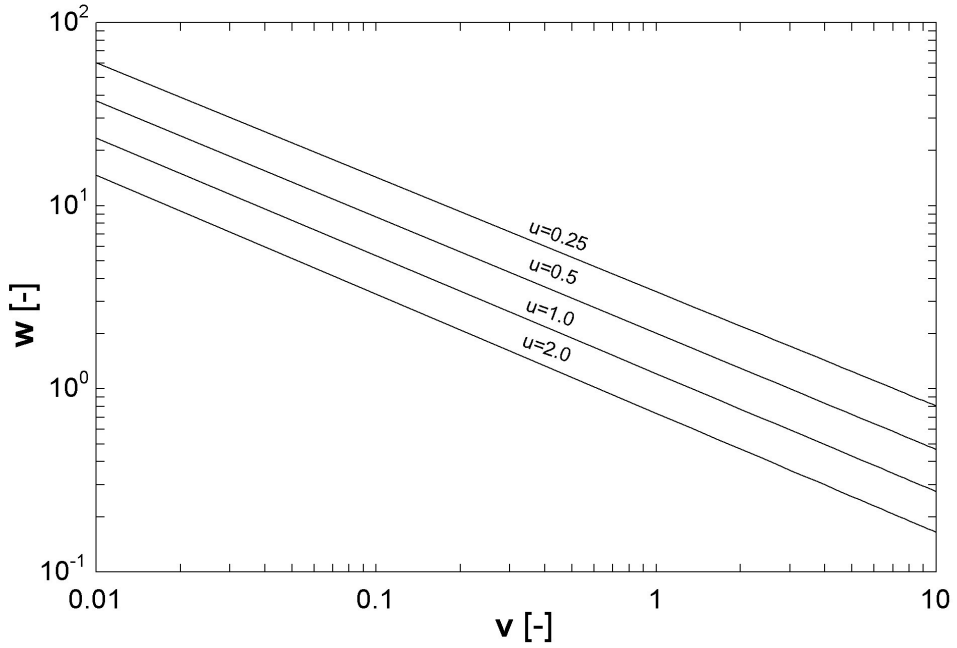

(ii)

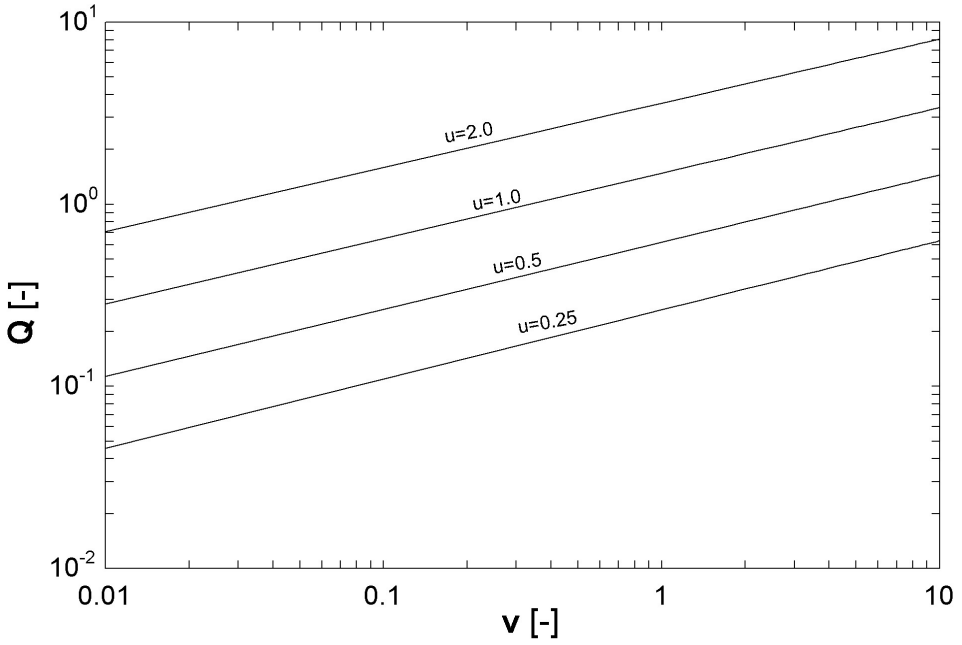

Figure 3-32 Optimization results for convex parabolic profile annular fin

The fitted regression equation with an error of ± 3% to actual data are given below:

$$w = c1 \cdot v^{n1}$$

$$Q = c2 \cdot v^{n2}$$

where the various parameters are related to fin heat transfer parameter (u) as

$$c1 = 1.21663 \cdot u^{-0.735782}$$

$$c2 = 1.49363 \cdot u^{1.25703}$$

$$n1 = -0.642233 - 0.0122127 \cdot ln(u)$$

$$n2 = 0.360687 - 0.0132649 \cdot ln(u)$$

3.10.4 Concave parabolic profile annular fin optimization

The optimization results are shown in Figure 3-33 for concave parabolic type of annular fin profile. It can be easily seen that for $u = 2$, as we decrease the non-dimensional volume, the curve approaches towards that of $u = 1$.Interestingly this do not happen for the corresponding values for determining the optimum heat transfer from the fin shown in Figure 3-33 (ii).

(i)

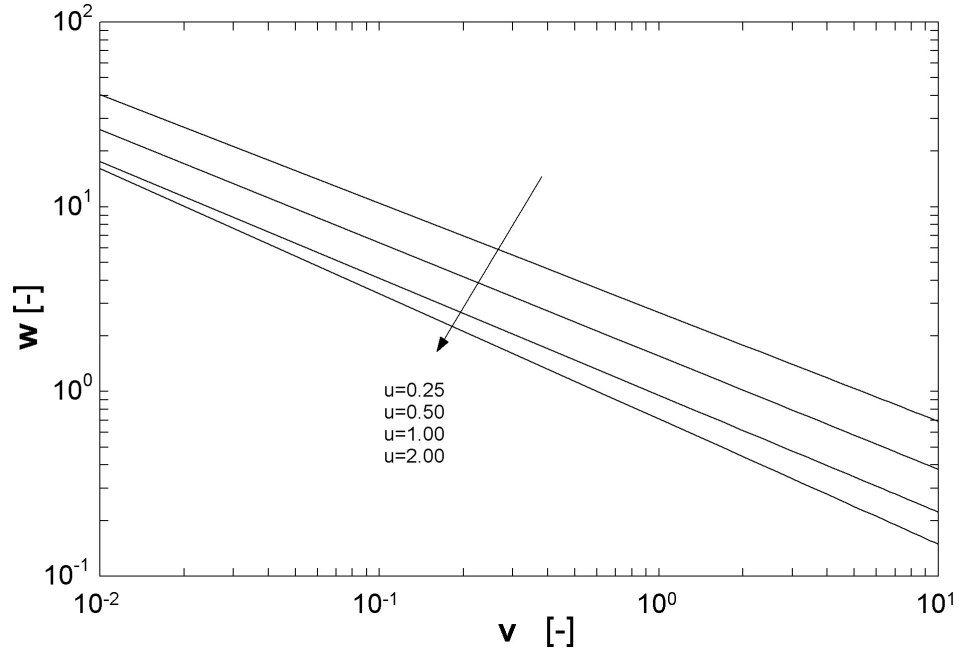

(ii)

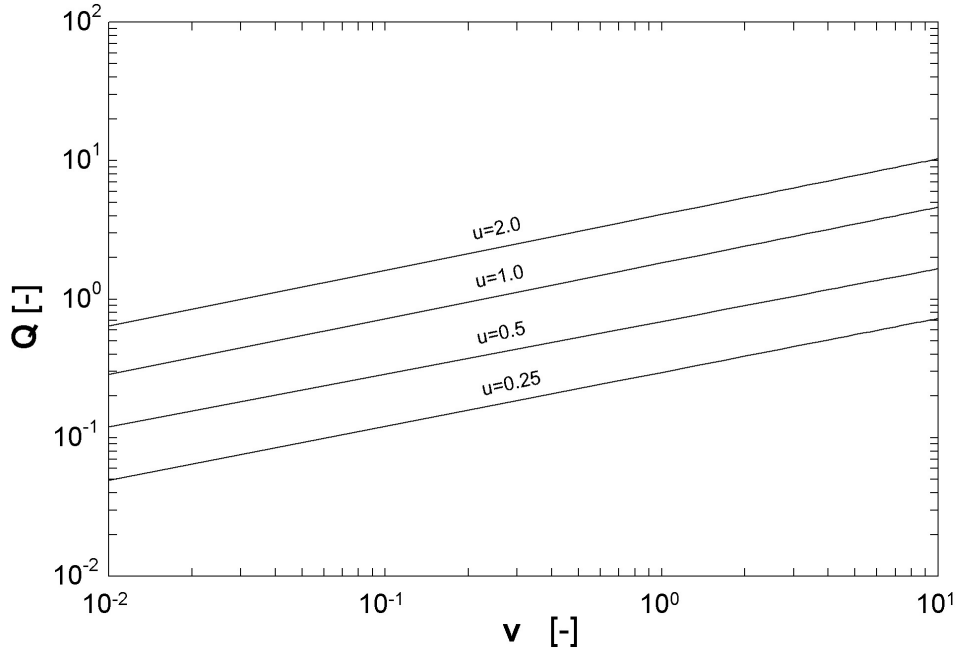

Figure 3-33 Optimization results for concave parabolic profile annular fin

The same results of optimum non-dimensional fin dimension and heat transfer for concave parabolic annular fin are best represented by the following regression model:

$$w = c1 \cdot v^{n1}$$

$$Q = c2 \cdot v^{n2}$$

where

$$c1 = 1.03739 \cdot u^{-0.645828}$$

$$c2 = 1.7313 \cdot u^{1.2766}$$

$$n1 = -0.583495 - 0.048166 \cdot u$$

$$n2 = 0.39673 + 0.00844871 \cdot ln(u)$$

3.10.5 Hyperbolic profile annular fin optimization

The heat transfer from this type of fin was mentioned in equation (3.5.9) and can be written in the following non-dimensional form

$$Q_b = \left(\frac{u'}{w}\right)^{2/3} \left[\frac{-Ai'(C_1)\,Bi'(C_2) + Ai'(C_2)\,Bi'(C_1)}{Ai'(C_1)\,Bi(C_2) - Ai(C_2)\,Bi'(C_1)}\right] \tag{3.8.11}$$

Where

$$C_1 = \left(u' \sqrt{w}\right)^{2/3} \left(1 + \frac{v\,w}{2}\right) \tag{3.8.12}$$

$$C_2 = \left(u' \sqrt{w}\right)^{2/3} \tag{3.8.13}$$

$$Q_b = \frac{Q_b^*}{k\, 2\pi\, r_b^* \left(\theta_b^* + \theta_p^*\right)} \tag{3.8.14}$$

$$u' = \sqrt{\left(\frac{2\,h\,r_b^{*}\left(1+b_2\,B\right)}{k} \right)} \tag{3.8.15}$$

$$v = \frac{2}{w}\left[\frac{r_t^{*}}{r_b^{*}} - 1 \right] \tag{3.8.16}$$

$$w = \frac{r_b^{*}}{t_b^{*}} \tag{3.8.17}$$

So again we can fix the value of u' and v and find out that w which will give us the maximum Q. The same results are computed and are compared with the numerical solution in Figure 3-34. This graph closely resembles the rectangular fin case. The numerical results predict higher maximum heat transfer but lesser optimum fin-base radius.

The fitted regression model best depicting the data presented in the figures below is

$$w = c1 \cdot v^{n1}$$

$$Q = c2 \cdot v^{n2}$$

where the various parameters are

$$c1 = 1.78863 \cdot u^{-0.599547}$$

$$c2 = 0.78741 \cdot u^{1.2158}$$

$$n1 = -0.681613 + 0.0169324 \cdot ln\left(u\right) - 0.00385546 \cdot u \cdot ln\left(u\right)$$

$$n2 = 0.376657 - 0.0186014 \cdot ln\left(u\right)$$

(i)

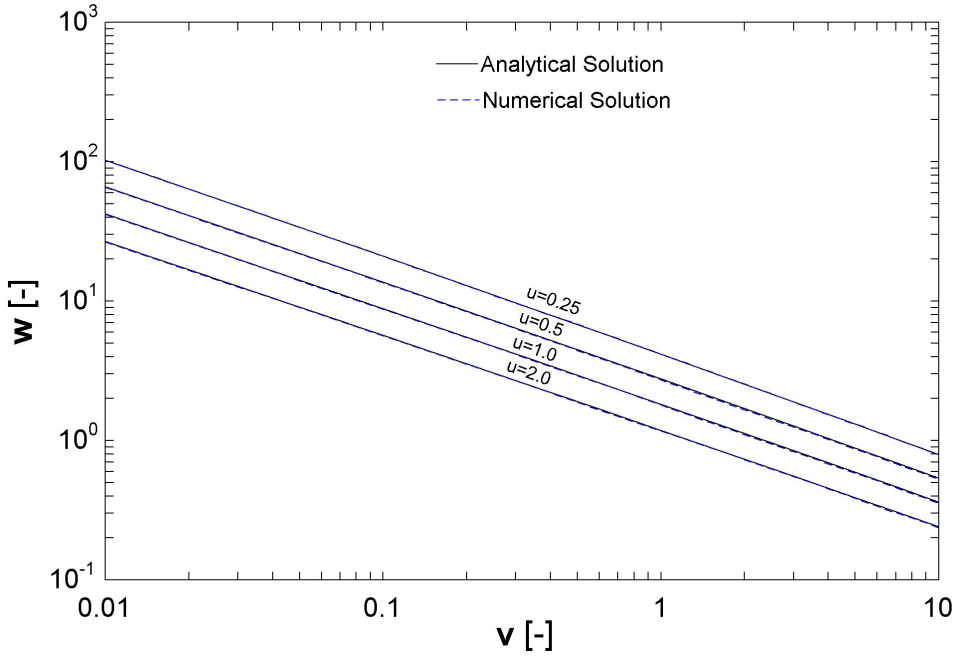

(ii)

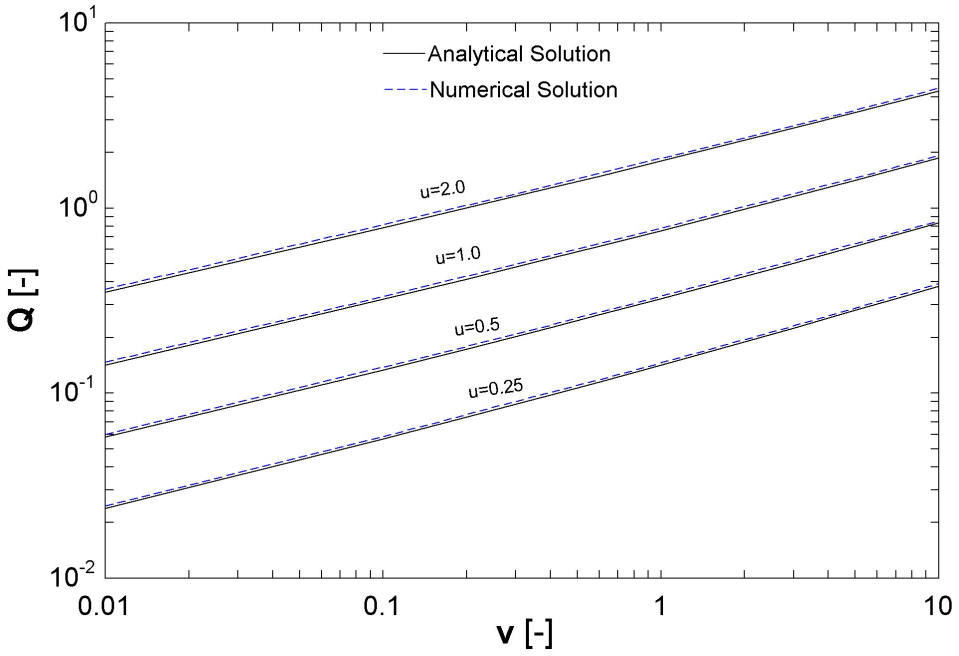

Figure 3-34 Optimization comparison with analytical solution for hyperbolic profile annular fin

CHAPTER 4

TWO-DIMENSIONAL FIN ANALYSIS

This chapter deals with the two dimensional (2-D) analysis of annular fins. In section 4.1 we present the generalized mathematical model for the two-dimensional case. The governing equations with analytical solution for dry fin case is presented in section 4.3 and is taken from Ref. [66]. This is followed by fin optimization model. In section 4.5 grid independence and validation is achieved. Finally, the results are presented and discussed for heat transfer, efficiency and optimum dimensions taking into account both isotropic and orthotropic materials.

4.1 Two Dimensional Fully Wet Fin Model

The two dimensional heat diffusion equation for steady state condition with no internal energy generation is mentioned in every heat transfer book. Figure 4-1 shows the heat transfer scenario on an element of the two-dimensional domain.

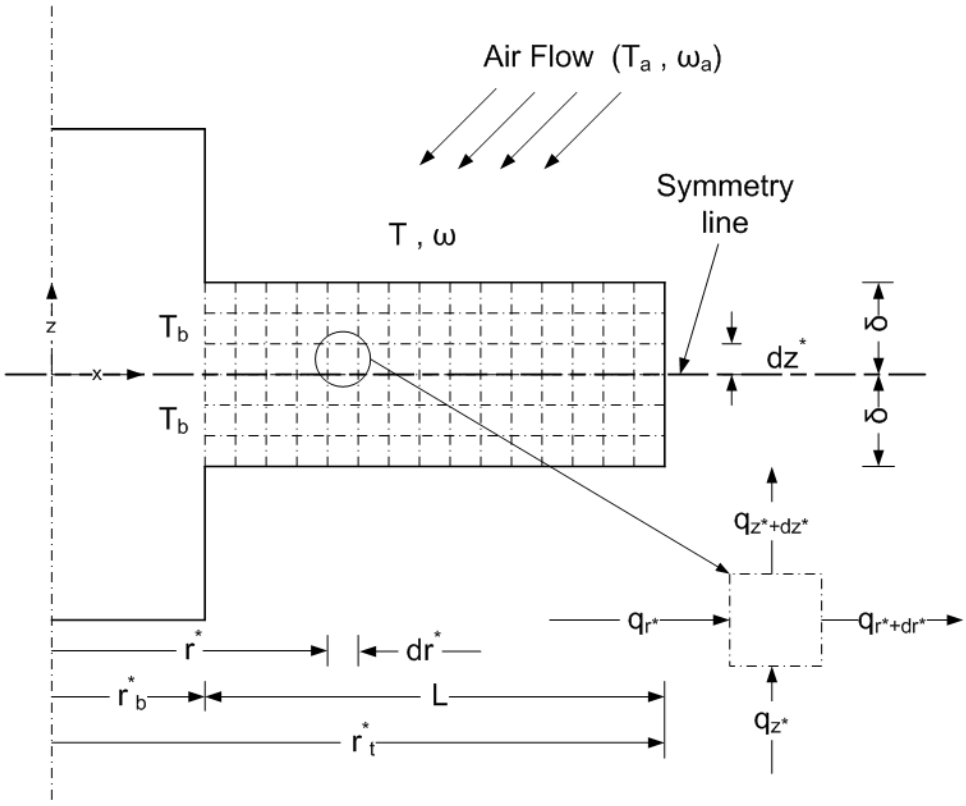

Figure 4-1 Cross-sectional view of an annular fin showing two-dimensional heat transfer

When energy balance is applied to a differential control volume in polar coordinates, the conduction heat transfer governing relation is as follows

$$\frac{1}{r^*}\frac{\partial}{\partial r^*}\left(k_r\, r^*\,\frac{\partial T}{\partial r^*}\right)+\frac{\partial}{\partial z^*}\left(k_z\,\frac{\partial T}{\partial z^*}\right)=0 \tag{4.1.1}$$

Where k_r and k_z are thermal conductivities in r^* and z^* directions, respectively. Defining some new non-dimensional parameters as

$$x=\frac{r^*}{r_t^*} \tag{4.1.2}$$

$$z=\frac{z^*}{\delta} \tag{4.1.3}$$

$$\beta=\frac{k_r}{k_z} \tag{4.1.4}$$

$$K=\frac{1}{\sqrt{\beta}}\left(\frac{r_t^*}{\delta}\right) \tag{4.1.5}$$

Plugging these parameter and recalling the definition of θ from equation (3.2.15), equation(4.1.1) yields

$$\frac{1}{x}\frac{\partial}{\partial x}\left(x\frac{\partial\theta}{\partial x}\right)+K^2\frac{\partial^2\theta}{\partial z^2}=0 \tag{4.1.6}$$

The boundary conditions are

- At fin base:

$$\text{at}\quad x=\frac{r_b^*}{r_t^*}=R_r\quad\text{and}\quad\text{any}\quad z;\quad\theta=1\quad\text{and}\quad\Omega=1 \tag{4.1.7}$$

- At symmetry line:

$$\text{at} \quad \text{any} \quad x \quad \text{and} \quad z = 0; \quad \frac{d\theta}{dz} = 0 \tag{4.1.8}$$

- At fin surface:

Applying energy balance on the fin surface cell

$$q_{conduction} = q_{convection} + q_{condensation} \tag{4.1.9}$$

$$k_z \frac{dT}{dz^*} = h\,(T_a - T) + h_D\, i_{fg}\,(\omega_a - \omega) \tag{4.1.10}$$

Using the definitions defined in section 3.2 and above we get

$$-\left(\frac{k_z}{h\,\delta}\right)\frac{d\theta}{dz} = [\theta + Co\,\Omega] \tag{4.1.11}$$

Defining Biot number in z-direction as

$$Bi_z = \frac{h\,\delta}{k_z} = Bi_r\,\beta \tag{4.1.12}$$

$$Bi_r = \frac{h\,\delta}{k_r} \tag{4.1.13}$$

The boundary conditions become

$$\text{at} \quad \text{any} \quad x \quad \text{and} \quad z = 1; \quad \frac{d\theta}{dz} + Bi_z\,[\theta + Co\,\Omega] = 0 \tag{4.1.14}$$

- Similarly at the fin tip with simultaneous heat and mass transfer the equation becomes:

$$\text{at} \quad x=1 \quad \text{and} \quad \text{any} \quad z; \quad \frac{d\theta}{dx}+Bi_r\,K\left[\theta+Co\,\Omega\right]=0 \qquad \text{convective tip} \tag{4.1.15}$$

$$\text{at} \quad x=1 \quad \text{and} \quad \text{any} \quad z; \quad \frac{d\theta}{dx}=0 \qquad \text{insulated tip} \tag{4.1.16}$$

Since we need one more relation between θ and Ω, we use the psychrometric correlations provide by Ref. [63].

The dimensionless heat transfer rate from the fin is the summation of heat transfer from the surface and the fin tip. Hence,

$$Q=Q_s+Q_t \tag{4.1.17}$$

Where

$$dQ_s=\frac{h\left(2\pi r^* dr^*\right)\left(T_a-T\right)+h\left(2\pi r^* dr^*\right)B\left(\omega_a-\omega\right)}{2\pi r_b^*\,k_z\left(T_a-T_b\right)} \tag{4.1.18}$$

which upon simplification becomes

$$Q_s=Bi_z\frac{K\sqrt{\beta}}{R_r}\int_{Rr}^{1}\left[\theta+Co\,\Omega\right]x\,dx \tag{4.1.19}$$

Similarly for a convective tip

$$dQ_t=\frac{h\left(2\pi r_t^* dz^*\right)\left[\left(T_a-T\right)+B\left(\omega_a-\omega\right)\right]}{2\pi r_b^*\,k_z\left(T_a-T_b\right)} \tag{4.1.20}$$

becomes

$$Q_t = \frac{Bi_r\,\beta}{R_r}\int_0^1 \left[\theta + Co\,\Omega\right] dz \tag{4.1.21}$$

The maximum heat transfer from the fin will be when the entire fin is at the base temperature and base humidity ratio and is given by

$$Q_{\max} = \frac{2\pi h\left[\left(T_a - T_b\right) + B\left(\omega_a - \omega_b\right)\right]\left\{\left(r_t^{*2} - r_b^{*2}\right) + r_t^{*}\left(2\,\delta\right)\right\}}{2\pi\, r_b^{*}\, k_z\left(T_a - T_b\right)} \tag{4.1.22}$$

Which reduces to

$$Q_{\max} = \frac{Bi_z}{R_r}\left(\theta_b + Co\,\Omega_b\right)\left[K\left(1 - R_r^{\,2}\right) + 2\right] \tag{4.1.23}$$

Finally, the efficiency of the fin is the ratio of total heat transfer from the fin to maximum possible i.e.

$$\eta = \frac{Q}{Q_{\max}} \tag{4.1.24}$$

As it should be, the total heat transfer from the fin surface is a function of differences in temperatures and humidity ratios of the ambient air and the fin. In addition to this, the efficiency of the fin is dependent on the distribution of temperature and humidity ratio. The above presented derivation is a general case in which we can have multiple combinations. For example, we can have insulated tip or convective tip condition. If the tip is convective then we can have different Biot numbers at the tip surface and at the fin surface. Furthermore, we can even change the thermal conductivities in r^* and z^* directions. These combinations can be evaluated for heat transfer as well as heat and

mass transfer. However, the base case would be when Biot numbers as well as the thermal conductivities are equal and the tip is convective for heat transfer case.

4.2 Two Dimensional Partially Wet Fin Model

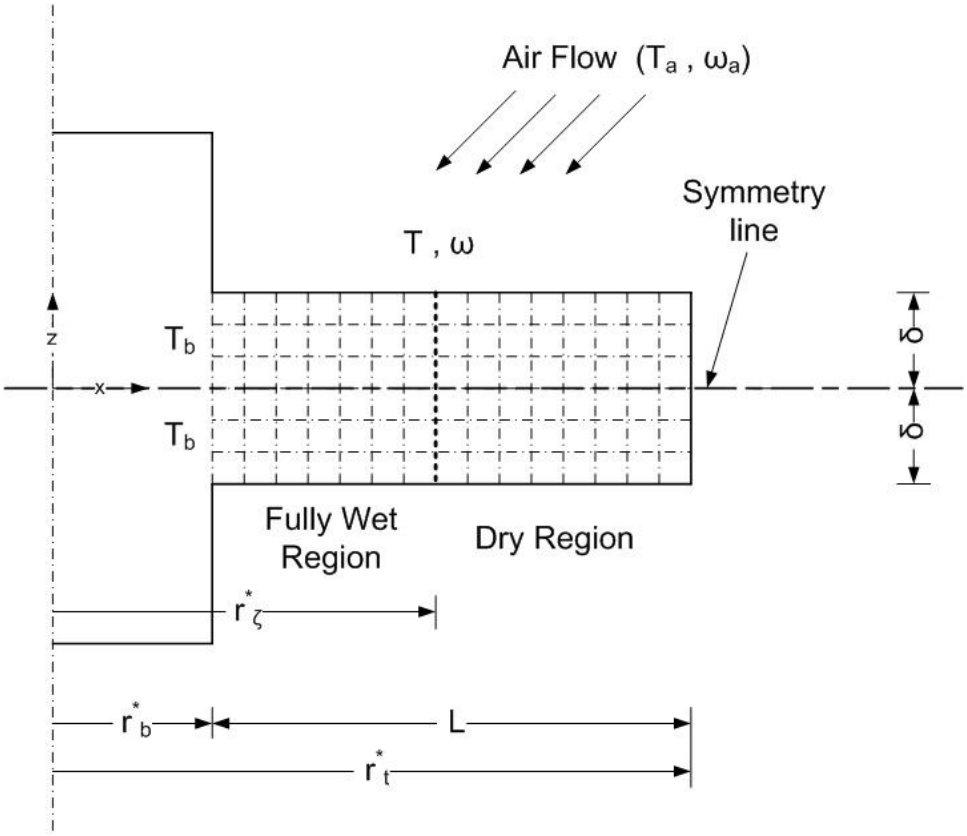

Figure 4-2 Schematic of a Partially Wet Two Dimensional Fin

As it was the case with one-dimensional model, there exist a radial distance r^*_ζ before which the fin is fully wet and after it the fin is dry. Under these conditions we need to write separate governing equations for the boundary condition in order to calculate the heat transferred from/to the fin surface.

The boundary conditions mentioned in equation (4.1.7) and (4.1.8) will still hold but the other two will change as follows:

- At the fin surface i.e. at any x and $z=1$,

For $R_r \le x \le x_\zeta$

$$\frac{d\theta}{dz} + Bi_z\left[\theta + Co\,\Omega\right] = 0 \tag{4.2.1}$$

For $x_\zeta \le x \le 1$

$$\frac{d\theta}{dz} + Bi_z\theta = 0 \tag{4.2.2}$$

- At the fin tip i.e. at $x=1$ and any z

$$\frac{d\theta}{dx} + Bi_r\,K\,\theta = 0 \quad \text{convective tip} \tag{4.2.3}$$

$$\frac{d\theta}{dx} = 0 \quad \text{insulated tip} \tag{4.2.4}$$

Now the heat transfer from the fin surface will become,

$$Q_s = Bi_z\frac{K\sqrt{\beta}}{R_r}\left[\int_{Rr}^{x_\zeta}\left[\theta + Co\,\Omega\right]x\,dx + \int_{x_\zeta}^{1}\theta\,x\,dx\right] \tag{4.2.5}$$

And that from the convective tip will be,

$$Q_t = \frac{Bi_r\,\beta}{R_r}\int_0^1 \theta\,dz \tag{4.2.6}$$

The total heat transfer from the fin will become the summation of the previous two equations, i.e.

$$Q = Q_s + Q_t \tag{4.2.7}$$

Using the relation of $Q_{\max}$ from equation (4.1.23) we finally have,

$$\eta = \frac{Q_s + Q_t}{Q_{\max}} \tag{4.2.8}$$

It should be noted that for an insulated tip $Q_t = 0$.

4.3 Dry Fin Case

This case represents heat transfer solution with same Biot numbers and thermal conductivities in r^* and z^* directions that is for isotropic material with $\beta = 1$. It is a special case to our solution and matches with that of Cotta and Mikhailov [66] which is presented below.

The dimensionless governing equation is

$$\frac{1}{x}\frac{\partial}{\partial x}\left(x\frac{\partial \theta'(x,z)}{\partial x}\right) + K^2\frac{\partial^2 \theta'(x,z)}{\partial z^2} = 0, \qquad R_r < x < 1, \quad 0 < z < 1 \tag{4.2.9}$$

With the boundary conditions as follows:

$$\theta'(R_r, z); \quad \frac{\partial \theta'(1,z)}{\partial x} + Bi_t\, K\, \theta'(1,z) = 0, \quad 0 < z < 1 \tag{4.2.10}$$

And

$$\frac{\partial \theta^{'}(x,0)}{\partial z}=0;\quad \frac{\partial \theta^{'}(x,1)}{\partial z}+Bi_s\,\theta^{'}(x,1)=0,\quad R_r<x<1 \tag{4.2.11}$$

With the following dimensionless groups

$$\theta^{'}(x,z)=\frac{T(r^{*},z^{*})-T_a}{T_b-T_a} \tag{4.2.12}$$

$$K=\frac{r_t^{*}}{\delta} \tag{4.2.13}$$

$$Bi_s=\frac{h_s\,\delta}{k} \tag{4.2.14}$$

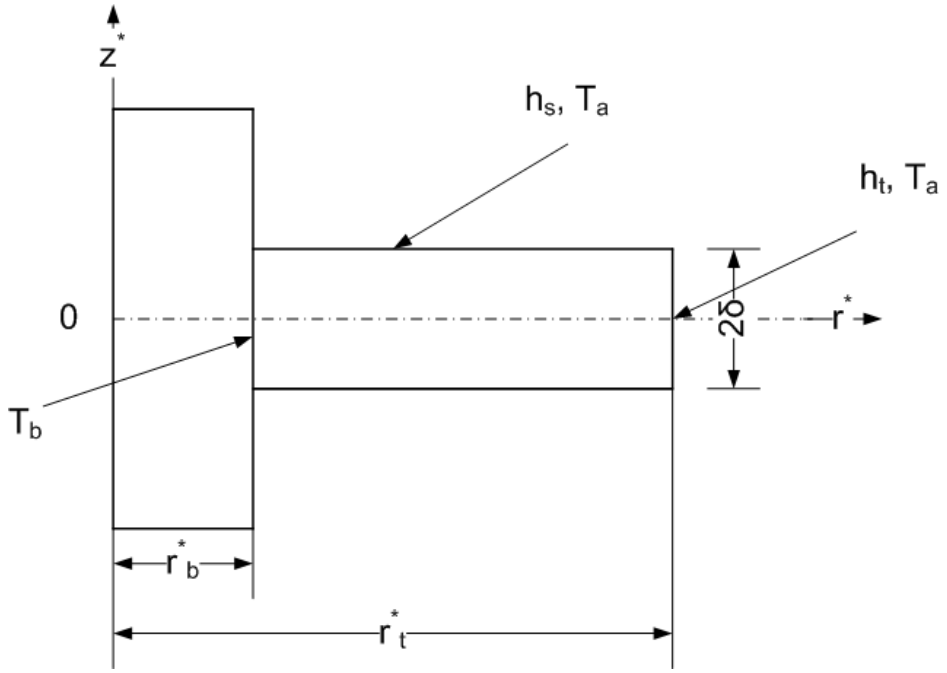

Figure 4-3 Geometry and coordinate system for radial fin analysis of Ref. [66]

$$Bi_t=\frac{h_t\,\delta}{k} \tag{4.2.15}$$

h_s and h_t are the heat transfer coefficients at the lateral surfaces and fin tip respectively.

The temperature distribution relation provided by the authors is something like this

$$\theta'(x,z) = 2\sum_{j=1}^{\infty} \frac{\sin\lambda_j \cos(\lambda_j z)}{\left[\lambda_j + \sin\lambda_j \cos\lambda_j\right]} F(\lambda_j, x) \tag{4.2.16}$$

Where

$$F(\lambda_j, x) = \frac{K_0(\lambda_j K x) C_3 - I_0(\lambda_j K x) C_4}{K_0(\lambda_j K R_r) C_3 - I_0(\lambda_j K R_r) C_4} \tag{4.2.17}$$

$$C_3 = Bi_t I_0(\lambda_j K) + \lambda_j I_1(\lambda_j K) \tag{4.2.18}$$

$$C_4 = Bi_t K_0(\lambda_j K) - \lambda_j K_1(\lambda_j K) \tag{4.2.19}$$

The non-dimensional heat transfer from the base of the fin given by the authors as

$$Q_b = \frac{q_b^*}{2\pi r_b^* k(T_b - T_a)} = \frac{-2}{K} \frac{d\theta_{av}(x)}{dx}\bigg|_{x=0} \tag{4.2.20}$$

Finally

$$Q_b = 4\sum_{j=1}^{\infty} \frac{\sin^2\lambda_j}{\left[\lambda_j + \sin\lambda_j \cos\lambda_j\right]} G(\lambda_j) \tag{4.2.21}$$

where

$$G(\lambda_j) = \frac{K_1(\lambda_j K R_r) C_3 + I_1(\lambda_j K R_r) C_4}{K_0(\lambda_j K R_r) C_3 - I_0(\lambda_j K R_r) C_4} \tag{4.2.22}$$

4.4 Two-Dimensional Fin Optimization

As we did for one-dimensional optimization, we will define some new terms. The non-dimensional volume for the fin shown in Figure 4-1 is written as

$$v = \frac{V}{\pi r_b^{*3}} = \frac{2\delta\pi\left(r_t^{*2} - r_b^{*2}\right)}{\pi r_b^{*3}} \tag{4.2.23}$$

Which is essentially the same as that mentioned in equation (3.8.3). In addition, fin base radius to base thickness may be written as

$$w' = \frac{r_b^*}{2\delta} \tag{4.2.24}$$

Now if we look at equation (4.1.17) through (4.1.21) and considering equations (4.1.5) and (4.1.12), we find that for isotropic materials ($\beta = 1$), Q is the function of radial Biot number Bi_r , fin base radius to base thickness ratio w_t and non-dimensional fin volume v .

$$Q_s = Bi_z \frac{w'}{R_r} \int_{R_r}^{1} \left[\theta + Co\,\Omega\right] x\, dx \tag{4.2.25}$$

$$Q_t = \frac{Bi_r\,\beta}{R_r} \int_{0}^{1} \left[\theta + Co\,\Omega\right] dz \tag{4.2.26}$$

Where R_r can be written as

$$R_r = \sqrt{\frac{1}{1 + v\,w'}} \tag{4.2.27}$$

A similar conclusion can be drawn when we see equations (4.2.5) to (4.2.7) for partially wet fins. So for a given fin volume and by fixing radial Biot number we can find the optimum fin base radius to base thickness ratio that will give us the maximum heat transfer at the operating conditions. In case of orthotropic materials, we will be having one more variable and that will be the ratio of thermal conductivities in the two fundamental directions and is defined by equation (4.1.4).

The numerical procedure is the same as was mentioned in section 3.6 but we need to do the grid independence again since we have now moved from one-dimensional analysis to two-dimensional analysis. The grid independence has been achieved for the base case and is presented in the following section.

4.5 Grid Independence and Validation

For achieving grid independence in two-dimensional modeling, the size of the fin domain was divided in to 11 X 11, 51 X 51, 101 X 101 and 151 X 151 numbers of nodes. The following figure represents the total amount of heat transfer (non-dimensional) from the fin surface to the ambient air under the following conditions. The Biot number at the tip is equal to that at the fin surface and its value was taken as 1, the ratio of fin base radius to fin tip radius was assumed as 0.3, ambient air at 27 ℃, base at 7 ℃ and the relative humidity as 20%. Under these operating conditions, the total heat transfer was calculated for various K values, which is given by equation (4.1.5). Analytical solution was also plotted on the same graph to check whether our numerical results were approaching the analytical ones or not. It can be seen from the figure that for 101 X 101 size matrix and 151 X 151 size matrix, the curves are almost overlapping. Moreover, they are closest to

the analytical result with maximum difference between them as 1.8%. This conclusion also validates our numerical model. Therefore, we can safely suggest that 101 X 101 size matrix will be able to give good results for our numerical solutions.

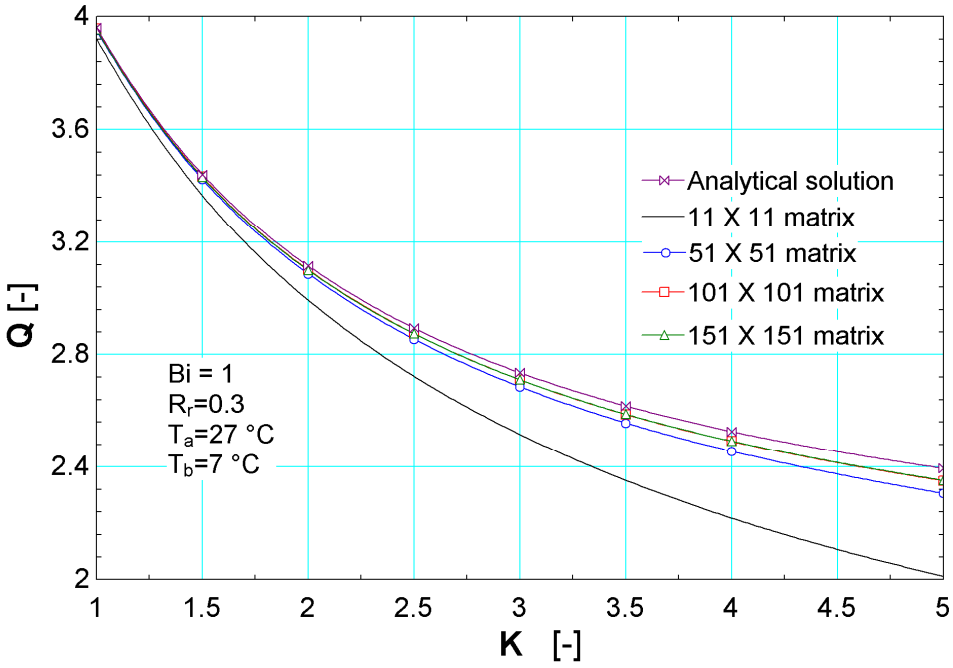

Figure 4-4 Grid independence for a two-dimensional domain for only heat transfer condition and comparison with Ref. [67]

4.6 Results and Discussion

We will compare our results with available analytical solution for only heat transfer first by considering the base case.

4.6.1 Heat transfer

Ref. [66] have given the results in tabular format for $h_s = h_t$, constant thermal conductivity k for $R_r = 0.3$. This tabular results are compared with our work and are shown in Table 4-1. The same is plotted in figure below

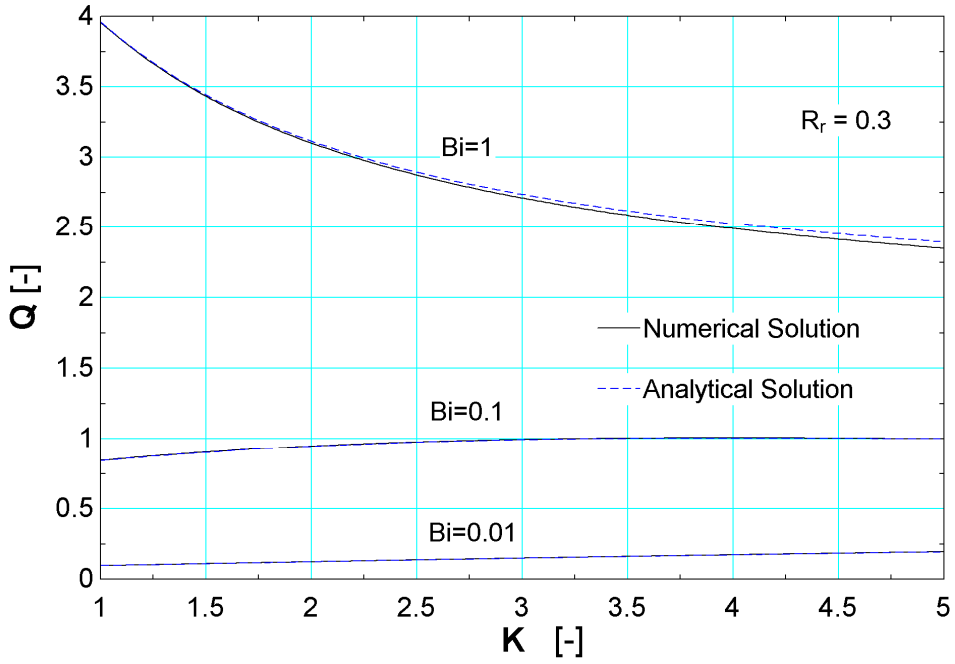

Figure 4-5 Comparison of analytical and numerical heat transfer solution for two-dimensional case

Table 4-1 Comparison of heat transfer rates for analytical and numerical solution at different Biot numbers and aspect ratios for 2-D model

$Bi_s = Bi_t = Bi$	K	Q	Q_b	*% Error*
0.01	1	0.0957	0.0956	-0.10%
0.01	1.5	0.1097	0.1095	-0.18%
0.01	2	0.1233	0.123	-0.24%
0.01	2.5	0.1364	0.1361	-0.22%
0.01	3	0.1491	0.1486	-0.34%
0.01	3.5	0.1612	0.1607	-0.31%
0.01	4	0.1728	0.1722	-0.35%
0.01	5	0.1942	0.1935	-0.36%
0.1	1	0.8441	0.8428	-0.15%
0.1	1.5	0.9035	0.9018	-0.19%
0.1	2	0.9467	0.9447	-0.21%
0.1	2.5	0.9762	0.9741	-0.22%
0.1	3	0.9944	0.9924	-0.20%
0.1	3.5	1.0039	1.0022	-0.17%
0.1	4	1.0066	1.0053	-0.13%
0.1	5	0.9984	0.9982	-0.02%
1	1	3.9561	3.9603	0.11%
1	1.5	3.433	3.4415	0.25%
1	2	3.101	3.1148	0.44%
1	2.5	2.8741	2.8934	0.67%
1	3	2.7102	2.7351	0.91%
1	3.5	2.5866	2.6168	1.15%
1	4	2.4902	2.5254	1.39%
1	5	2.3492	2.3936	1.85%

It can be seen from the Table 4-1 and Figure 4-5 that at lower Biot number the error between the two solutions is almost zero however, as we increase the Biot number value this error starts growing but is still in acceptable range. Also, at $Bi = 0.01$ the variation of heat transfer rate is very small as we increase the aspect ratio $K = r_t^* / \delta$. However this

variation is little bit more for $Bi = 0.1$ and maximum for $Bi = 1$. Moreover, on increasing the aspect ratio the heat transfer rate increases for lower Biot numbers, but for $Bi = 1$ it follows the reverse trend. This can be explained by the argument that when we are increasing K, r_t^* is increasing and δ is decreasing. So at low Biot numbers (ratio of conduction resistance within material to convection resistance at the surface), this would lead to thin and long fins which will be having temperatures close the base temperature. This results in higher heat transfer rate on increasing K. However, as we move to higher Biot numbers, the effect of two-dimensional heat transfer will start coming into picture. Now when we increase K, the conduction resistance will have significant effect due to increased fin length and already thick fin. That's why we observe a drop in heat transfer rate for $Bi = 1$.

Figure 4-6 shows the two dimensional temperature distribution contours for the half section of the fin above symmetry line under only heat transfer with convective tip. The input variable for this result were $R_r = 0.6$, $Bi = 1$, $K = 1$ and $RH_a = 0.2$

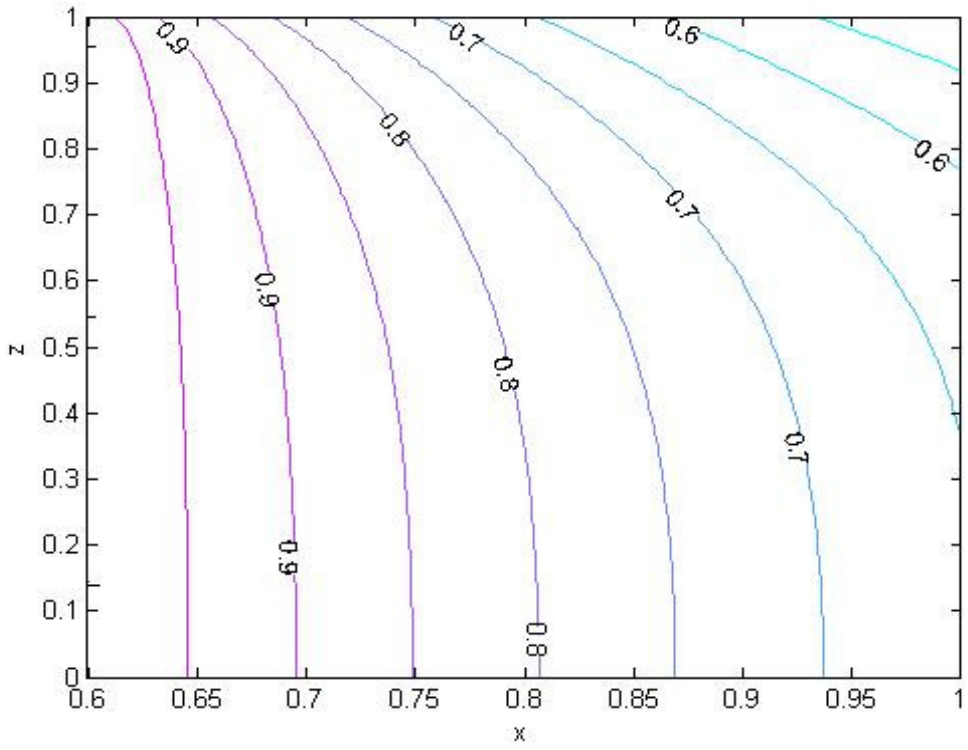

Figure 4-6 Contour of temperature in the region above symmetry line of 2D fin domain for dry fin

4.6.2 Heat and mass transfer

In this section, all the presented results are for identical thermal conductivity values in r^* and z^* directions. A graph similar to the dry fin temperature distribution is presented below for the same condition but for relative humidity as 100%. It is clearly visible that the temperature variation is more wide spread in comparison to dry fin case. The effect of heat transfer from the surface and tip of the fin is distinguishable from that of the symmetric line.

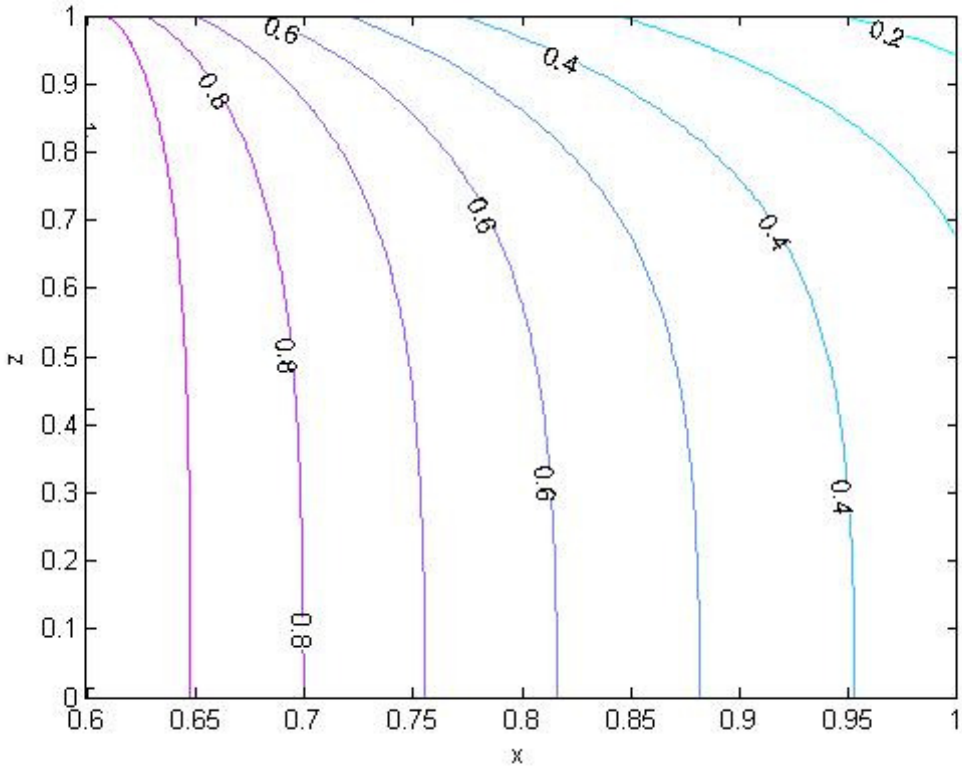

Figure 4-7 Contour of temperature in the region above symmetry of 2D fin domain for fin with heat and mass transfer

Figure 4-8 shows the effect of aspect ratio, K on the fin efficiency η operating at various relative humidity values for isotropic materials. The operating conditions are mentioned on the figure itself. We see that, irrespective of the relative humidity value, if we decrease the aspect ratio the fin efficiency increases. The graph shows that the more the thickness of the fin the better will be its output for constant tip radius.

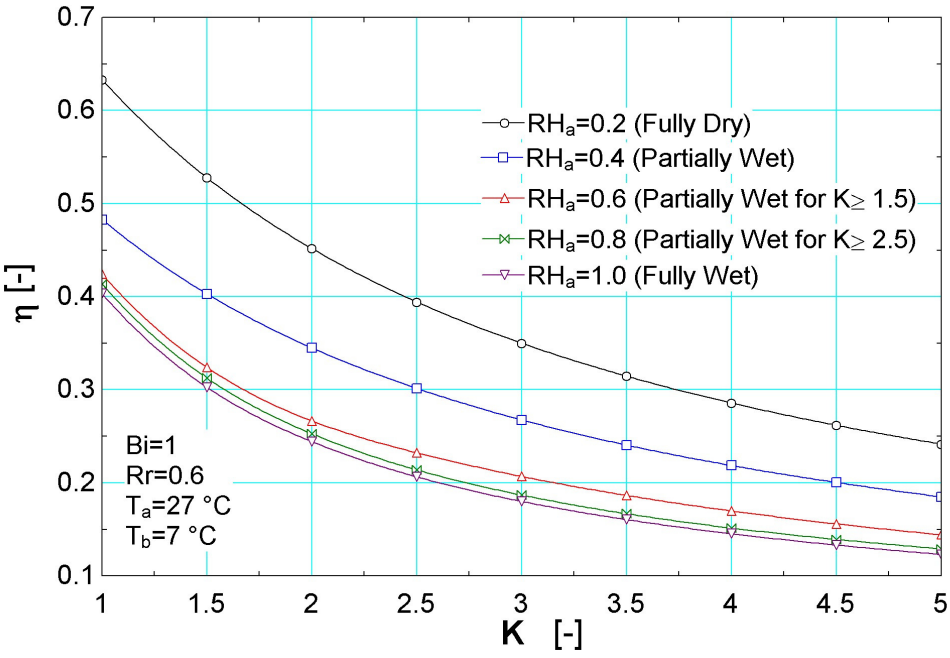

Figure 4-8 Effect of aspect ratio on the fin efficiency

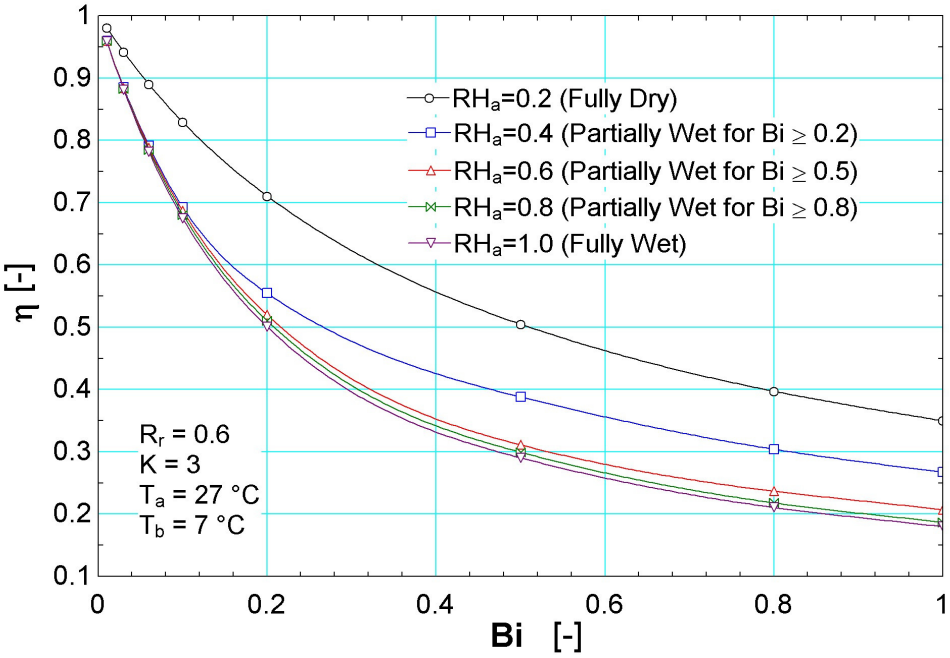

Figure 4-9 Effect of Biot number on the fin efficiency

The effect of variation of the Biot number on the fin efficiency for radius ratio of 0.6, aspect ratio value of 3, ambient air of 27 ℃ and base air temperature of 7 ℃ is shown in Figure 4-9 for various relative humidities. It clearly depicts that for lower values of Biot number, the fin efficiency is better at every relative humidity of the ambient air. The high fin efficiency at low Biot numbers doesn't mean that heat transfer rate is higher for these situations rather it implies that the maximum possible heat transfer rates are low at low Biot number. The condensation of water vapor further increases this $Q_{\max}$ thereby further decreases the fin efficiency.

In contrast to the previous two trends, for any value of relative humidity, as we increase the radius ratio R_r, the fin efficiency increases. This means that the shorter the fin length is, the more it is efficient (Figure 4-10).

It is worth noting that higher values of RH_a does not influence the fin efficiency considerably in comparison to medium range values. This can be observed from Figure 4-8 through Figure 4-10.

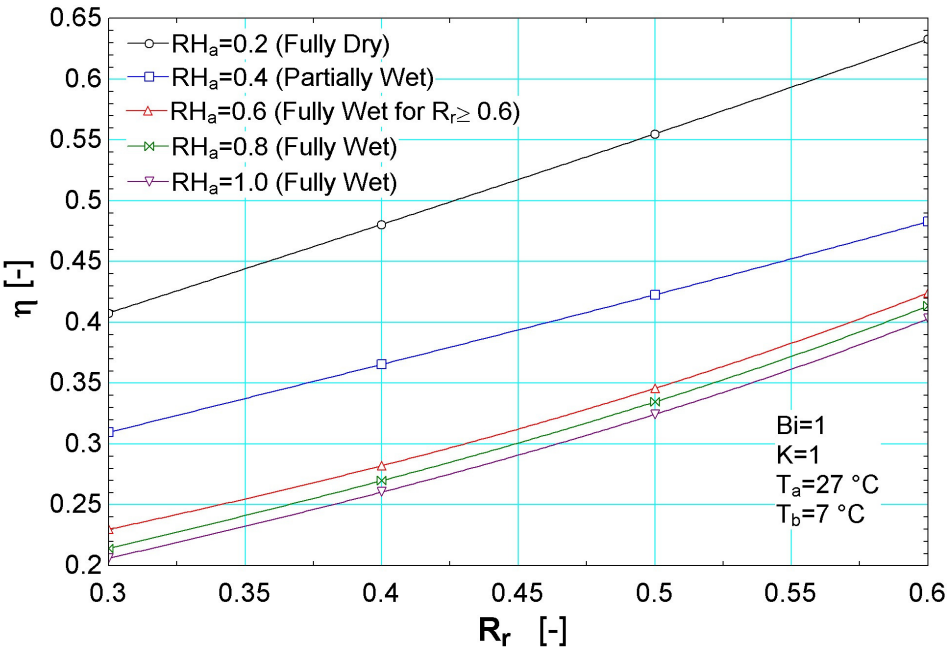

Figure 4-10 Variation of efficiency with radius ratio R_r

4.6.3 Effect of orthotropic thermal conductivity

Due to the advances in polymer composites, new materials have come into picture, which provide significant ease in molding, and have relatively low density than the conventional copper and aluminum. These composites, when added with high thermal conductivity continuous carbon fibers, display orthotropic behavior i.e. different thermal conductivity in the fundamental directions. The thermal conductivity ratio in fiber axis direction is sometimes two orders of magnitude higher than in the orthotropic direction (perpendicular to fiber axis). Some of the typical polymers and their properties are shown in Table 4-2.

Table 4-2 Polymer composite properties Ref. [59]

Filler	Matrix	Parallel to fibers (W/m-K)	Normal to fibers (W/m-K)	Density (g/cc)
Continuous carbon fiber	Polymer	330	3-10	1.8
Discontinuous carbon fiber	Polymer	10-100	3-10	1.7
Graphite	Epoxy	370	6.5	1.94
Short carbon fiber	PPS	25	4	1.7

Different values of thermal conductivities are assumed in r^* and z^* directions and for different ratios of these two, various results are obtained. Figure 4-11 shows the effect of thermal conductivity ratios on the heat transfer rate from the fin as a function of radial Biot number Bi_r .We find that the heat transfer rate increases upon increasing the value of Biot number in radial direction as well as the thermal conductivity ratio. On the other hand, reverse trend is obtained for fin efficiency vs. radial Biot number and is presented in Figure 4-12. That is, as the Biot number and β are increased, the fin efficiency decreases. The reason is that when we increase the Biot number and β, the maximum heat transfer possible also increase. This increase in $Q_{\max}$ is more than the increase in Q hence the fin efficiency decrease.

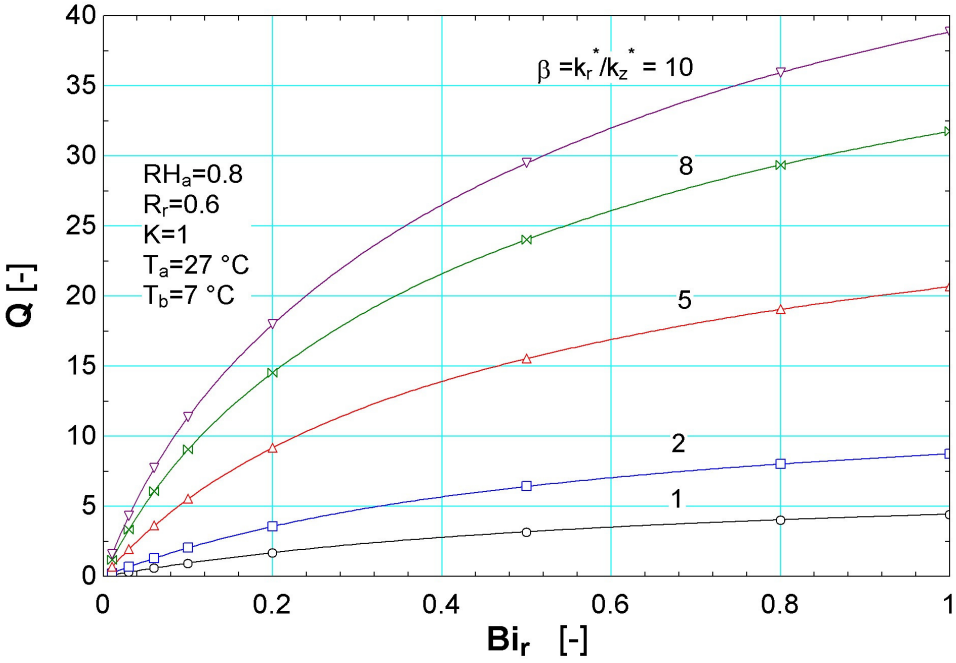

Figure 4-11 Effect of thermal conductivity ratio on the heat transfer rate

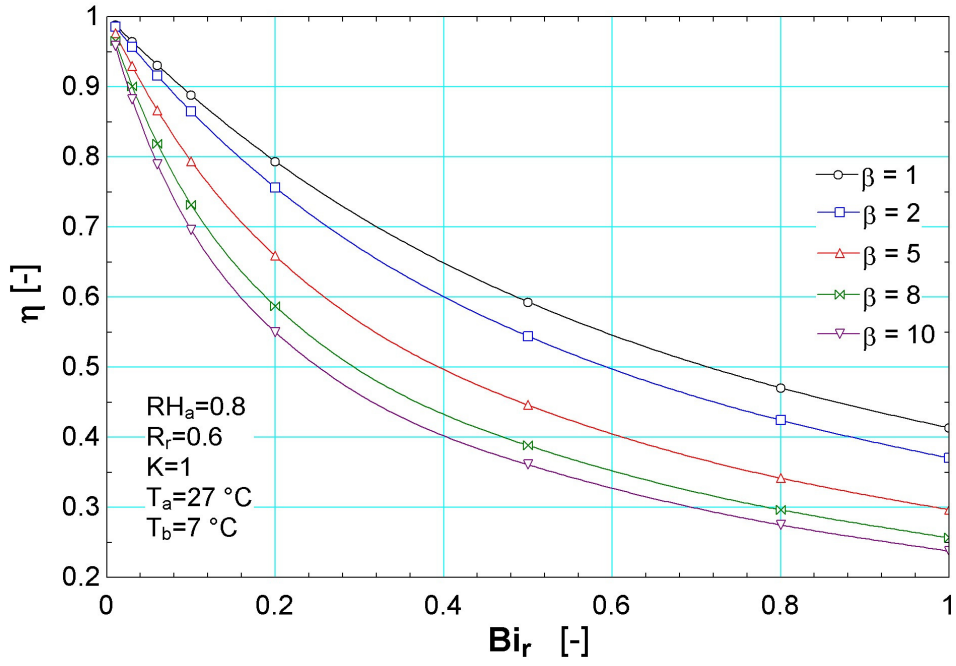

Figure 4-12 Efficiency vs. radial Biot number for various thermal conductivity ratios

4.6.4 Optimization

As it was mentioned in section 4.4, we will fix the values of radial Biot number and non-dimensional fin volume and try to find the optimum w' that will give us the maximum heat transfer at the operating conditions. As we shall demonstrate in the following paragraphs, it can be achieved for both orthotropic as well as isotropic fins. This optimization is achieved by using Matlab toolbox. Since we are optimizing with respect to only one variable, Matlab 'fminsearch' tool box creates a one-dimensional simplex and do a random search to find the minima of the function. We can manipulate the function to do maximization for us by making the function negative. So Matlab will search for a minima and that minima will be the maxima for our function.

Figure 4-13 shows the effect of fin volume on the optimum fin dimension. This result was obtained at a relative humidity of 80%, radial Biot number of 0.1 and for an isotropic material that is, $\beta = 1$. Although the optimum dimension increase with decreasing the fin volume, but there is not much change in the heat transfer value. It must be noted here that due to the chosen scale on the x-axis, it looks like that the curves for low fin volume does not have a peak but in fact, they do have a peak heat transfer rate which would be visible on a longer scale. Another interesting point is that the heat transfer rate at optimum fin dimension value is not very sensitive to non-dimensional fin volume. This leads to the conclusion that to find the optimum dimension for a required heat transfer rate, we have a range of fin volumes that will give us close to the desired output (heat transfer rate).

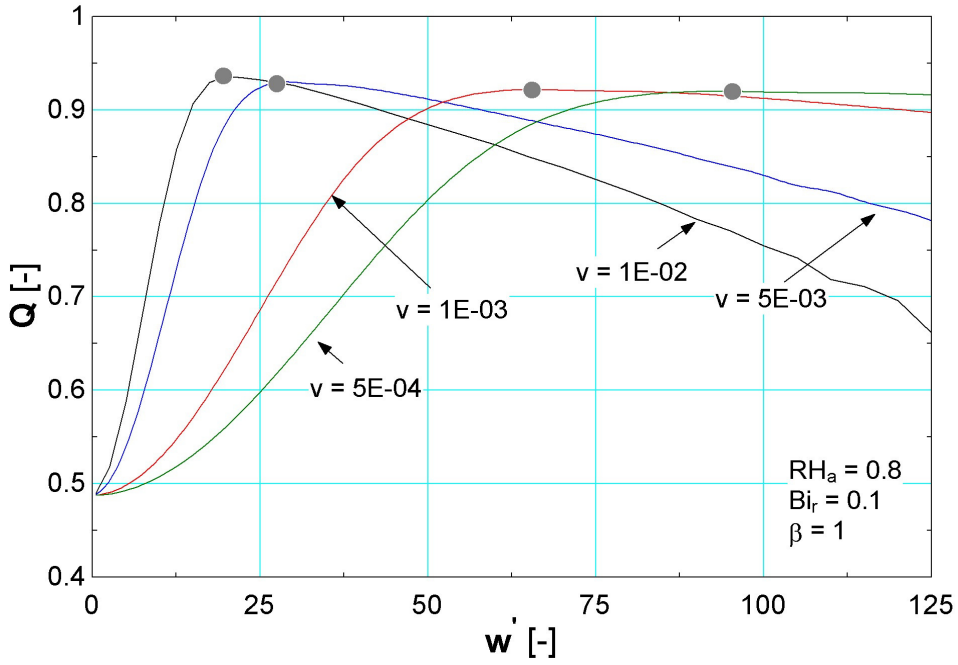

Figure 4-13 Effect of non-dimensional volume on the optimum fin dimensions

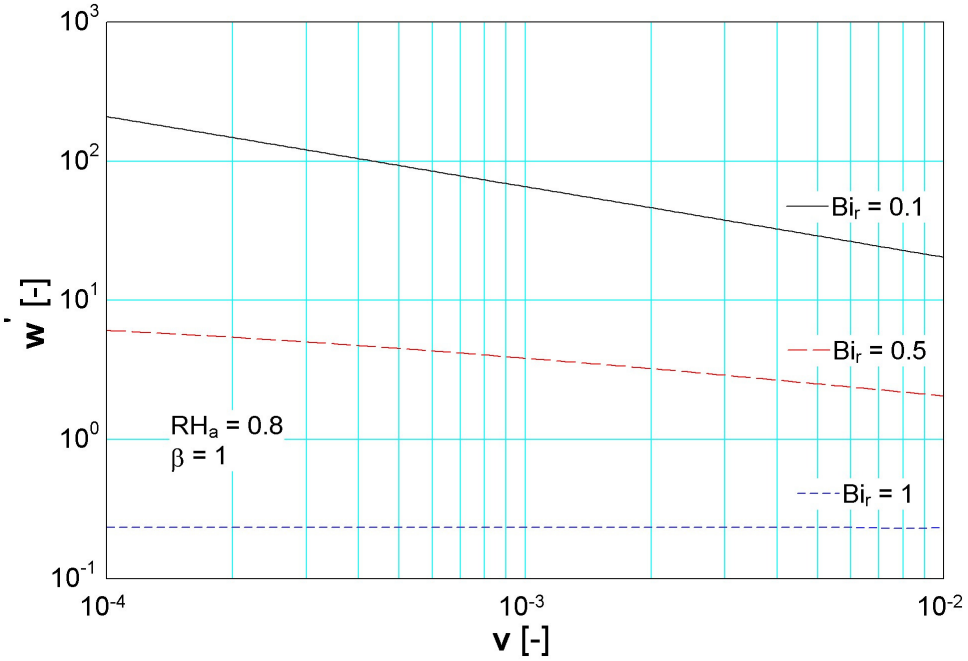

Figure 4-14 Optimum dimensions for various fin volumes at different radial Biot numbers

The locus of optimum fin dimensions for various radial biot numbers as a function of dimensionless fin volume is shown in the Figure 4-14, which is a log-log plot. It can be observed that as the biot number increases, the effect of fin volume on the optimum fin dimension decreases. For $Bi_r = 1$, it reaches its peak and the optimum fin aspect ratio is almost constant.

The effect of thermal conductivity in x and z directions on the optimum fin dimensions is shown in Figure 4-15 in the form of their ratio. The value of radial Biot number, relative humidity and fin volume is mentioned on the graph itself. We observe from the figure that as we increase the thermal conductivity ratio β, the fin base ratio starts reducing up till a value of 6, from there onwards the fin base ratio starts to increase as we further increase the thermal conductivity ratio.

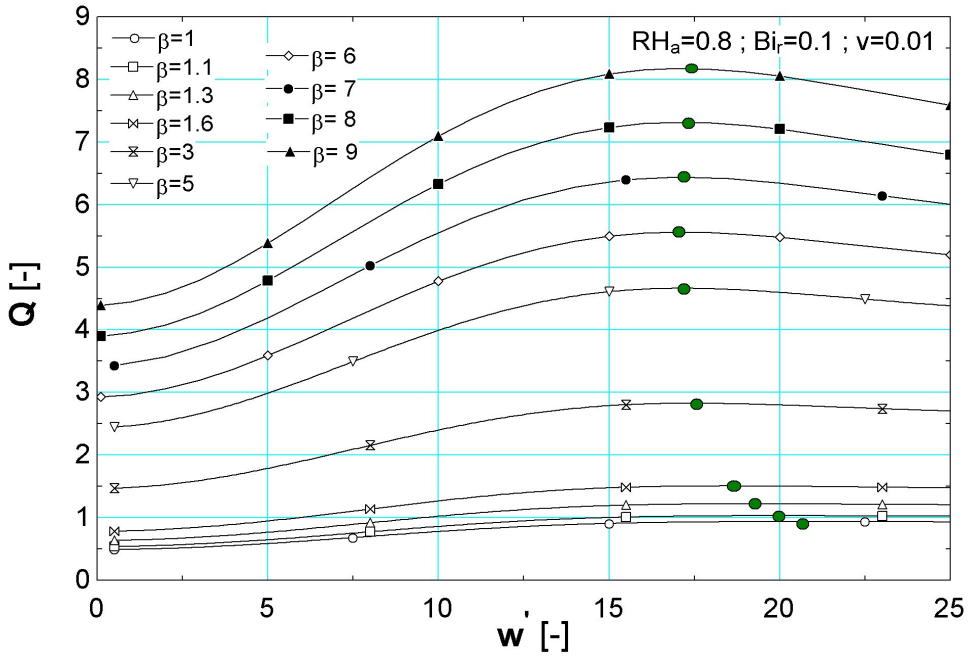

Figure 4-15 Effect of β on the optimum fin dimension for orthotropic materials

These two regions i.e., one showing decreasing optimum dimension and the other shows increasing trend are separated and shown in the figures below

(a)

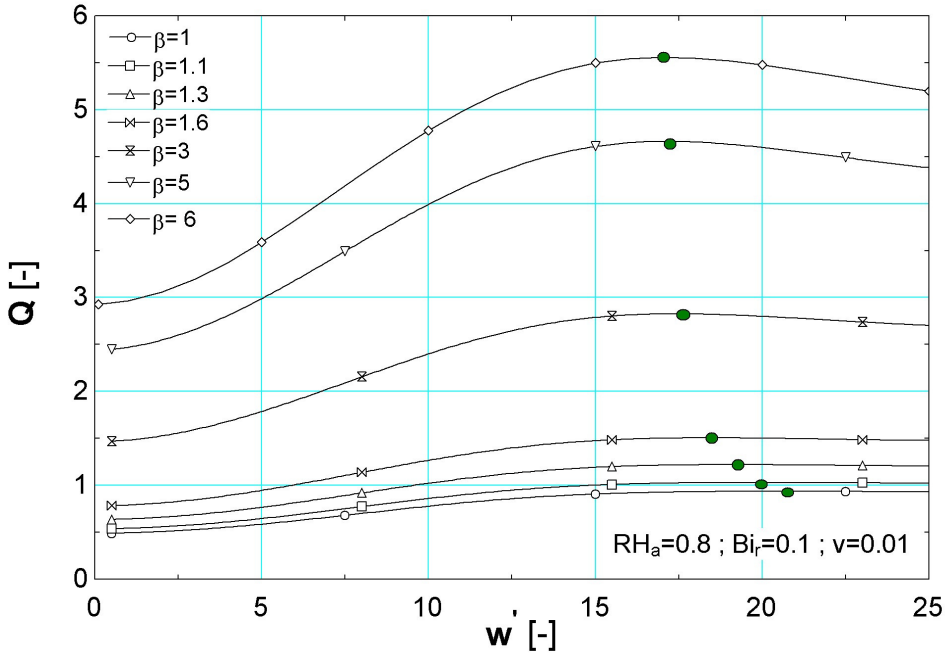

(b)

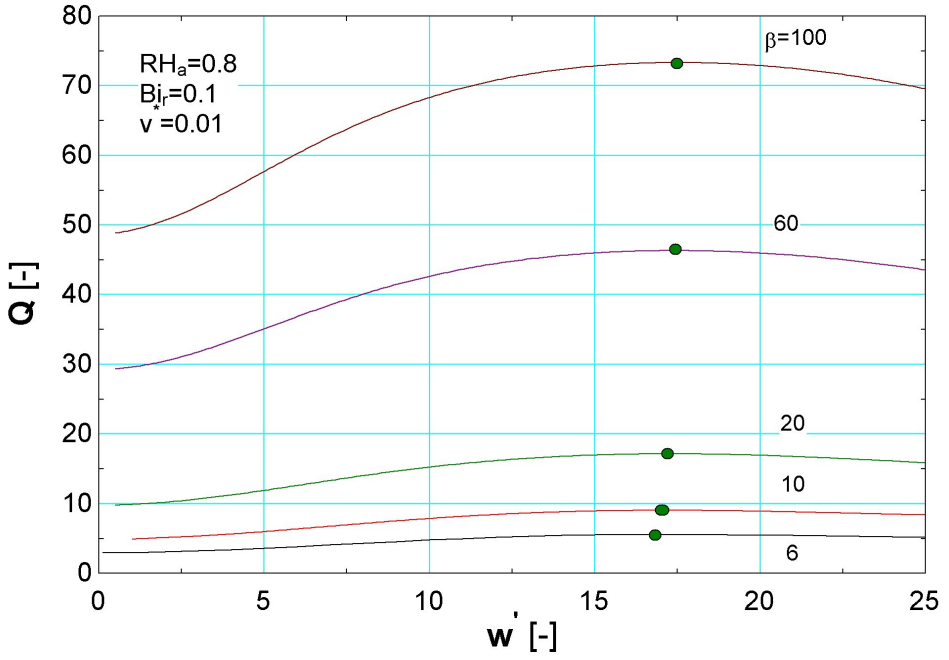

Figure 4-16 Heat transfer rate vs. optimum dimension for various thermal conductivity ratios: (a) Decreasing trend (b) Increasing trend

A graph similar to Figure 4-13 is shown in the Figure 4-17 for orthotropic material with a thermal conductivity ratio of 50. The trend is almost similar but the value of heat transfer rate at the optimum dimension of the fin has increased sharply. This clearly shows the importance of orthotropic material when specifying fins for thermal systems applications.

Again, a log-log plot is shown in Figure 4-18 for locus of optimum fin dimension at various thermal conductivity ratio values as a function of dimensionless fin volume. It is clearly visible that higher values of β does not affect the results much.

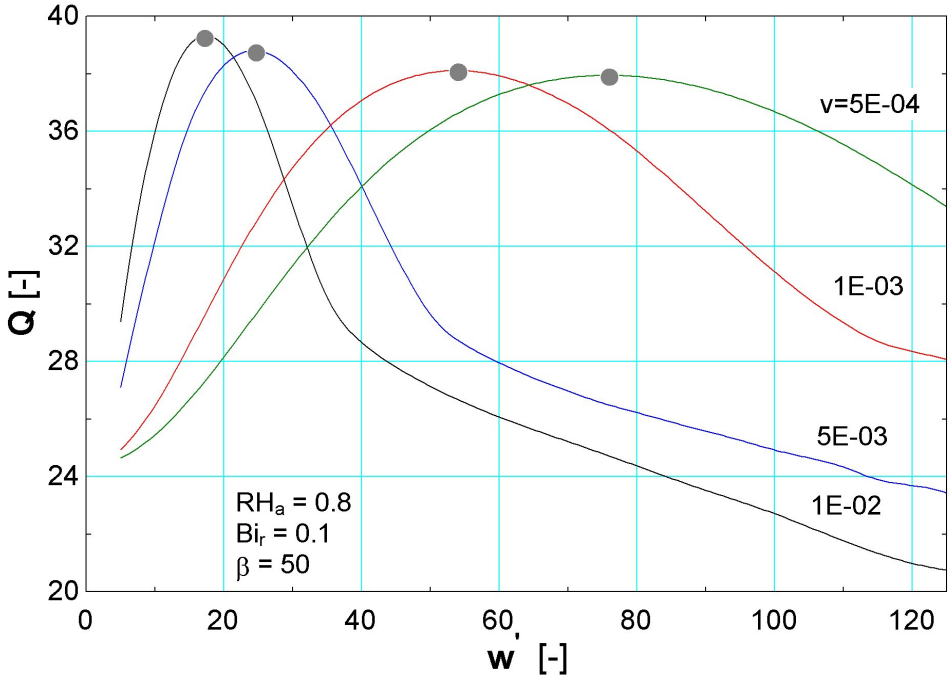

Figure 4-17 Effect of non-dimensional volume on the optimum fin dimensions for orthotropic materials

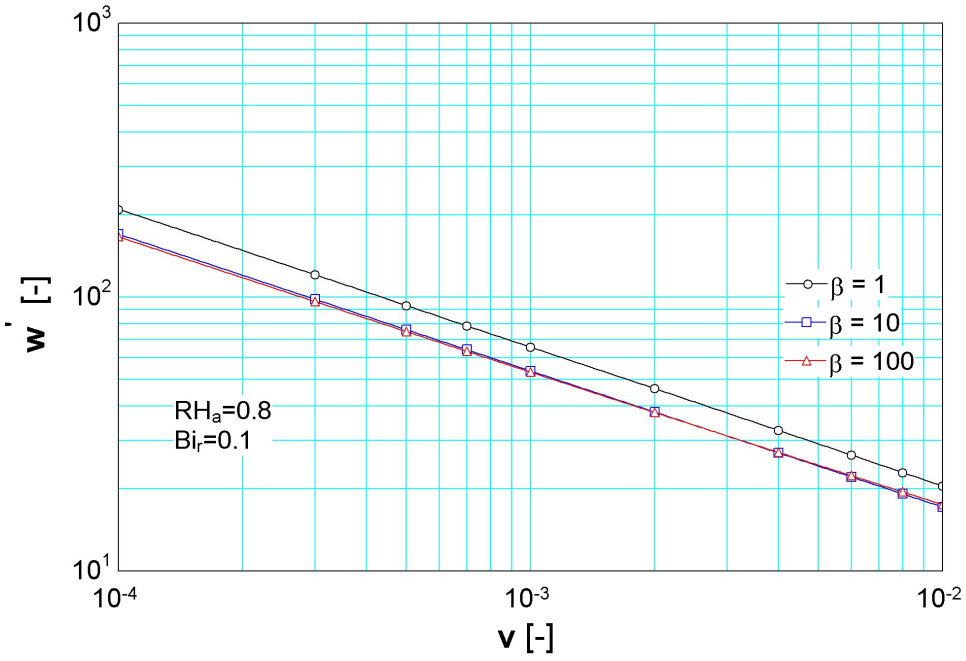

Figure 4-18 Optimum dimensions for various fin volumes at different β

CHAPTER 5

Conclusions and Recommendations

The objectives of this investigation were to study different types of annular fins under simultaneous heat and mass transfer and subsequently determining their optimum dimensions that give us the maximum heat transfer rate for a known quantity of fin material.

From the results obtained from the present study, the following conclusions can be deduced for one-dimensional case:

- Water condensation increases the surface temperature, which leads to lesser heat transfer and subsequently low efficiency.
- Upon increasing the fin parameter ($m_0 L$), the fin efficiency reduces.
- The transition from dry fin to partially wet fin produces more effect on the fin efficiency than from partially to fully wet condition.
- Fully dry fin always have the highest efficiency at any value of fin parameter at any radius ratio (R).

- As the radius ratio increases the efficiency of the fin decreases.
- Increase in the difference of the ambient air temperature and the fin base temperature decreases the efficiency.
- When condensation on the fin surface starts to occur, the relative humidity doesn't affect the efficiency much for low fin parameter values.
- For triangular and concave parabolic profile fins, when the relative humidity is low the temperature distribution curve is almost linear. This linearity is more visible for concave in comparison to triangular fin.
- Another conclusion regarding concave profile fin is that the temperature of the fin tip is always about the same as that of the ambient air irrespective of the humidity condition.
- For hyperbolic profile, analytical solution is obtained by modifying the fin parameter and the results are compared to numerical solution. It is observed that numerical results predict slightly higher efficiency.
- Optimum dimension results are presented in the form of graphs for all five types of annular profile fin, which could be very useful for a designer.
- Rectangular and hyperbolic profile fin results are compared with analytical solution. Numerical solution shows higher heat transfer rate with lesser corresponding aspect ratio compared to analytical results.
- From all the optimum dimension graphs, we see that if we know two parameters; like fin heat transfer parameter (u) and fin volume (v) or u and fin base ratio (w) or u and heat transfer rate (Q), we can identify the remaining two.

Heat transfer in two-dimensional domain is studied for annular fin of rectangular profile for isotropic as well as for orthotropic materials and the following conclusions are drawn:

- Generalized results are studied with respect to dimensionless variables such as fin aspect ratio K, radius ratio R_r, Biot number and radial-to-axial thermal conductivity ratios.
- The fin efficiency decreases as we increase the biot number regardless of the type of material.
- As with the one-dimensional case, relative humidity (RH_a) plays an important role in determining the fin efficiency.
- In case of isotropic materials, increasing the aspect ratio (K) of the fin has a negative effect on the efficiency whereas increasing the radius ratio R_r has a positive effect.
- For orthotropic materials, increasing the magnitude of the radial to orthogonal thermal conductivity ratio amplifies the heat transfer rate from the fin but reduces the fin efficiency.
- Optimal dimensions are computed and plotted for various non-dimensional fin volumes and for various radial to orthogonal thermal conductivity values.

Some of the suggested recommendations for future work are

- Studying heat and mass transfer interaction in fins for temperature dependent thermal conductivity.
- Analyzing the orthotropic behavior in more detail.

- To obtain heat and mass transfer solutions using a two-dimensional approach for other types of fins like triangular, concave parabolic and convex parabolic profiles.

Appendix

Corrected length for constant profile annular fin

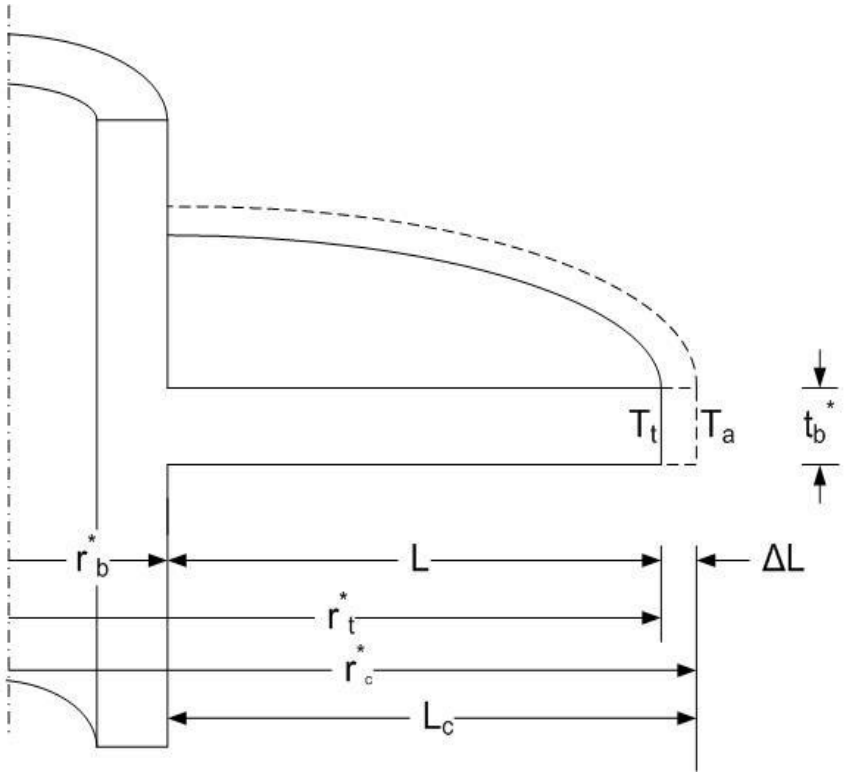

Figure A-1 Fictitious extension of fin length L to corrected adiabatic tip at L_c for rectangular profile annular fin

Without the extended tip, the heat transfer rate at $r^* = r_t^*$

$$q_t = h\left(2\pi r_t^* t_b\right)\left(T_a - T_t\right) + h_D\, i_{fg}\left(\omega_a - \omega_t\right)\left(2\pi r_t^* t_b\right)$$

and under the condition that $\frac{dT}{dr^*} = 0$ at $r^* = r_c^*$ at, ΔL must be such that q_t is all dissipated on the fictitious surface $2\Delta L$ or

$$h\left(2\pi r_t^* t_b\right)\left[\left(T_a - T_t\right) + B\left(\omega_a - \omega_t\right)\right] = 2h\left(2\pi r_t^* \left(L_c - L\right)\right)\left[\left(T_a - T_t\right) + B\left(\omega_a - \omega_t\right)\right]$$

which yields

$$L_c = L + \frac{t_b}{2}$$

Nomenclature

a_2	Constant defined in equation. (3.4.8), (kg_w/ kg_a)
A	fin cross-sectional area, (m^2)
b_2	constants defined in equation (3.4.9), (kg_w/ kg_a K)
B	parameter defined in equation (3.2.11), (℃)
Bi_r	Biot number in radial direction as mentioned in equation (4.1.13)
Bi_z	Biot number in orthogonal direction as mentioned in equation (4.1.12)
Co	constant defined in equation (3.2.20), (kg_w/ kg_a)
C	constant defined in equation (3.2.28), (kg_w/ kg_a K)
C_p	specific heat of incoming moist air stream, (J/kg.K)
h	heat transfer coefficient on the air side, (W/m^2K)
h_D	mass transfer coefficient, (kg/ m^2.s)
i_{fg}	latent heat of condensation of water vapor, (J/kg)
k	thermal conductivity of the fin material, (W/m K)
K	parameter defined in equation (4.1.5)

L fin length, (m)

Le Lewis number

$m_0 L$ fin parameter, (m^{-1})

m wet fin parameter defined in equation (3.4.11), (m^{-1})

n index of the fin profile mentioned in equation (3.2.19)

P_{atm} atmospheric pressure, (kPa)

q heat transfer rate, (W)

Q dimensionless heat transfer rate

RH_a relative humidity of incoming air stream

t dimensionless fin thickness

T Temperature, (℃)

R fin radius ratio, given as r_t^* / r_b^*

R_r Radius ratio for 2D case, given as r_b^* / r_t^*

r dimensionless radius

r_ζ dimensionless radius that separates between wet and dry regions on the fin surface

u dimensionless heat transfer parameter defined in equation (3.8.2)

u' dimensionless heat transfer parameter defined in equation (3.8.15)

v dimensionless fin volume defined in equation (3.8.3) or (3.8.4) for hyperbolic fin

w ratio of base radius to base thickness defined in equation (3.8.5)

w' ratio of base radius to base thickness defined in equation (4.2.24)

x dimensionless radius given by equation (4.1.2)

X dimensionless length of the fin

z dimensionless height of the fin given by equation (4.1.3)

Greek Symbols

β radial to orthogonal thermal conductivity ratio given by equation (4.1.4)

δ half thickness of the fin shown in Figure 4-1

η fin efficiency

θ dimensionless temperature as defined in equation (3.2.15)

θ^* dimensional temperature defines by equation (3.4.6)

θ' dimensionless temperature as defined in equation (4.2.12)

ω humidity ratio of the air, (kg_w/kg_a)

Ω dimensionless humidity ratio of the air as defined in equation (3.2.16)

Ψ fin aspect ratio = $\left(t_b^* / 2\right) / L$

Subscripts

a air

b fin base

c fictitious extended fin tip

dew dew point

max maximum

r radial direction

s fin surface

t fin tip

z direction perpendicular to radius

Superscripts

* dimensional parameter

References

[1] Donald Q.Kern and Allan D.Kraus, *Extended Surface Heat Transfer* Macgraw-Hill, New York, 1972.

[2] W.M.Murray, "Heat transfer through an annular disc or fin of uniform thickness," *ASME Journal of Applied Mechanics*, Vol. 60, p. A78, 1938.

[3] K.A.Gardner, "Efficiency of extended surface," *American Society of Mechanical Engineers*, Vol. 67, pp. 621-631, 1945.

[4] A. D. Kraus, "Sixty-five years of extended surface technology (1922-1987)," *Appl. Mech. Rev*, Vol. 41, No. 9, pp. 321-364, 1988.

[5] F.P.Incropera and D.P.Dewitt, *Fundamentals of Heat and Mass Transfer*, Fifth ed John Wiley & Sons Inc., NY, 2002.

[6] Iftakhar Alam and P.S.Ghoshdastidar, "A study of heat transfer effectiveness of circular tubes with internal longitudinal fins having tapered lateral profiles," *International journal of heat and mass transfer*, Vol. 45, No. 6, pp. 1371-1376, 2002.

[7] Hong-Sen Kou, Ji-Jen Lee, and Chi-Yuan Lai, "Thermal analysis of a longitudinal fin with variable thermal properties by recursive formulation," *International journal of heat and mass transfer*, Vol. 48, No. 11, pp. 2266-2277, 2005.

[8] H.J.Lane and P.J.Heggs, "Extended surface heat transfer—the dovetail fin," *Applied Thermal Engineering*, Vol. 25, No. 16, pp. 2555-2565, 2005.

[9] M.N.Bouaziz and S.Hanini, "Efficiency and optimisation of fin with temperature-dependent thermal conductivity: a simplified solution," *Heat and Mass Transfer*, Vol. 4, No. 1, pp. 1-9, 2007.

[10] A.Ullmann and H.Kalman, "Efficiency and optimized dimensions of annular fins of different cross-section shapes," *International journal of heat and mass transfer*, Vol. 32, No. 6, pp. 1105-1110, 1989.

[11] A.Brown, "Optimum Dimensions of Uniform Annular Fins," *International journal of heat and mass transfer*, Vol. 8, pp. 655-662, 1965.

[12] Inmaculada Arauzo, Antonio Campo, and Cristóbal Cortés, "Quick estimate of the heat transfer characteristics of annular fins of hyperbolic profile with the power series method," *Applied Thermal Engineering*, Vol. 25, No. 4, pp. 623-634, 2005.

[13] Antonio Campo and Jianhong Cui, "Temperature/Heat Analysis of Annular Fins of Hyperbolic Profile Relying on the Simple Theory for Straight Fins of Uniform Profile," *Journal of Heat Transfer*, Vol. 130, No. 5, pp. 054501-1-054501-4, 2008.

[14] B.Kundu and P.K.Das, "Performance analysis and optimization of elliptic fins circumscribing a circular tube," *International journal of heat and mass transfer*, Vol. 50, No. 1-2, pp. 173-180, 2007.

[15] E.Assis and H.Kalman, "Transient temperature response of different fins to step initial conditions," *International journal of heat and mass transfer*, Vol. 36, No. 17, pp. 4107-4114, 1993.

[16] K.Loar and H.Kalman, "Performance and optimum dimensions of different cooling fins with a temperature-dependent heat transfer coefficient," *International journal of heat and mass transfer*, Vol. 39, No. 9, pp. 1993-2003, 1995.

[17] B.Kundu and P.K.Das, "Performance analysis and Optimization of Straight Taper Fins with Variable Heat Transfer Coefficient," *International journal of heat and mass transfer*, Vol. 45, pp. 4739-4751, 2002.

[18] B.Kundu and P.K.Das, "Performance and optimum design analysis of convective fin arrays attached to flat and curved primary surfaces," *International Journal of Refrigeration*, Vol. 32, No. 3, pp. 430-443, 2009.

[19] J.L.Threlkeld, *Thermal Environmental Engineering*, 2nd edition ed Prentice-Hall Inc., 1970.

[20] F.C.McQuiston, "Fin Efficiency with Combined Heat and Mass Transfer," *ASHRAE Transactions*, Vol. 81, No. 1, pp. 350-355, 1975.

[21] G.Wu and T.Y.Bong, "Overall Efficiency of a Straight Fin with Combined Heat and Mass Transfer," *ASHRAE Transactions*, Vol. 100, No. 1, pp. 367-374, 1994.

[22] A.H.Elmahdy and R.C.Briggs, "Efficiency of Extended Surfaces with Simultaneous Heat and Mass Transfer," *ASHRAE Transactions*, Vol. 89, No. 1A, pp. 135-143, 1983.

[23] B.Kundu, "Performance and Optimum Design Analysis of Longitudinal and Pin Fin with Simultaneous Heat and Mass Transfer: Unified and Comparative Investigation," *Applied Thermal Engineering*, Vol. 27, pp. 976-987, 2007.

[24] H.Kazeminejad, "Analysis of one-dimensional fin assembly heat transfer with dehumidification," *International journal of heat and mass transfer*, Vol. 38, No. 3, pp. 455-462, 1995.

[25] Mostafa H.Sharqawy and Syed M.Zubair, "Efficiency and optimization of straight fins with combined heat and mass transfer – An analytical solution," *Applied Thermal Engineering*, Vol. 28, No. 17-18, pp. 2279-2288, 2008.

[26] B.Kundu and A.Miyara, "An analytical method for determination of the performance of a fin assembly under dehumidifying conditions: A comparative study," *International Journal of Refrigeration*, Vol. 32, No. 2, pp. 369-380, 2009.

[27] S.Y.Liang, M.Liu, T.N.Wong, and G.K.Nathan, "Analytical study of evaporator coil in humid environment," *Applied Thermal Engineering*, Vol. 19, No. 11, pp. 1129-1145, 1999.

[28] G. Adomian, *Nonlinear stochastic operator equations* Academic Press, 1986.

[29] Mostafa H.Sharqawy and Syed M.Zubair, "Efficiency and optimization of an annular fin with combined heat and mass transfer an analytical solution," *International Journal of Refrigeration*, Vol. 30, pp. 751-757, 2007.

[30] B.Kundu, "An analytical study of the effect of dehumidification of air on the performance and optimization of straight tapered fins," *International Communications in Heat and Mass Transfer*, Vol. 29, No. 2, pp. 269-278, 2002.

[31] B.Kundu and P.K.Das, "Performance and Optimization Analysis for Fins of Straight Taper with Simultaneous Heat and Mass Transfer," *Transaction of the ASME*, Vol. 126, pp. 862-868, 2004.

[32] B.Kundu, D.Barman, and S.Debnath, "An analytical approach for predicting fin performance of triangular fins subject to simultaneous heat and mass transfer," *International Journal of Refrigeration*, Vol. 31, No. 6, pp. 1113-1120, 2008.

[33] D.C.Look and H.S.Kang, "Optimization of a thermally non-symmetric fin : preliminary evaluation," *International journal of heat and mass transfer*, Vol. 35, No. 8, pp. 2057-2060, 1992.

[34] L.Rosario and M.M.Rahman, "Overall efficiency of a radial fin assembly under dehumidifying conditions," *Journal of Energy Resources Technology*, Vol. 120, pp. 299-304, 1998.

[35] P.Naphon, "Study on The Heat Transfer Characteristics of The Annular Fin under Dry-Surface, Partially Wet-Surface, and Fully Wet-Surface Conditions," *International Communications in Heat and Mass Transfer*, Vol. 33, pp. 112-121, 2006.

[36] S.Y.Laing, T.N.Wong, G.K., and Nathan, "Comparison of One-Dimensional and Two-Dimensional Methods for Wet-Surface Fin Efficiency of a Plate Fin-Tube Heat Exchanger," *Applied Thermal Engineering*, Vol. 20, pp. 941-962, 2000.

[37] B.Kundu, "Analysis of thermal performance and optimization of concentric circular fins under dehumidifying conditions," *International journal of heat and mass transfer*, Vol. 52, No. 11-12, pp. 2646-2659, 2009.

[38] J.E.Coney, C.G.Sheppard, and E.A.El-Shafei, "Fin Performance with Condensation from Humid Air: a Numerical Investigation," *International Journal of Heat and Fluid Flow*, Vol. 10, pp. 224-231, 1989.

[39] E.Schmidt, "Die Warmeubertragung durch Rippen," *Zeitschrift des Vereines Deutscher Ingenieure*, Vol. 70, pp. 885-951, 1926.

[40] S.M.Zubair, A.Z.Al-Garni, and J.S.Nizami, "The optimal dimensions of circular fins with variable profile and temperature-dependent thermal conductivity," *International journal of heat and mass transfer*, Vol. 39, No. 16, pp. 3431-3439, 1996.

[41] Jameel-ur-Rehman Khan and S.M.Zubair, "The optimal dimensions of convective-radiating circular fins," *Heat and Mass Transfer*, Vol. 35, No. 6, pp. 469-478, 1999.

[42] Antonio Campo, Biagio Morrone, and Salah Chikh, "Easy and rapid computation of the transfer of heat from annular fins of nearly optimal profile with the finite-difference technique and the shooting method," *International Journal of Numerical Methods for Heat & Fluid Flow*, Vol. 14, No. 8, pp. 1002-1010, 2004.

[43] Cihat Arslanturk, "Simple correlation equations for optimum design of annular fins with uniform thickness," *Applied Thermal Engineering*, Vol. 25, No. 14-15, pp. 2463-2468, 2005.

[44] Chi-Yuan Lai, Hong-Sen Kou, and Ji-Jen Lee, "Optimum thermal analysis of annular fin heat sink by adjusting outer radius and fin number," *Applied Thermal Engineering*, Vol. 26, No. 8-9, pp. 927-936, 2006.

[45] S.Ravi Kumar, G.Ramamurthy, and K.V.Sharma, "Numerical Analysis for Optimal Dimensions of a Circular Fin with Hyperbolic Profile,", 33 ed 2008, pp. 633-637.

[46] A.Sonn and A.Bar-Cohen, "Optimum Cylindrical Pin Fin," *Journal of Heat Transfer*, Vol. 103, pp. 814-815, 1981.

[47] M.Almogbel and A.Bejan, "Cylindrical trees of pin fins," *International journal of heat and mass transfer*, Vol. 43, No. 23 2000.

[48] Raj Bahadur and Avram Bar-Cohen, "Thermal Design and Optimization of Staggered Polymer Pin Fin Natural Convection Heat Sinks," *Ninth Intersociety Conference on Thermal and Thermomechanical Phenomena in Electronic Systems*, 2004.

[49] Han-Ting Chen, Po-Li Chen, Jenn-Tsong Horng, and Ying-Huei Hung, "Design Optimization for Pin-Fin Heat Sinks," *Journal of Electronic Packaging*, Vol. 127, No. 4, pp. 397-406, 2005.

[50] Ko-Ta Chiang and Fu-Ping Chang, "Application of response surface methodology in the parametric optimization of a pin-fin type heat sink," *International Communications in Heat and Mass Transfer*, Vol. 33, No. 7, pp. 836-845, 2006.

[51] Leonid Hanin and Antonio Campo, "A new minimum volume straight cooling fin taking into account the "length of arc"," *International journal of heat and mass transfer*, Vol. 46, No. 26, pp. 5145-5152, 2003.

[52] Panagiotis Razelos, "Discussion: "Performance and Optimization Analysis for Fins of Straight Taper with Simultaneous Heat and Mass Transfer"," *Journal of Heat Transfer*, Vol. 129, No. 9, pp. 1304-1305, 2007.

[53] H. S. Kang and D. C. Look Jr, "Two dimensional trapezoidal fins analysis," *Computational Mechanics*, Vol. 19, No. 3, pp. 247-250, 1997.

[54] H. S. Rang and D. C. Look, "A Comparison of Four Solution Methods for the Analysis of a Trapezoidal Fin," *Journal of Mechanical Science and Technology*, Vol. 13, No. 6, pp. 487-495, 1999.

[55] S. Y. Liang, T. N. Wong, and G. K. Nathan, "Comparison of one-dimensional and two-dimensional models for wet-surface fin efficiency of a plate-fin-tube heat exchanger," *Applied Thermal Engineering*, Vol. 20, No. 10, pp. 941-962, 2000.

[56] C. N. Lin and J. Y. Jang, "A two-dimensional fin efficiency analysis of combined heat and mass transfer in elliptic fins," *International journal of heat and mass transfer*, Vol. 45, No. 18, pp. 3839-3847, 2002.

[57] Cihat Arslanturk, "Performance analysis and optimization of a thermally non-symmetric annular fin," *International Communications in Heat and Mass Transfer*, Vol. 31, No. 8, pp. 1143-1153, 2004.

[58] P. Malekzadeh and H. Rahideh, "IDQ two-dimensional nonlinear transient heat transfer analysis of variable section annular fins," *Energy Conversion and Management*, Vol. 48, No. 1, pp. 269-276, 2007.

[59] Raj Bahadur and Avram Bar-Cohen, "Orthotropic thermal conductivity effect on cylindrical pin fin heat transfer," *International Communications in Heat and Mass Transfer*, Vol. 50, pp. 1155-1162, 2007.

[60] J.E.Coney, H.Kazeminejad, and C.G.Sheppard, "Dehumidification of Air on a Vertical Rectangular Fin: A Numerical Study," *Journal of Mechanical Engineering Science*, Vol. 203, pp. 165-175, 1988.

[61] J.E.Coney, H.Kazeminejad, and C.G.Sheppard, "Dehumidification of Turbulent Air Flow over a Thick Fin: An Experimental Study," *Journal of Mechanical Engineering Science*, Vol. 203, pp. 177-188, 1988.

[62] T. H. Chilton and A. P. Colburn, "Analogy between heat and mass transfer," *Ind Eng Chem*, Vol. 26, p. 1183, 1934.

[63] R.W.Hyland and W.Wexler, "Formulations for The Thermodynamic Properties of The Saturated Phases of H2O from 173.15 K to 473.15 K," *ASHRAE Transactions*, Vol. 89, No. 2, pp. 500-519, 1983.

[64] M. Abramowitz and I. A. Stegun, *Handbook of mathematical functions with formulas, graphs, and mathematical table* Courier Dover Publications, 1965.

[65] J.Patrick, *Fundamental of Computational Fluid Dynamics* Hermosa Publishers, 1998.

[66] R. M. Cotta and M. D. Mikhailov, *Heat conduction: lumped analysis, integral transforms, symbolic computation* Wiley New York, 1997.

[67] Allan D.Kraus, Abdul Aziz, and James Welty, *Extended Surface Heat Transfer* John Wiley & Sons, Inc., 2001.

Vita

- Abdurrahman Moinuddin
- Born in 1985, Delhi, India
- Received Bachelor of Technology (B.Tech) with honors in Mechanical Engineering from Jamia Millia Islamia, New Delhi - 110025, India, 2006.
- Joined Mechanical Engineering Department at King Fahd University of Petroleum and Minerals (KFUPM), Dhahran, Saudi Arabia, as Research Assistant in February 2007.
- Received Master of Science (M.S) in Mechanical Engineering from KFUPM in 2009.
- E-mail: abdur.rahman11@gmail.com